中子皮及其在核反应中的效应

方 德 清

复旦大学

目 录

不稳定核中的新现象与新物理

稳定核($N \approx Z$)

原子核壳模型

$R \approx 1.2 \times A^{1/3}$

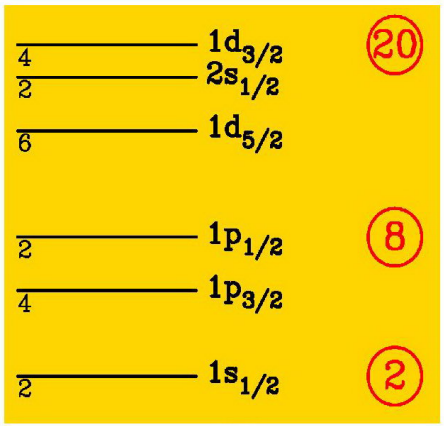

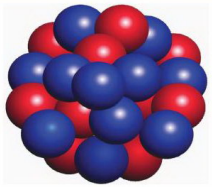

稳定核：~300；理论预言：~8000；已发现：~3000

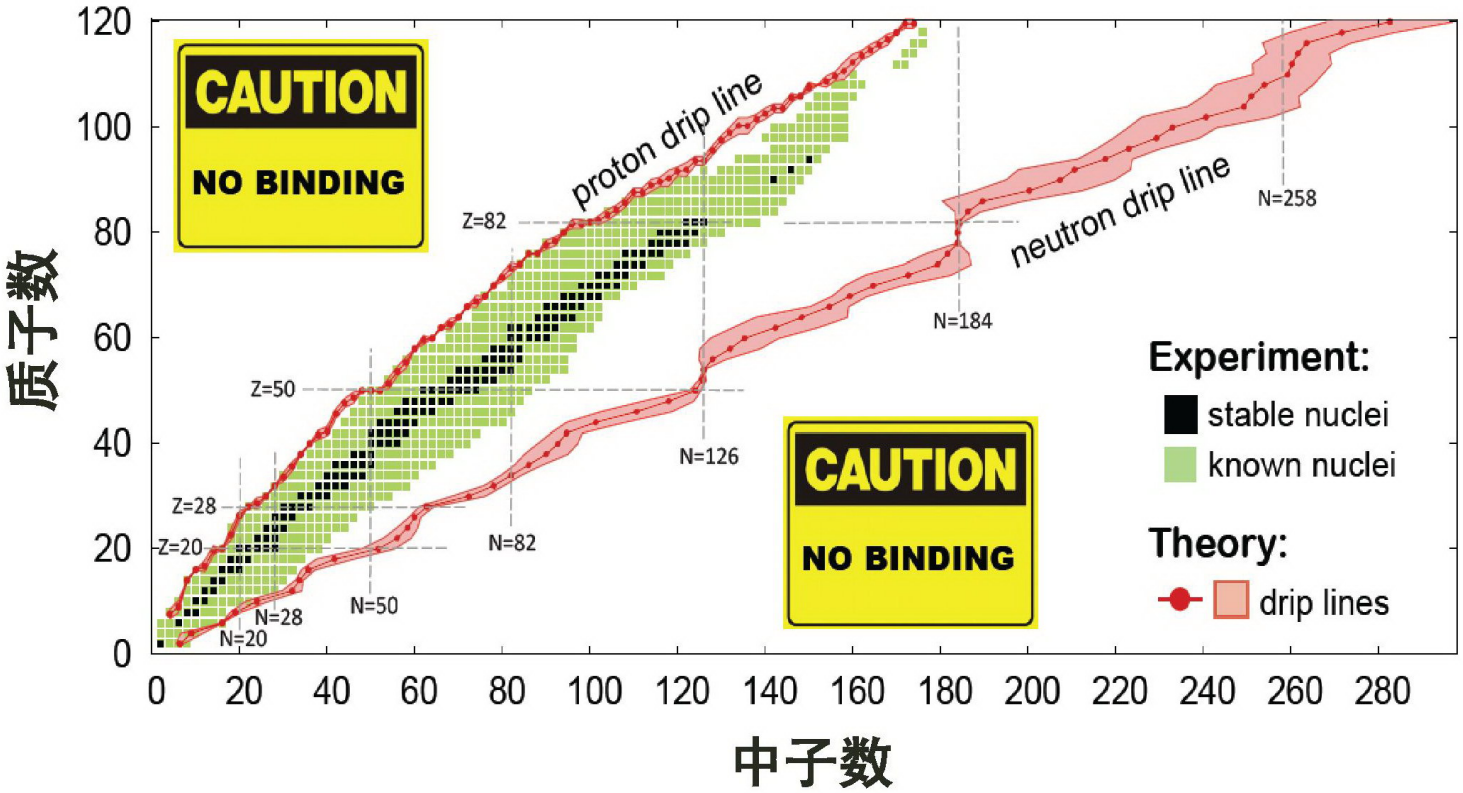

- **壳层结构的改变**
- **幻数的消失与新幻数的出现**
- **晕结构**
- **集团结构**
- **奇异放射性**
- **……**

现象❶：幻数的消失与新幻数的出现

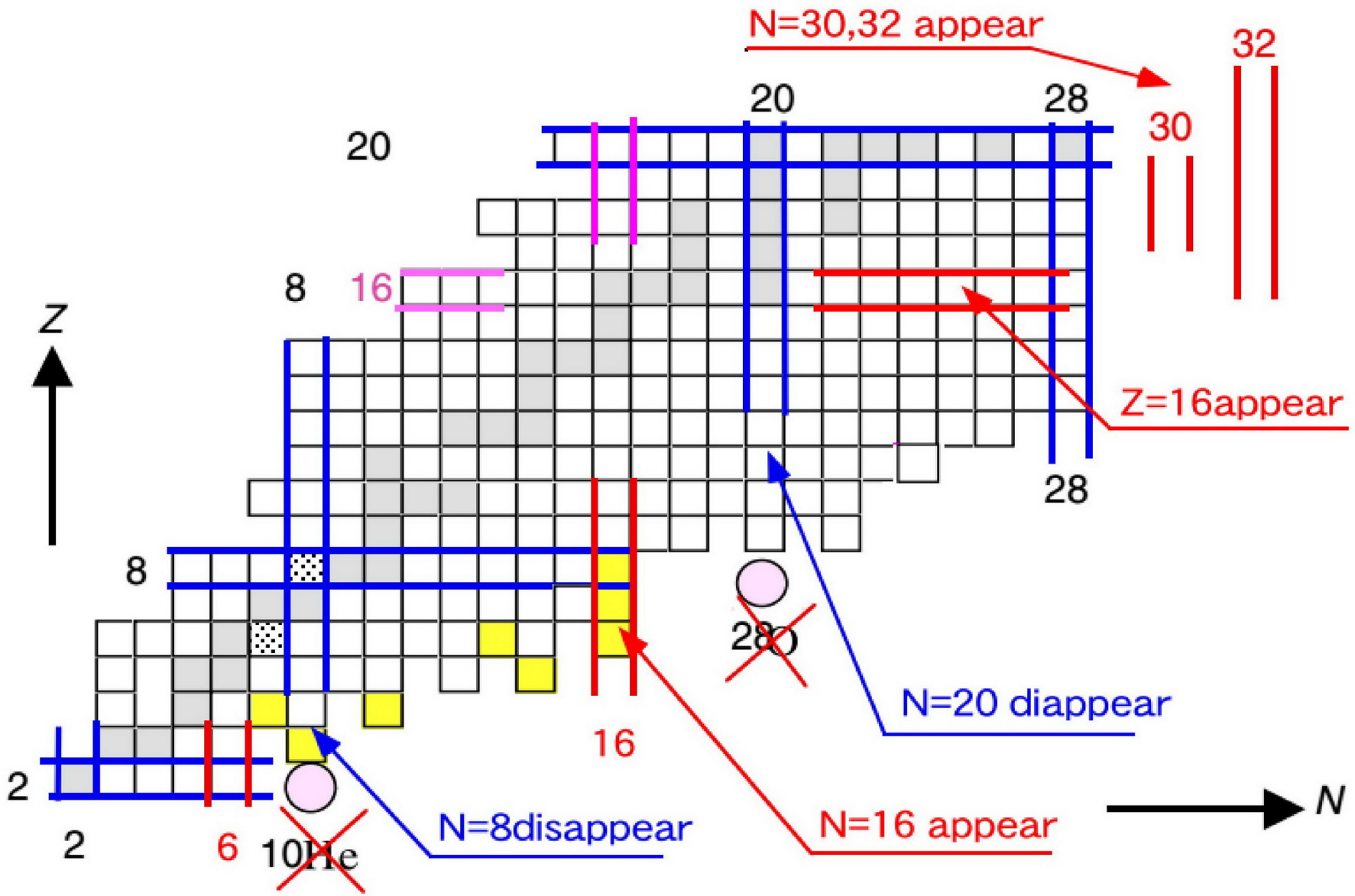

现象❷：晕结构

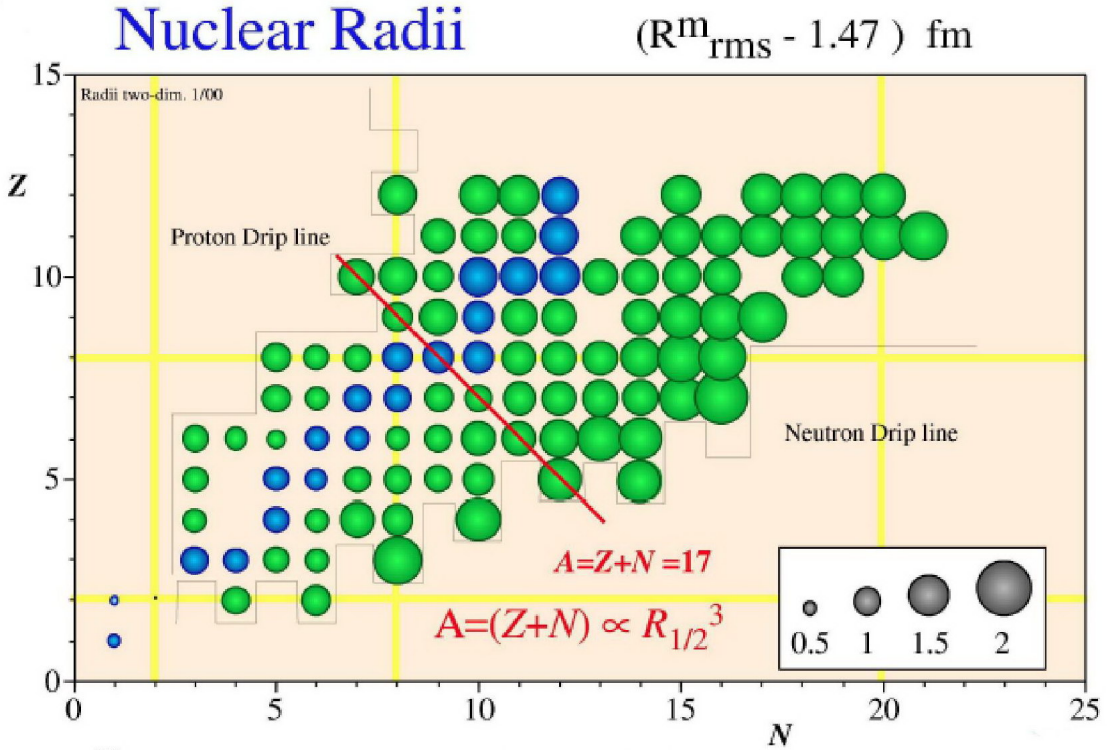
Nuclear Radii
$(R^m_{rms} - 1.47)$ fm
Radii two-dim. 1/00
Proton Drip line
Neutron Drip line
A=Z+N =17
$A=(Z+N) \propto R_{1/2}^3$
0.5 1 1.5 2
Z
N

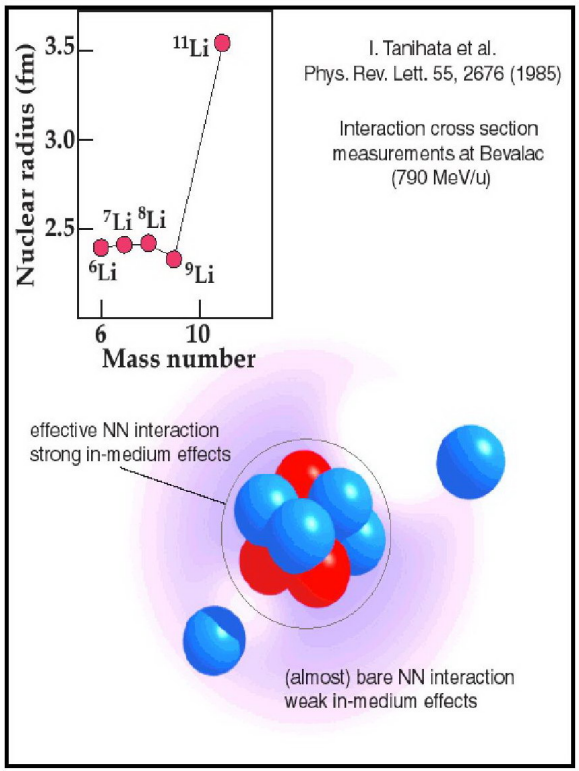
Nuclear radius (fm)
Mass number
^{11}Li
^{7}Li ^{8}Li
^{6}Li
^{9}Li
I. Tanihata et al.
Phys. Rev. Lett. 55, 2676 (1985)
Interaction cross section
measurements at Bevalac
(790 MeV/u)
effective NN interaction
strong in-medium effects
(almost) bare NN interaction
weak in-medium effects

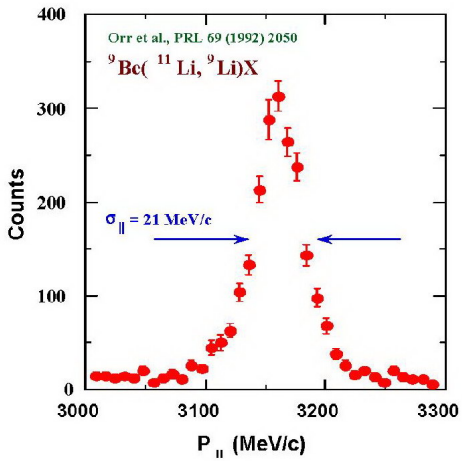
Orr et al., PRL 69 (1992) 2050
^{9}Be(^{11}Li, ^{9}Li)X
$\sigma_{\parallel}$ = 21 MeV/c
Counts
$P_{\parallel}$ (MeV/c)

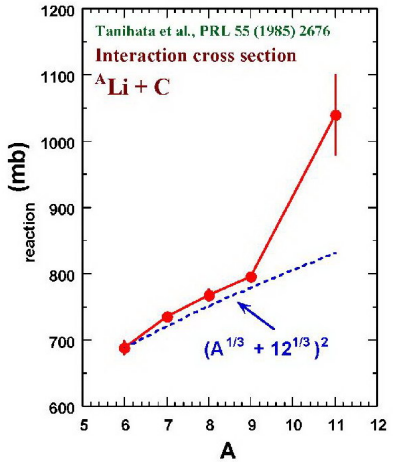
Tanihata et al., PRL 55 (1985) 2676
Interaction cross section
^{A}Li + C
reaction (mb)
$(A^{1/3} + 12^{1/3})^2$
A

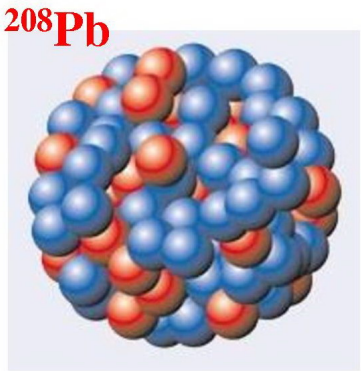
^{208}Pb

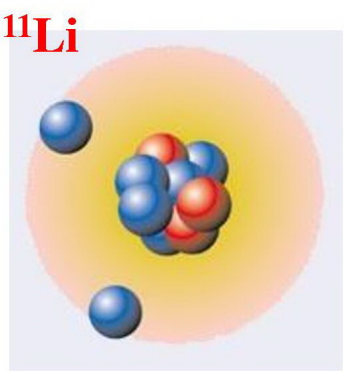
^{11}Li

晕 (皮) 核与稳定核的差异

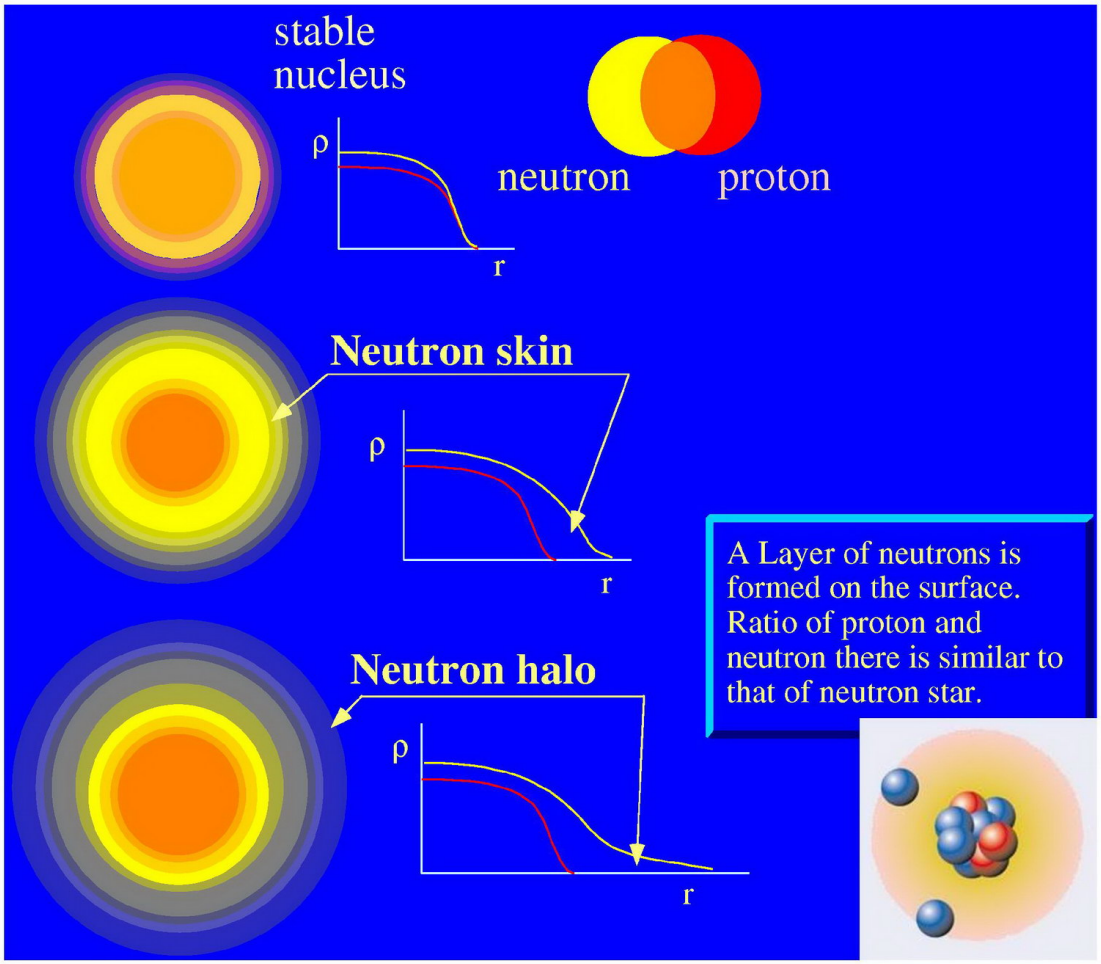

A Layer of neutrons is formed on the surface. Ratio of proton and neutron there is similar to that of neutron star.

1. $A=(Z+N) \propto R_{1/2}{}^3$
2. Surface diffuseness is constant
3. $\rho_p(r) \propto \rho_n(r)$

$$\text{Weight} = \frac{4}{3}\pi R^3 \rho$$

^{11}Li case

$$P_{out} = 4\pi \int_{R_{core}}^{\infty} |\phi(r)|^2 r^2 dr > 0.5$$

价核子在核芯外的几率大于 0.5！

影响晕核形成的主要因素

【3-dim. square-well potential】

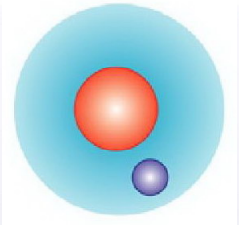

$$-\frac{\hbar^2}{2m}\frac{d^2u(r)}{dr^2}+\left(\frac{\hbar^2}{2m}\frac{l(l+1)}{r^2}+V(r)\right)u(r)=E\,u(r),\quad rR(r)=u(r)$$

for $\ell=0$

inner： $u(r)\propto\exp(-ikr)$

outer： $u(r)\propto\exp(-\kappa r)$

$$\kappa=\sqrt{2m|E|}/\hbar$$

$$\therefore\quad R(r)\propto\exp(-\kappa r)/r$$

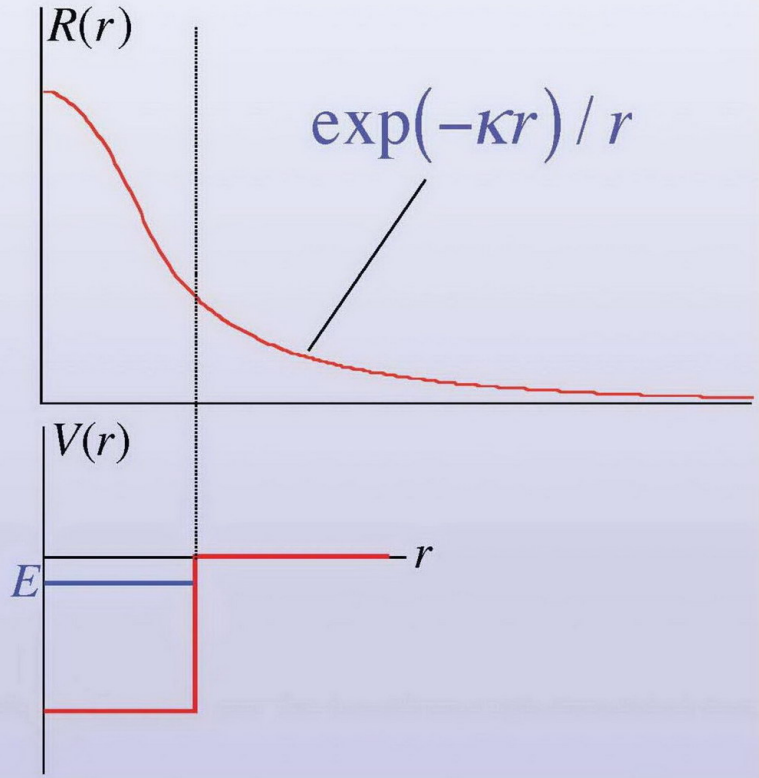

影响晕核形成的主要因素

outer :

$$R(r) \propto \exp(-\kappa r)/r$$

$$\kappa = \sqrt{2m|E|}/\hbar$$

|E| small → κ small

a long tail in R(r)

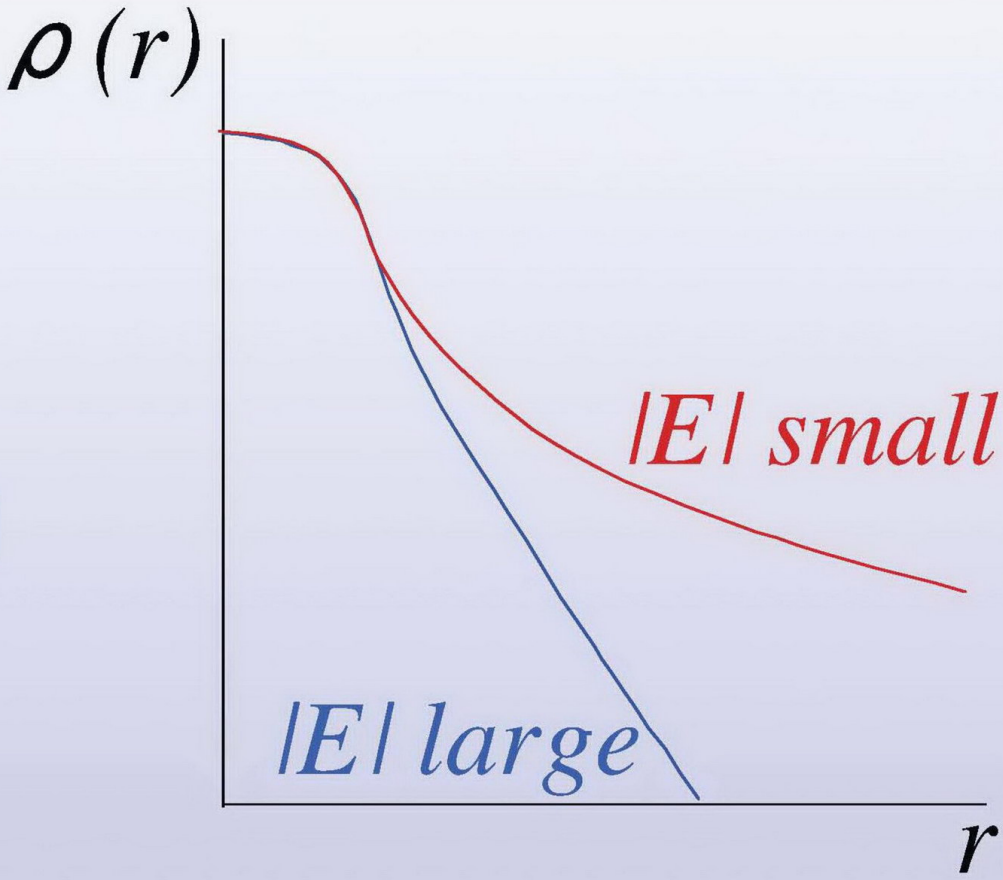

影响晕核形成的主要因素

$S_n(^{15}C)$=1.218 MeV

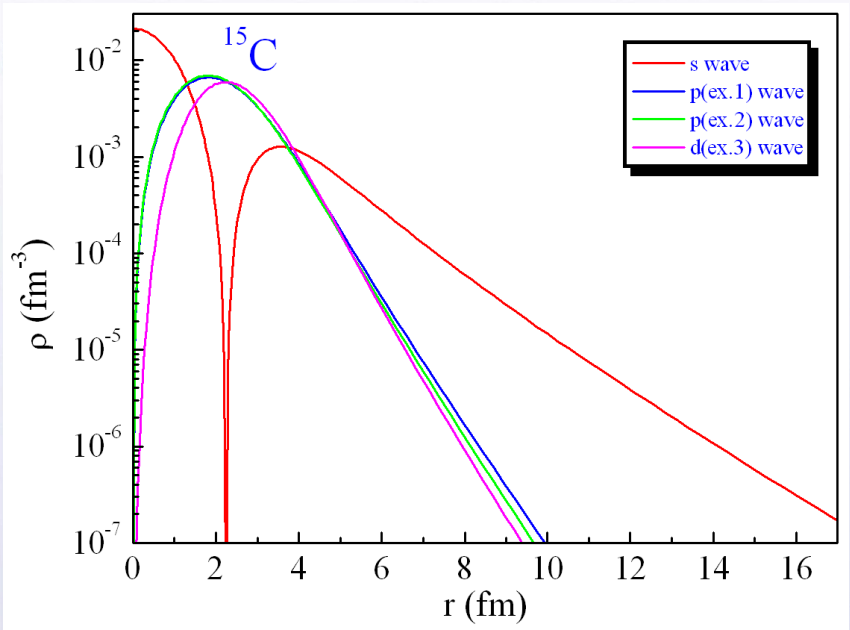

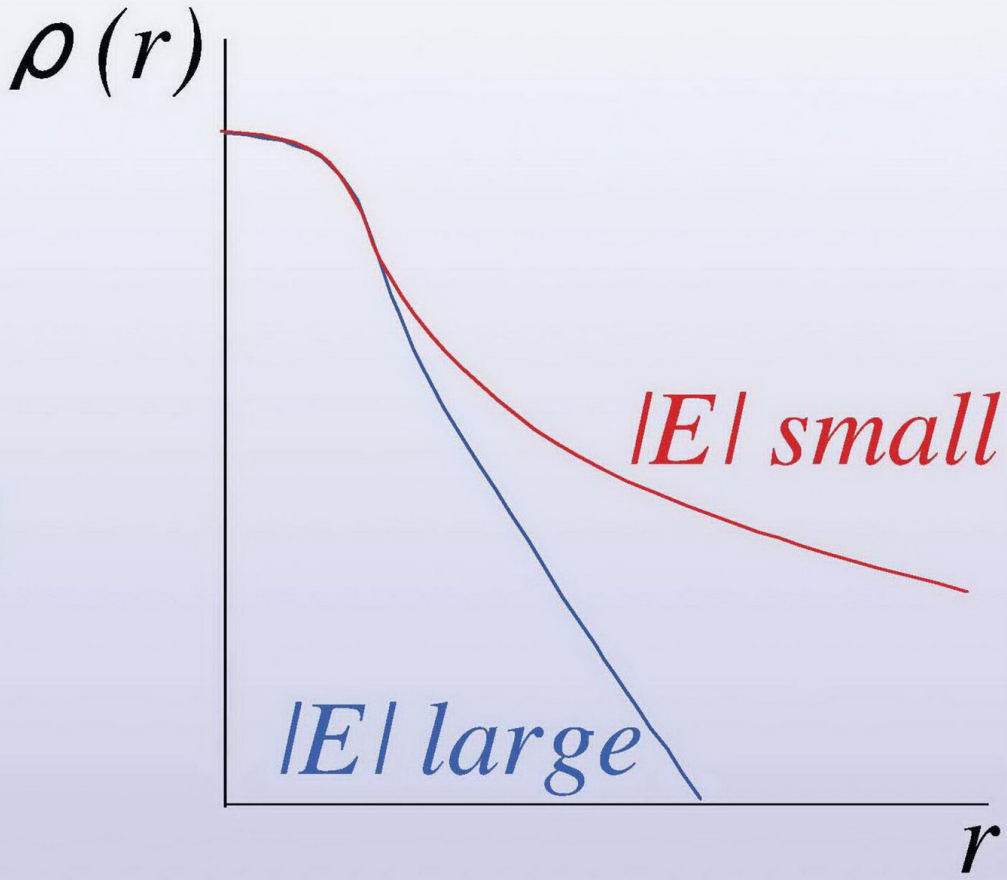

|E| small → κ small

a long tail in R(r)

晕核研究进展

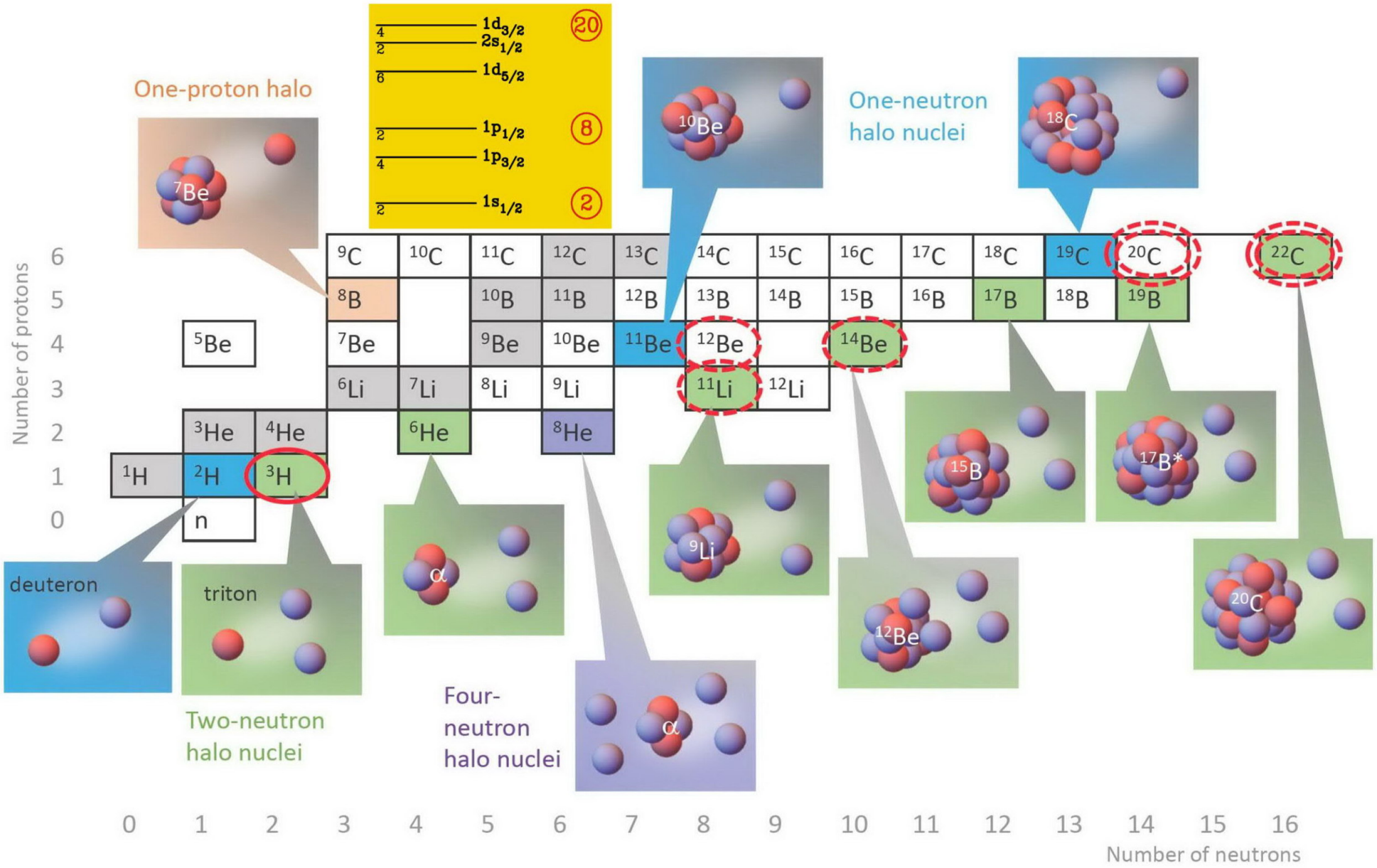
One-proton halo
One-neutron halo nuclei
Two-neutron halo nuclei
Four-neutron halo nuclei
deuteron
triton
Number of protons
Number of neutrons
1d3/2
2s1/2
1d5/2
1p1/2
1p3/2
1s1/2
20
8
2

晕核研究进展

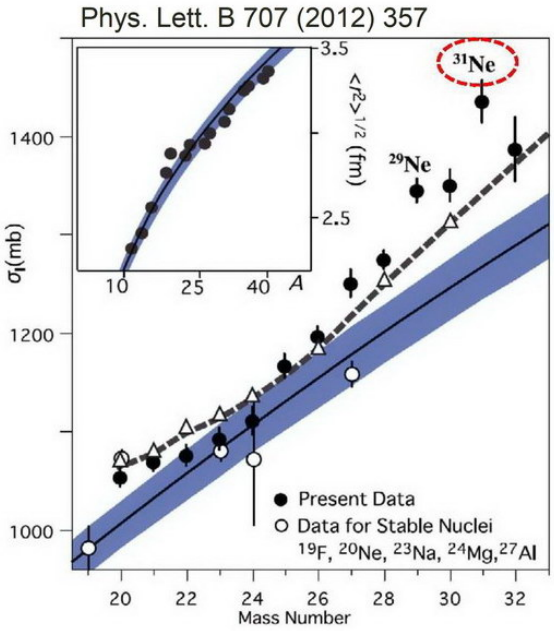
Phys. Lett. B 707 (2012) 357
^{31}Ne
^{29}Ne
σ_I(mb)
$\langle r^2\rangle^{1/2}$ (fm)
Present Data
Data for Stable Nuclei
^{19}F, ^{20}Ne, ^{23}Na, ^{24}Mg,^{27}Al
Mass Number

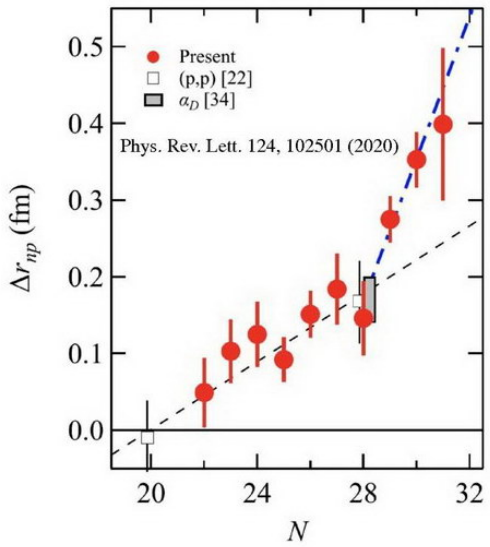
Present
(p,p) [22]
α_D [34]
Phys. Rev. Lett. 124, 102501 (2020)
Δr_{np} (fm)
N

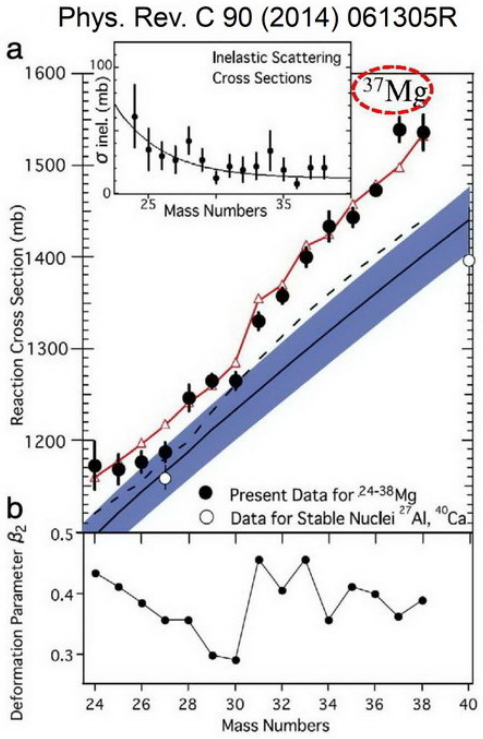
Phys. Rev. C 90 (2014) 061305R
Inelastic Scattering Cross Sections
^{37}Mg
Present Data for $^{24-38}$Mg
Data for Stable Nuclei ^{27}Al, ^{40}Ca
Reaction Cross Section (mb)
Deformation Parameter β_2
Mass Numbers

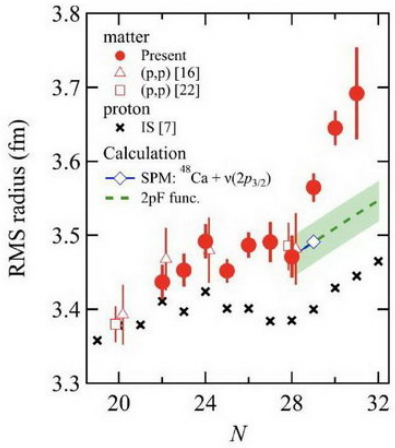
matter
Present
(p,p) [16]
(p,p) [22]
proton
IS [7]
Calculation
SPM: ^{48}Ca + $\nu(2p_{3/2})$
2pF func.
RMS radius (fm)
N

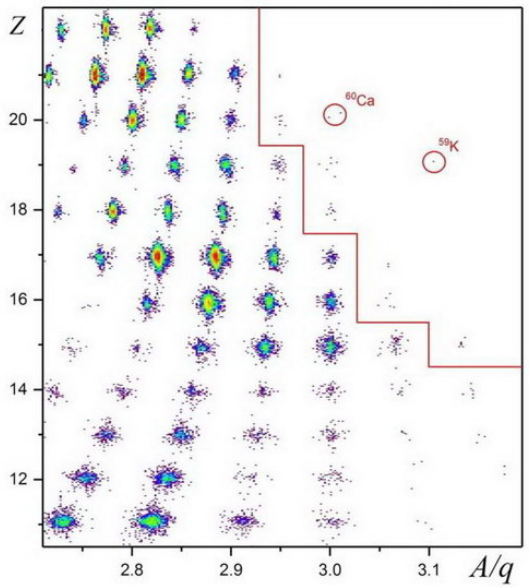
RIBF
Phys. Rev. Lett. 121, 022501 (2018).
Z
^{60}Ca
^{59}K
A/q

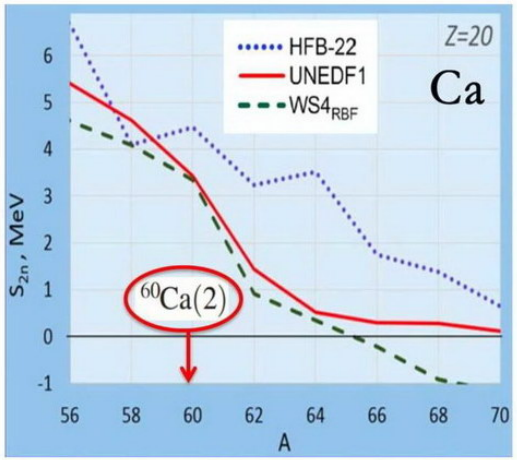
HFB-22
UNEDF1
WS4$_{RBF}$
Z=20
Ca
^{60}Ca(2)
S_{2n}, MeV
A

现象❸：集团结构

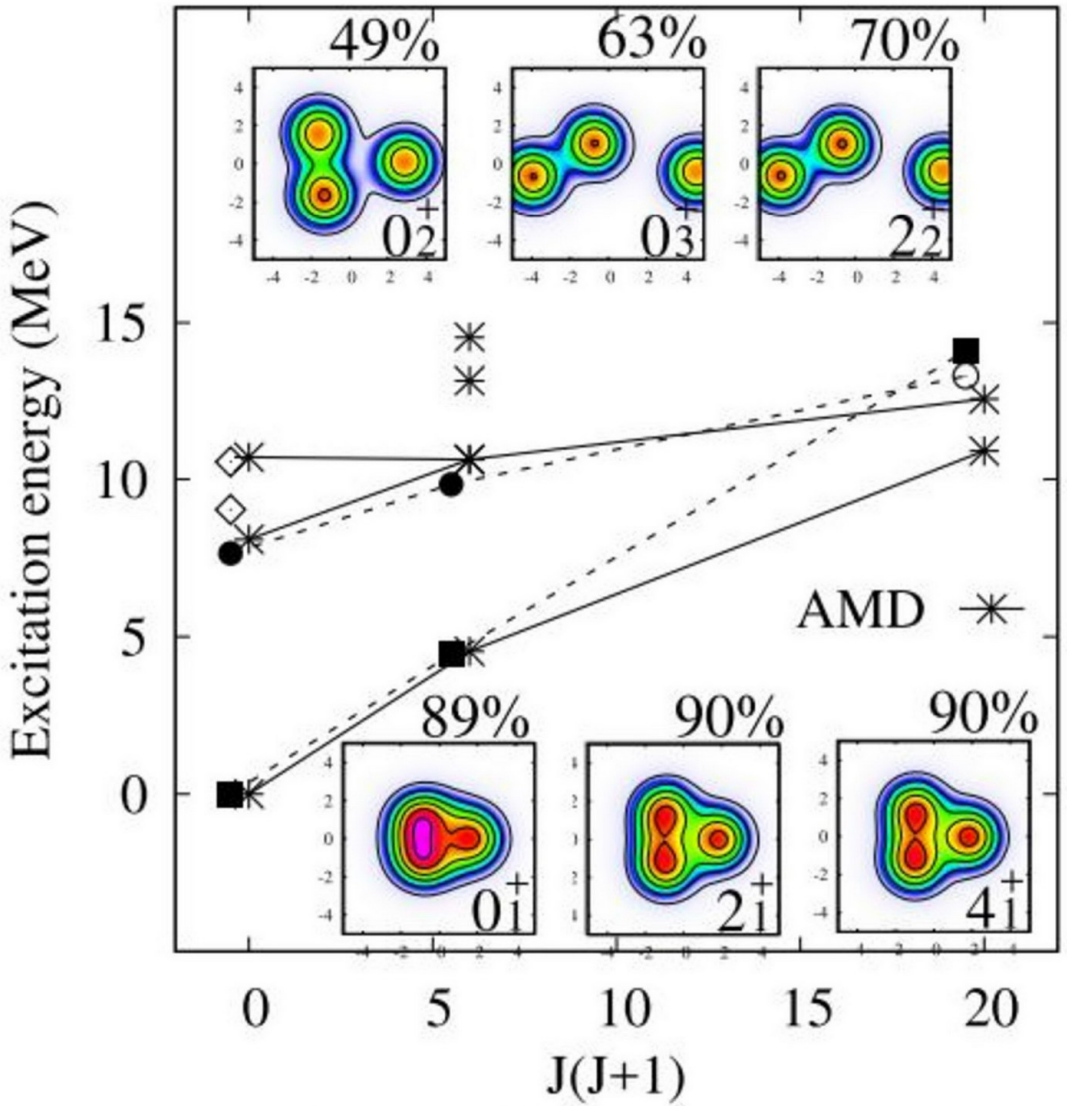

^{12}C的集团结构(AMD模型)

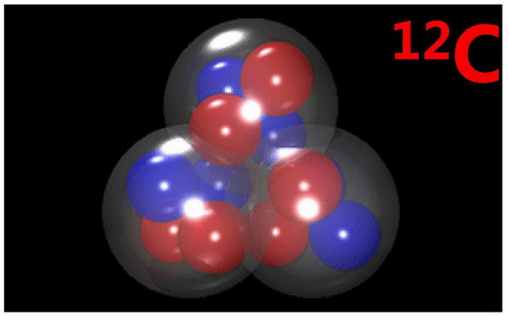

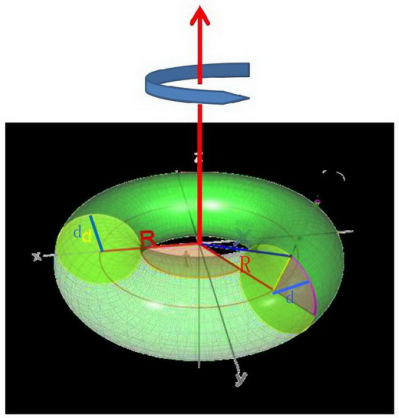

^{28}Si

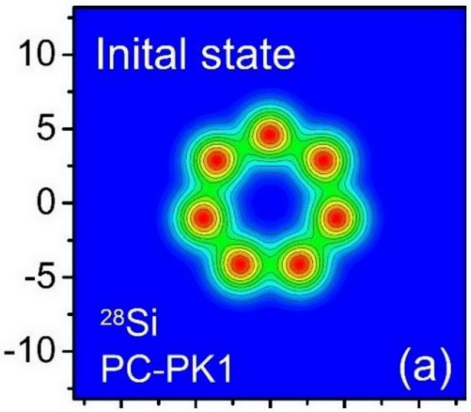

现象❹：奇异放射性

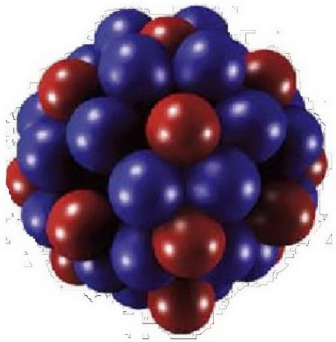

新的衰变模式

α 放射性

β 放射性

γ 放射性

裂变

质子/中子放射性

β 缓发质子/中子

重离子放射性

现象❹：奇异放射性

- 单质子/中子衰变
- 双质子/中子衰变
- β－缓发中子
- β－缓发质子

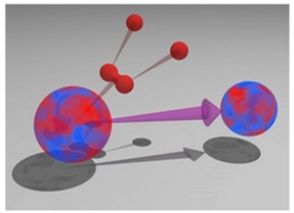
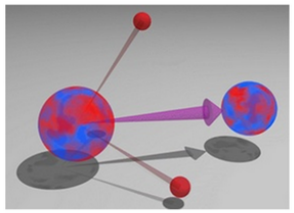
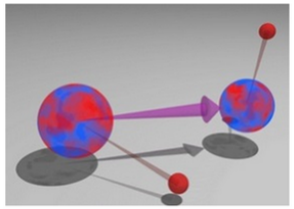

^{2}He 集团发射 三体发射 级联发射

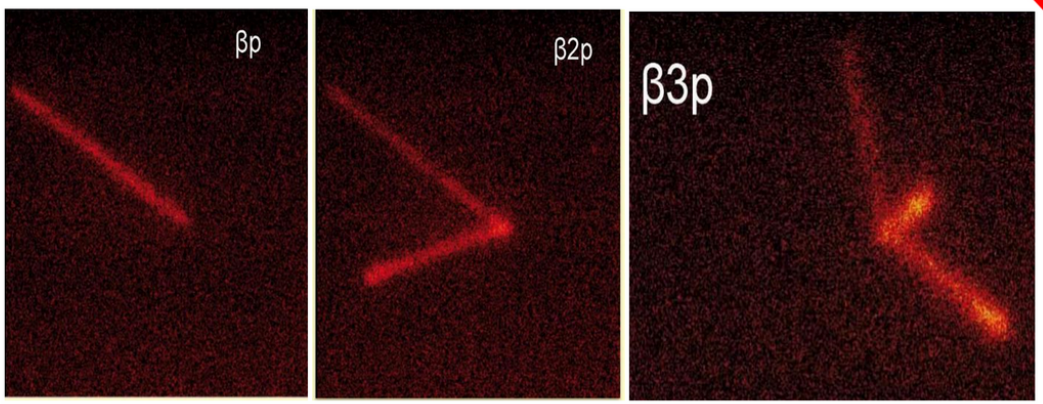

双质子发射研究进展

基态的双质子发射

V. Goldanskii, Nucl. Phys. 19 (1960) 482

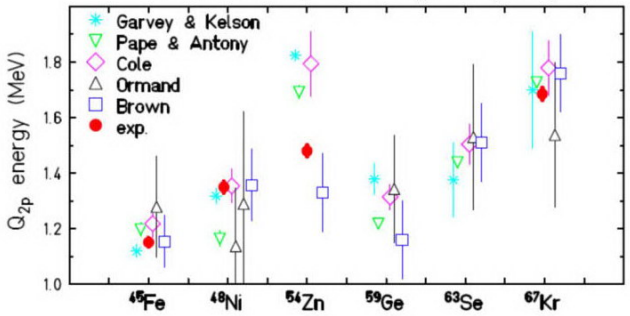

^{45}Fe, Giovinazzo *et al.*, PRL89, 102501 (2002)
^{48}Ni, Dossat *et al.*, PRC72, 054315 (2005)
^{54}Zn, B. Blank *et al.*, PRL94, 232501 (2005)
^{19}Mg, I. Muhka et al., PRL99, 182501 (2007)
^{67}Kr, T. Goigoux *et al.*, PRL117, 162501 (2016)

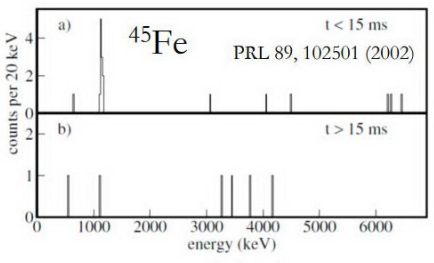

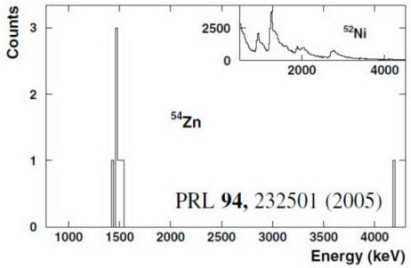

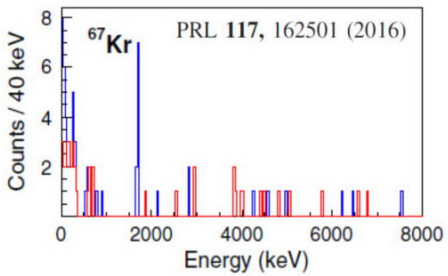

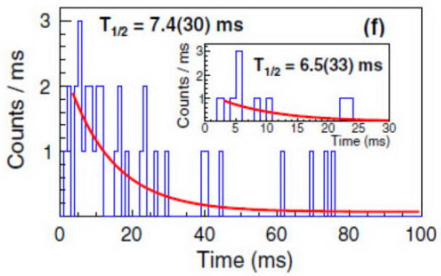

激发态的双质子发射

^{43}Cr: Giovinazzo *et al.*, PRL99, 102501 (2007)
Audirac et al., EPJA48, 179 (2012)
^{31}Ar: Axelsson *et al.*, NPA628, 345 (1998)
Fynbo et al., NPA677, 38 (2000)
^{26}P: Cable et al., PRC30, 1276 (1984)
^{22}Al: Cable et al., PRL50, 404 (1983)
Jahn et al., PRC31, 1576 (1985)
Blank et al., NPA615, 62 (1997)
Achouri et al., EPJA27, 287(2006)
^{18}Ne: Raciti et al., PRL100, 192503(2008)

^{28,29}S 、 ^{27,28}P 、 ^{22}Si等:
C. J. Lin *et al.*, PRC 80, 014310 (2009).
X. X. Xu *et al.*, PLB 727, 126 (2013).
X. X. Xu *et al*, PLB 766, 321 (2017).

双质子发射研究进展

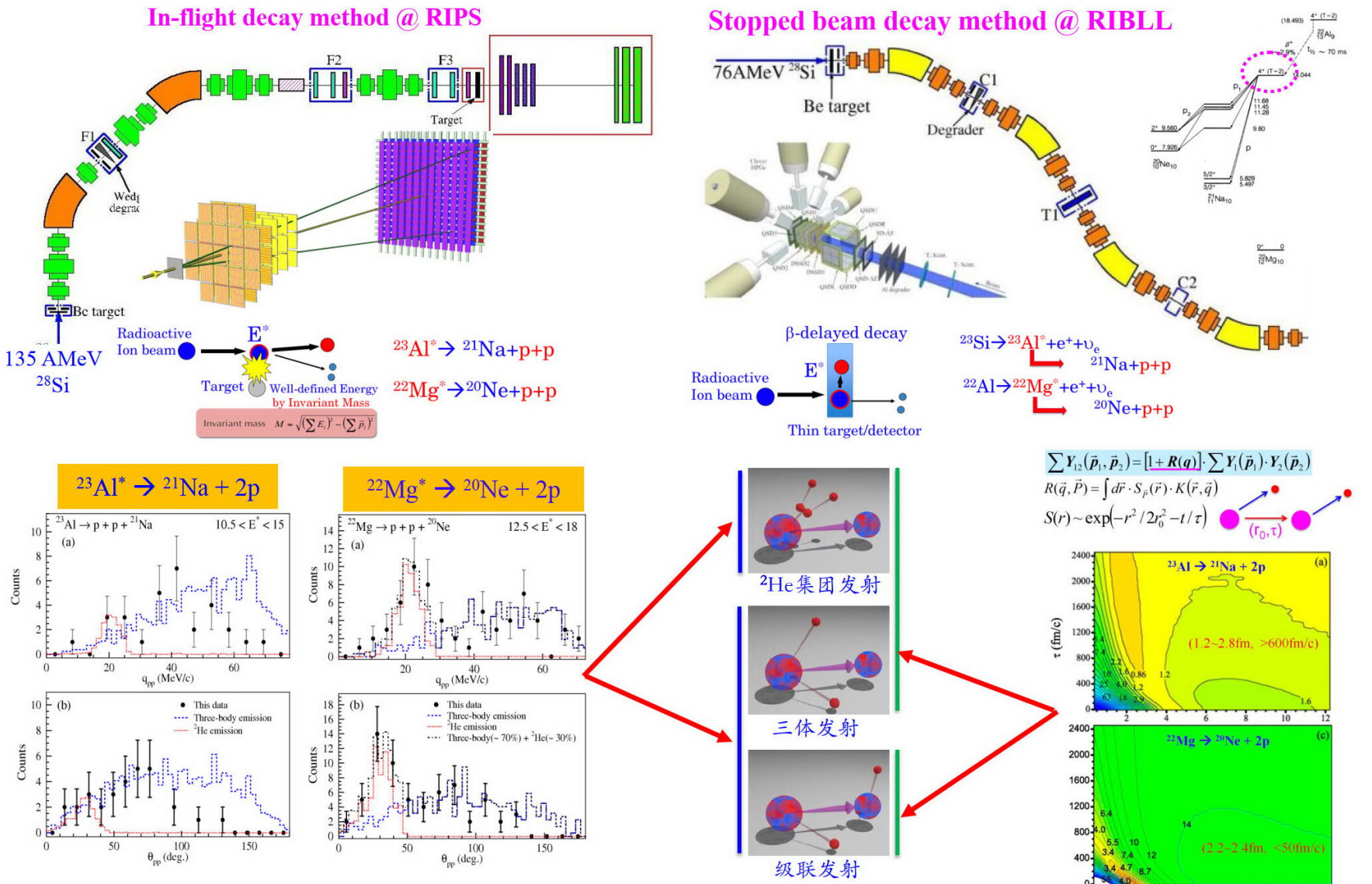

Y. G. Ma, D. Q. Fang et al., Phys. Lett. B 743 (2015) 306; D. Q. Fang, Y. G. Ma et al., PRC 94, 044621 (2016);
Y. T. Wang, D. Q. Fang et al., Phys. Lett. B 784,12 (2018); Y. T. Wang, D. Q. Fang et al., Eur. Phys. J A 54,107 (2018);
K. Wang, D. Q. Fang et al., IJPE 27, 1850014 (2018).

放射性核束物理

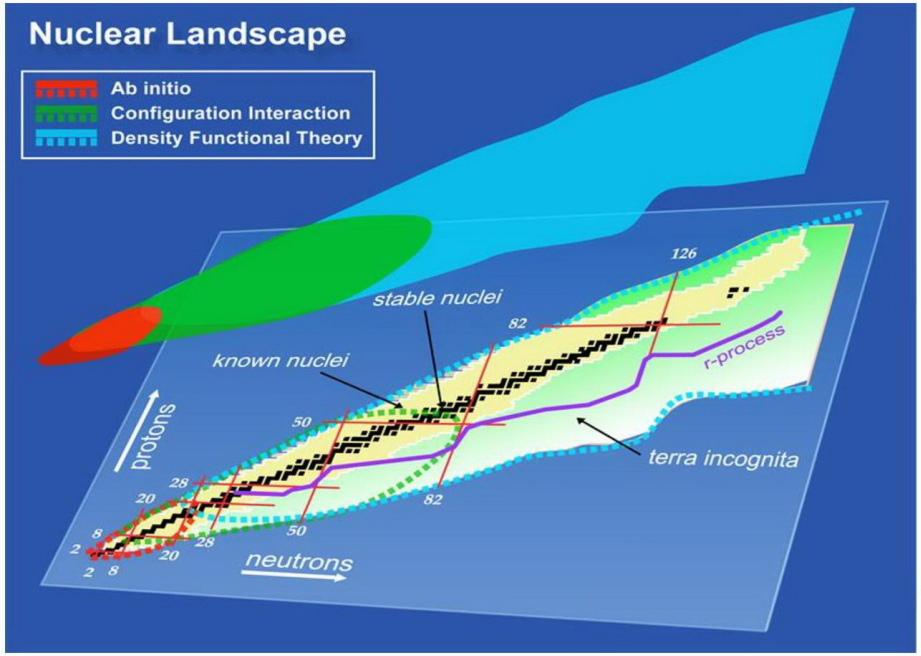

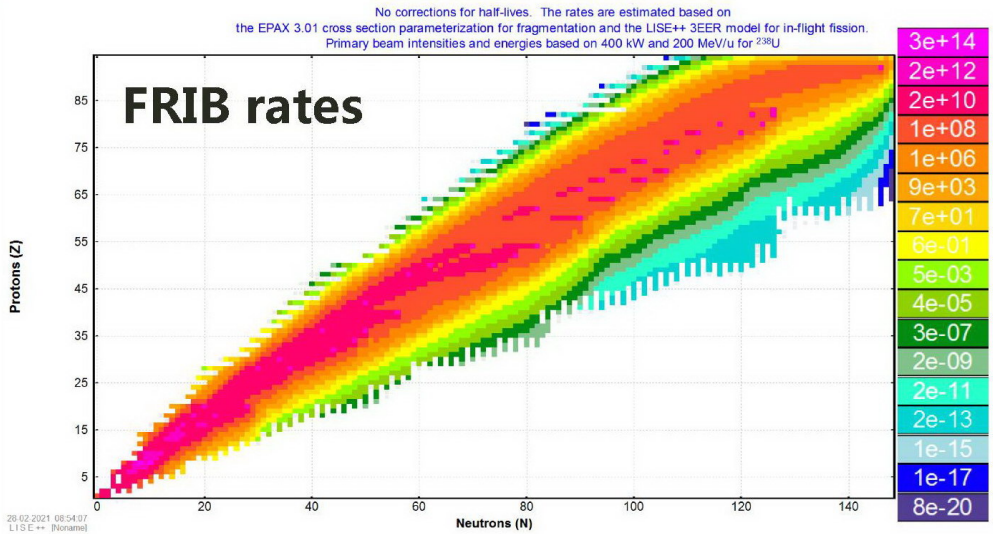

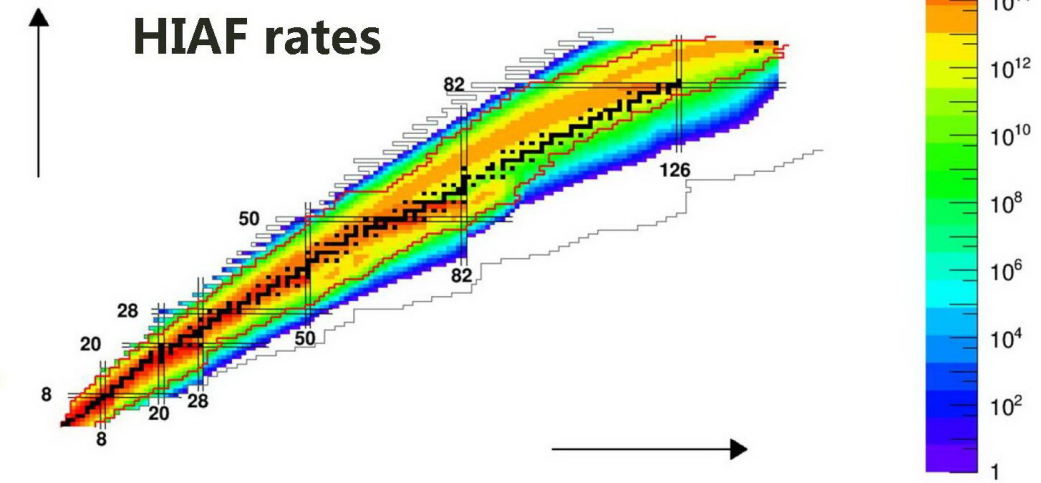

研究目标与方法

依托重离子加速器，产生不稳定原子核并测量其结构与衰变特性，发现新现象、探索新物理！

观测 ⇒ 理论 ⇒ 预言 ⇒ 实验/观测

国际放射性束流大科学装置发展

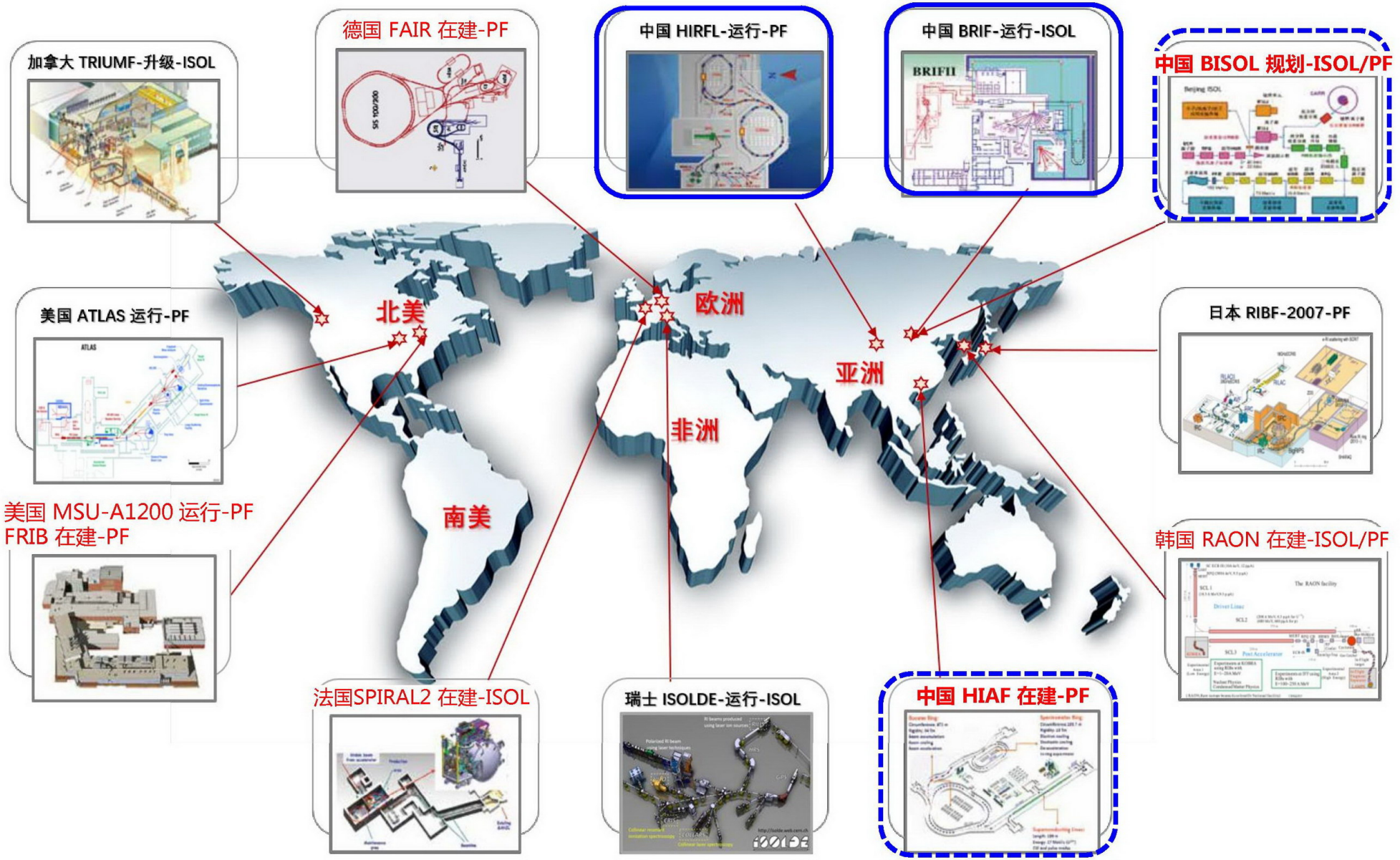

中子皮：$\Delta R_{np} = R_n - R_p$

- The proton radii can be determined to a high acurracy from the charge density distribution in experiments using electromagnetic probes, like electron scattering experiments. In contrast, it is much difficult to acurrately determine the neutron density distribution by any experimental probes

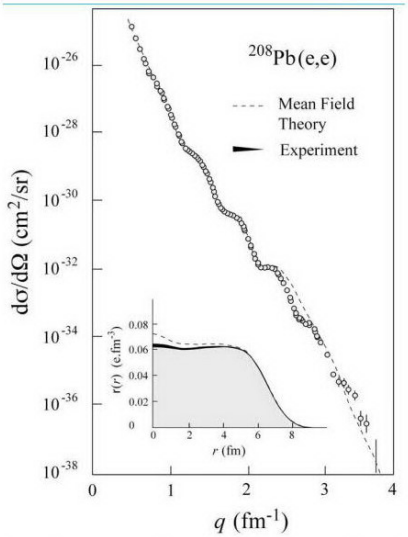

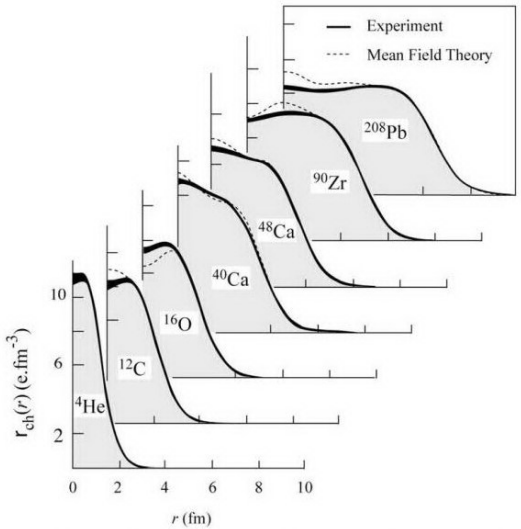

- Serveral attempts have been made to determine the neutron density distribution by using proton scattering, interaction cross section in heavy ion collisions, and also a promising new method by measuring the parity violation effect in polarized electron scattering (G. Fricke et al., At. Data Nucl. Data Tables, 60 (1995) 177, C. J. Horowitz et al., PRC 63 (2001) 025501, T. Suzuki et al., PRL 75 (1995) 3421).

- So far, the acurracy of neutron radii determinations is poor compared to that of proton radii, especially for exotic nuclei.

核物质状态方程

Nuclear EOS at T=0, density ρ and isospin asymmetry

EOS of asymmetric nuclear matter $E(\rho,\delta) \approx E(\rho,\delta=0) + E_{sym}(\rho)\delta^2, \quad \delta = \frac{\rho_n - \rho_p}{\rho_n + \rho_p}$

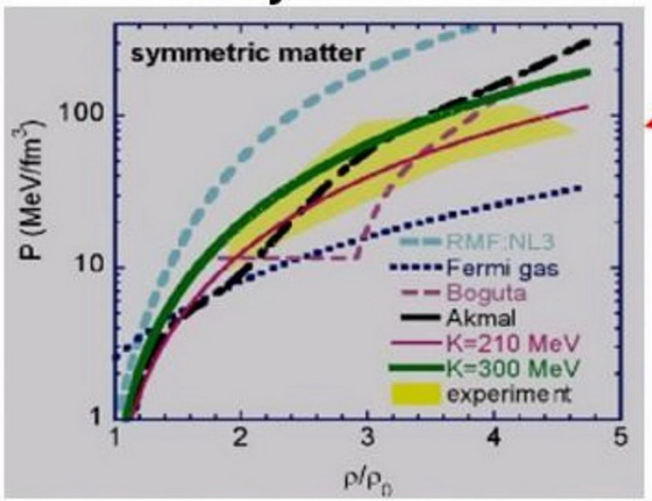

Symmetry energy $E_{sym}(\rho) = E_{sym}(\rho_0)u^{\gamma}, \quad u = \rho/\rho_0$

Symmetry energy coefficient $E_{sym}(\rho_0) \approx 30$ MeV

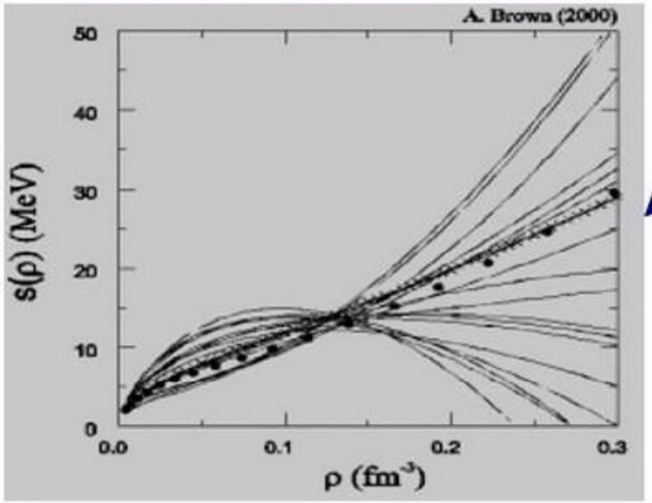

Pressure $P_{sym}(\rho,\delta) = \rho^2 \frac{\partial E_{sym}}{\partial \rho}\delta^2$

$= \rho_0 E_{sym}(\rho_0)\gamma u^{\gamma+1}\delta^2$

Compressibility $K_{sym} = 9\rho_0^2 \left.\frac{\partial^2 E_{sym}(\rho)}{\partial^2 \rho}\right|_{\rho=\rho_0}$

Danilewicz, Lacey, Lynch, Science 298,1592 (2002)

Density dependence of symmetry energy is largely unconstrained below and above the saturation density.

中子皮与非对称核物质状态方程

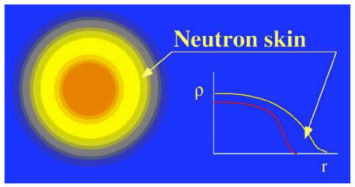

$$\Delta R_{np} = R_n - R_p = \sqrt{\langle r_n^2 \rangle} - \sqrt{\langle r_p^2 \rangle}$$

Strong correlation between neutron skin thickness and:

$E_{sym}(\rho_0)$------ nuclear symmetry energy at saturation density ρ_0

L ------the slope of symmetry energy

K_{sym}------the curvature of the nuclear symmetry energy at ρ_0

L / J ratio------J is the symmetry energy coefficient at the saturation density ρ_0

$J-a_{sym}$------a_{sym} is the symmetry energy coefficient of finite nuclei

K_v------nuclear incompressibility

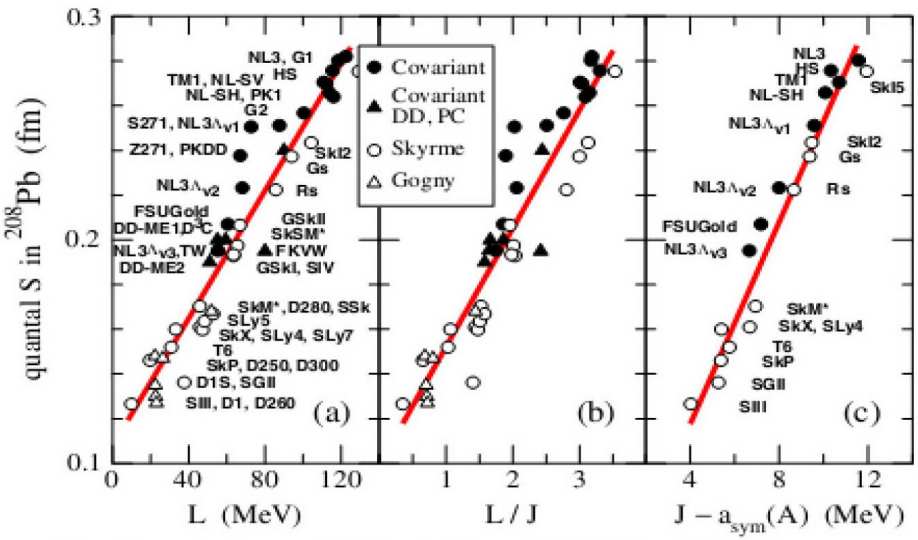

M. Centelles, PRL 102, 122502 (2009)

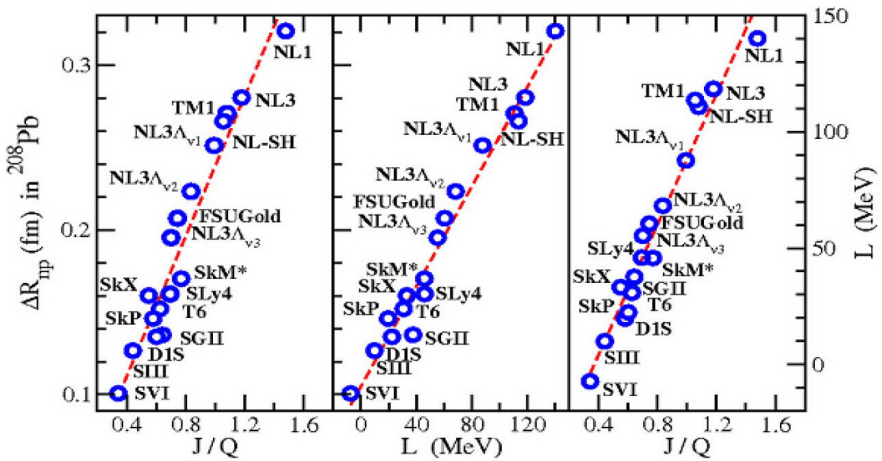

M. Warda, PRC 80, 024316 (2009)

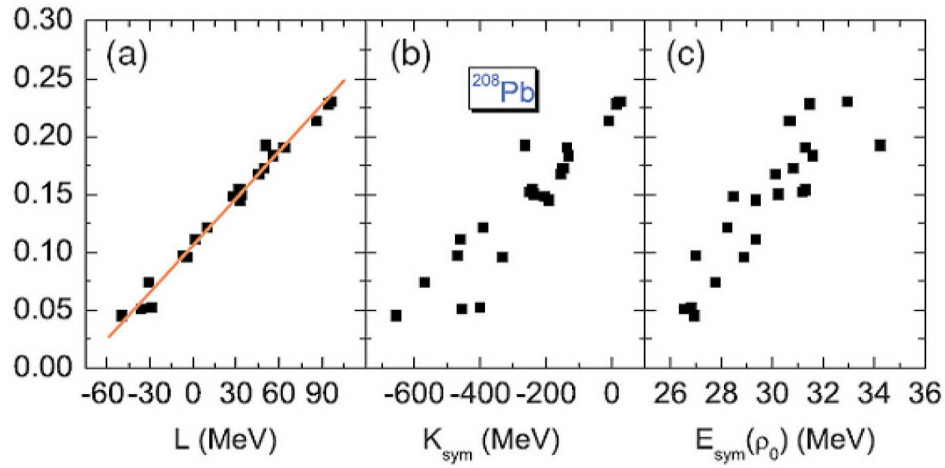

Lie-Wen Chen, PRC 72, 064309 (2005)

中子皮与中子星

- 丰中子核物质的状态方程是理解中子星等致密核天体性质的重要依据，中子星的质量与半径关系、壳-芯转变、冷却等性质依赖于核态方程。
- 核物理实验测量能提取核态方程，从而可以对中子星的性质提供约束。

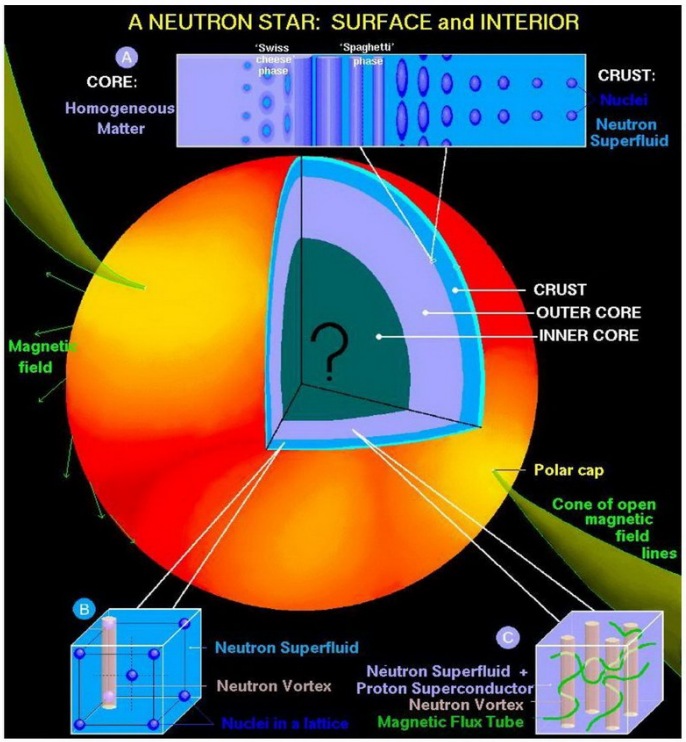

不同的核态方程对应的不同的中子星质量、半径关系

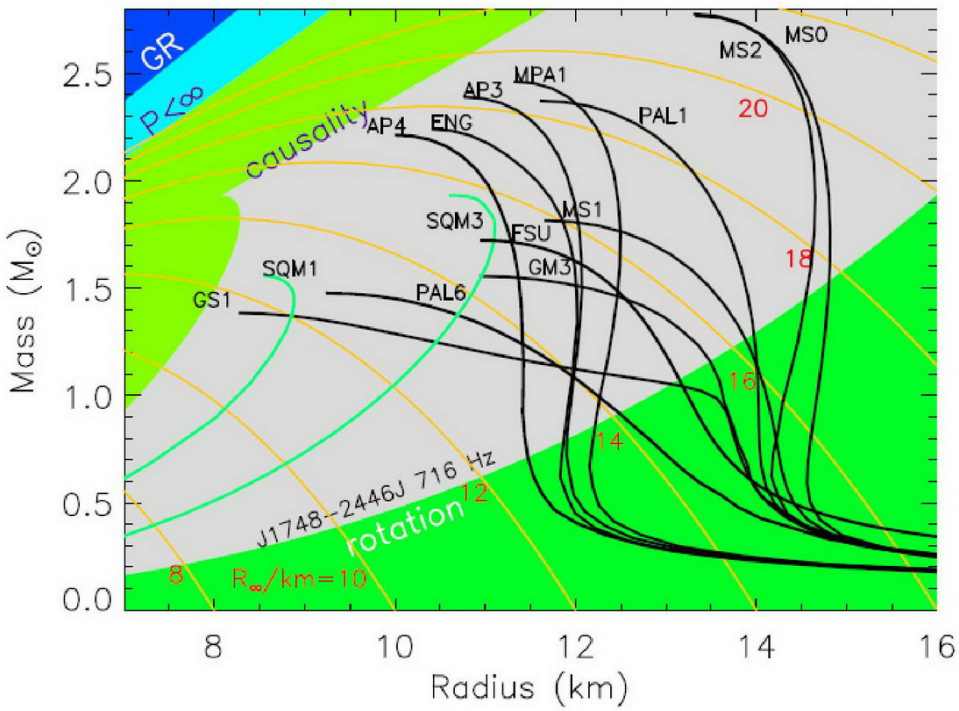

H. Huber et al, Phys. Rev. C 50 (1994) 1287 (R).
J.M. Lattimer, M. Prakash, Phys. Rep. 621 (2016) 127.

- ☆ 中子皮与中子擦去截面
- ☆ 中子皮与轻粒子产额比
- ☆ 中子皮与弹核碎裂反应 (同位旋标度现象等)
- ☆ 中子皮与集团结构
- ☆ 中子皮与核表面张力
- ☆ 中子皮与核温度
- ☆ 高能重离子碰撞中的中子皮效应

同位旋相关的量子分子动力学模型 (IQMD)

- Quantum molecular dynamics (QMD) with the isospin factor and many important quantum features included, e.g. Pauli blocking.
- The nucleons are treated as a Gaussian wave packet

$$f_i(\vec{r},\vec{p},t)=\frac{1}{\pi^3\hbar^3}\mathrm{e}^{-(\vec{r}-\vec{r}_i(t))^2\frac{2}{L}}\mathrm{e}^{-(\vec{p}-\vec{p}_i(t))^2\frac{L}{2\hbar^2}}$$

- The evolution of every single nucleon follows the Hamilton canonical equation

$$\dot{\vec{r}}=\frac{\partial H}{\partial\vec{p}},\dot{\vec{p}}=-\frac{\partial H}{\partial\vec{r}}$$

- The effective potential can be written as 4 parts:

$$U(\rho)=U_{\mathrm{Sky}}+U_{\mathrm{Coul}}+U_{\mathrm{Yuk}}+U_{\mathrm{sym}}$$

- IQMD distinguish n,p in simulation, could give us detailed phase space information both on the nucleon and fragments
- Construct fragments after freezing-out by the coalescence method

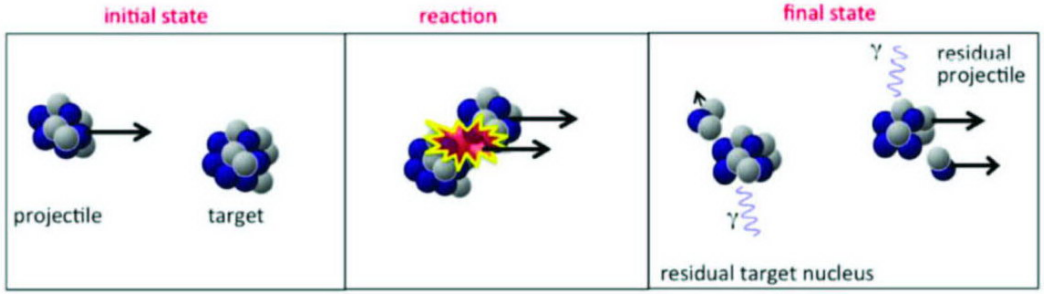

统计擦碎模型 (Statistical Abrasion-Ablation, SAA)

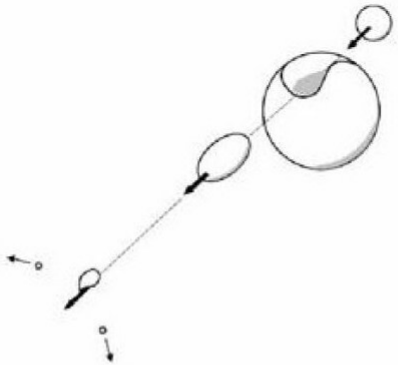

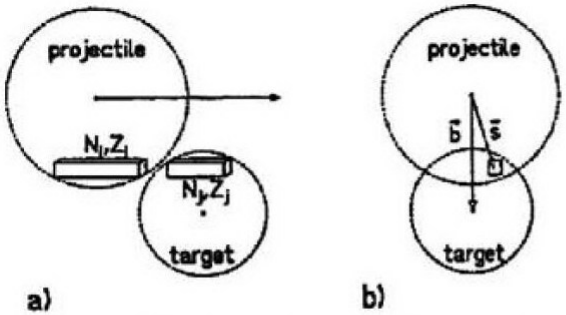

Schematic view of two nuclei collision in straight-line geometry.
a)Side view of a peripheral collision via collisions of tube pairs;
b)Seen in beam direction, the vectors s and b are defined in the plane perpendicular to the beam.

T. Brohm, K.H. Schmidt, NPA**569**(1994)821.

Transmission probability for an incident nucleon (k=n for neutron, k=p for proton)

$$t_{j,k} = \exp\left(-\frac{1}{F}(N_j\sigma_{nk} + Z_j\sigma_{pk})\right)$$

Average number of nucleons removed in a collision of tube pairs

$$< \Delta A_i >= N_i(1 - t_{j,n})) + Z_i(1 - t_{j,p}) =< \Delta N_i > + < \Delta Z_i >$$

Binomial distributions are assumed for $< \Delta N_i >$ and $< \Delta Z_i >$. The total number of removed nucleons in a collision at a given impact parameter is obtained by the sum of the above equation.

- **Abrasion stage:**

  Prefragment with the mass and charge numbers determined by the statistical abrasion method, the excitation energy given by the hole-energy model (13.3 MeV per hole, J.-J. Gaimard, K.-H. Schmidt, NPA**531**(1991)109.)

- **Ablation stage:**

  Final fragment after the deexcitation process using the conventional statistical evaporation model

模型中的密度分布

sity distribution in Droplet
lel:

$$= \frac{\rho_i^0}{1+\exp(\frac{r-C_i}{f_i t_i/4.4})}, i = n, p$$

cting condition: RMS radius,
ng energy and δ_{np}.

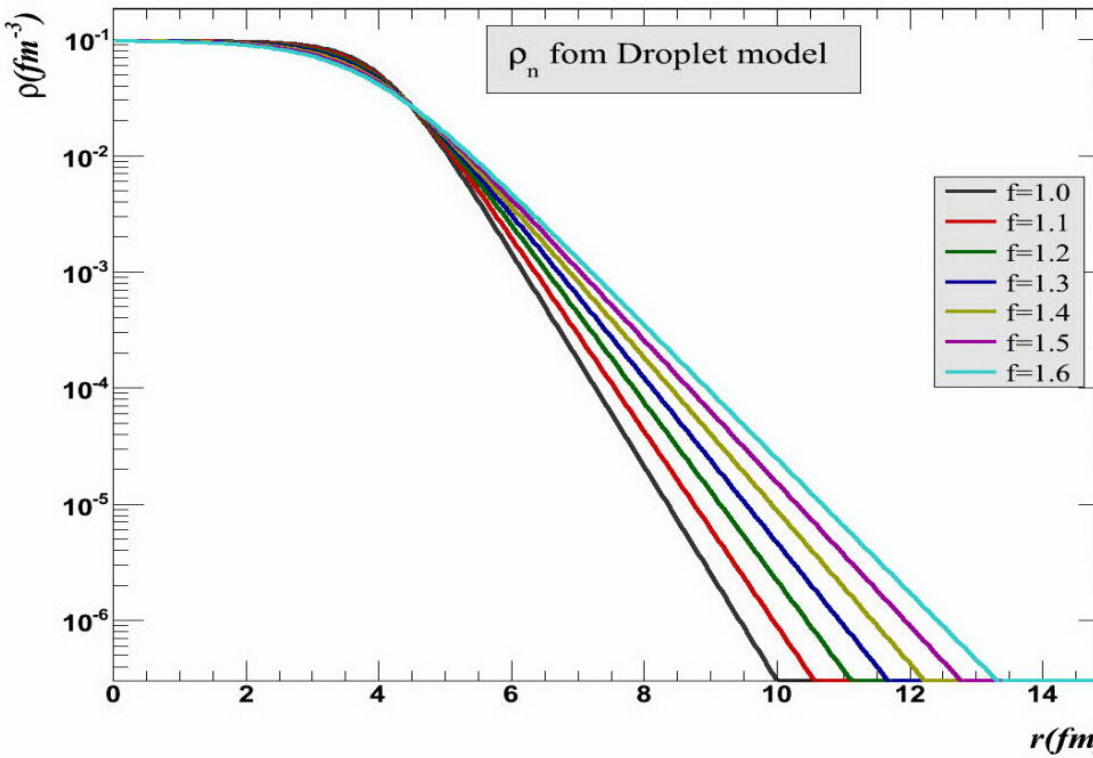

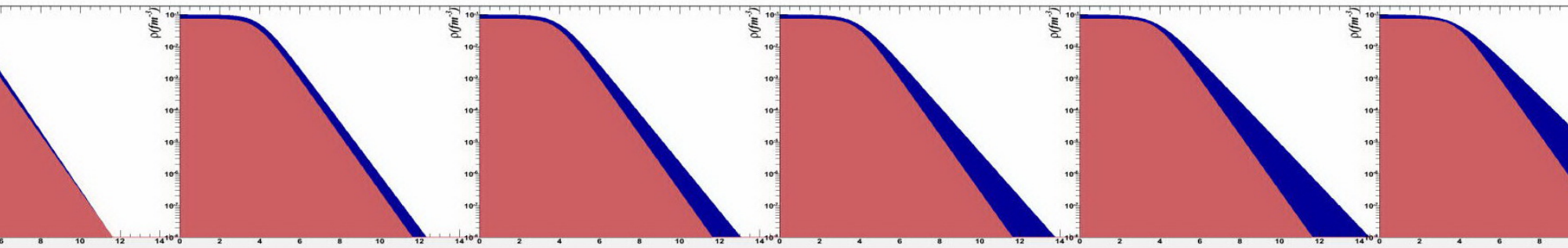

IQMD 模型计算的同位素分布

Z. T. Dai, D. Q. Fang et al., Phys. Rev. C 91 (2015) 034618

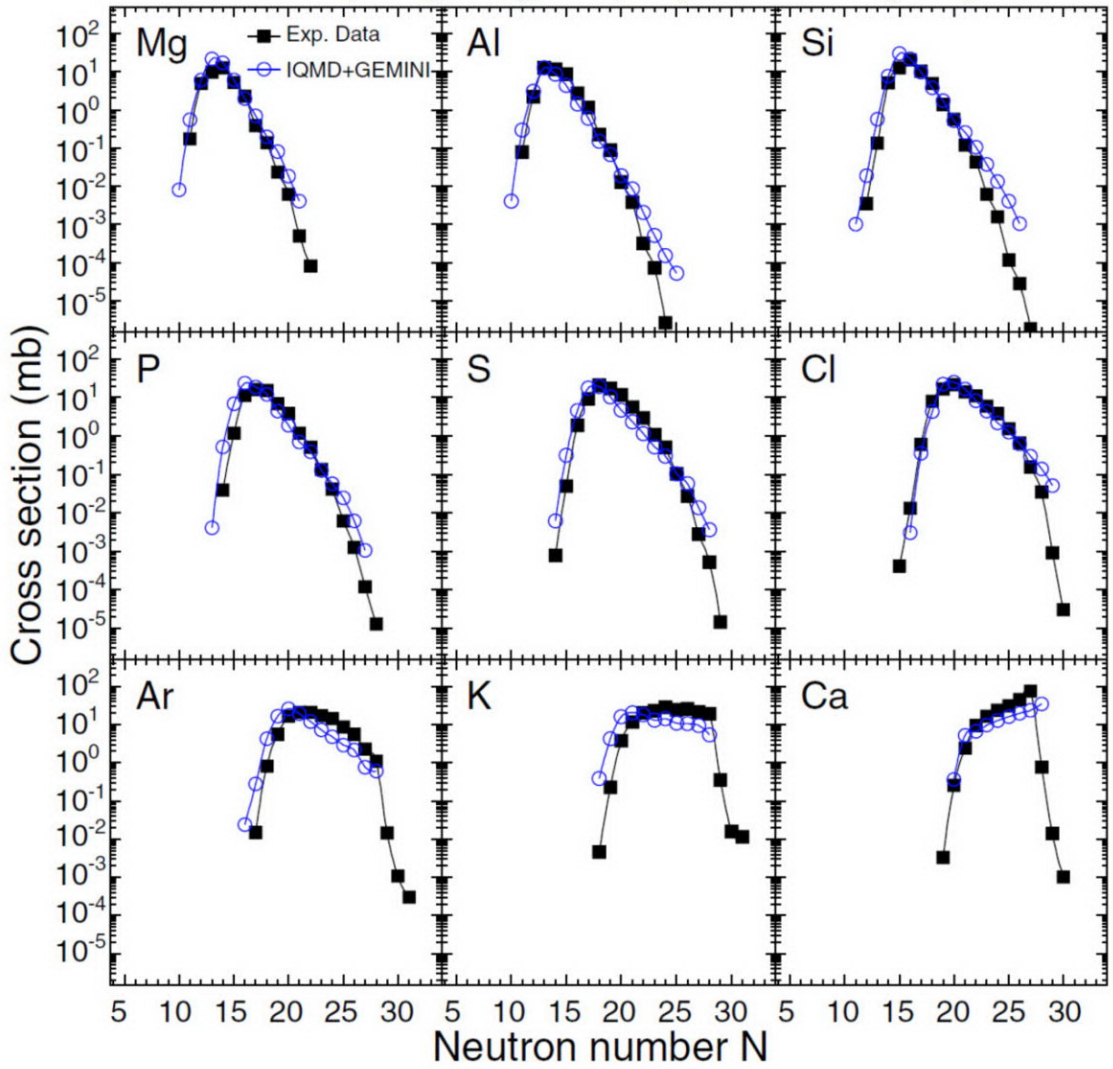

FIG. 3. (Color online) Isotopic distributions as a function of neutron number N for elements with $12 \leqslant Z \leqslant 20$ in 140 MeV/nucleon ^{48}Ca+^{9}Be. Solid squares are the experimental data from Ref. [47], and open circles are the calculated results with IQMD plus GEMINI.

SAA 模型计算的同位素分布

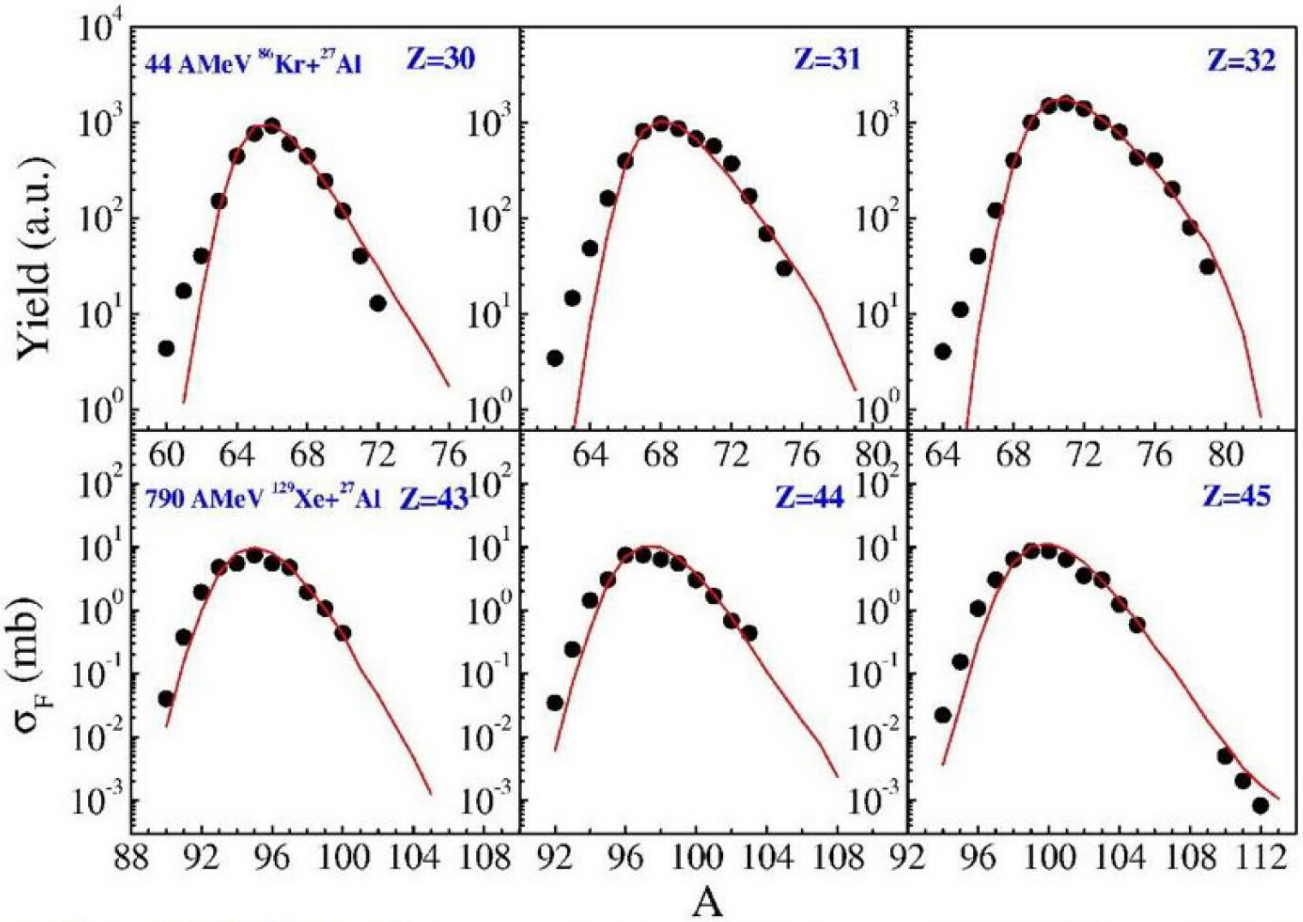

The experimental data (Upper panels from D. Bazin *et al.*, NPA**515**(1990)349; lower panels from J. Reinhold *et al.*, PRC**58**(1998)247) can be well reproduced by the SAA model.

D. Q. Fang et al., Phys. Rev. C 61 (2000) 044610;
Eur. Phys. J. A 10 (2001) 381; J. Phys. G 34 (2007) 2173

中子皮与中子擦去截面 (SAA)

$$\sigma_{-N} = \sum_{i=1}^{N} \sigma(i,0), \qquad \sigma(\Delta N, \Delta Z) = \int d^2b P(\Delta N, b) P(\Delta Z, b),$$

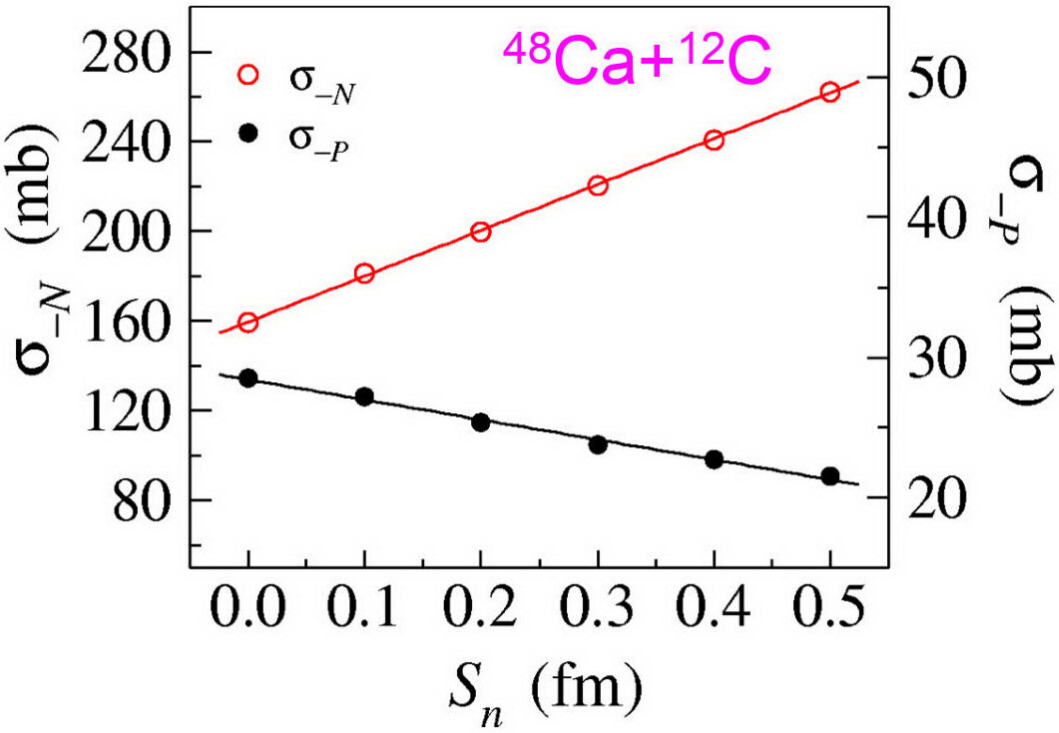

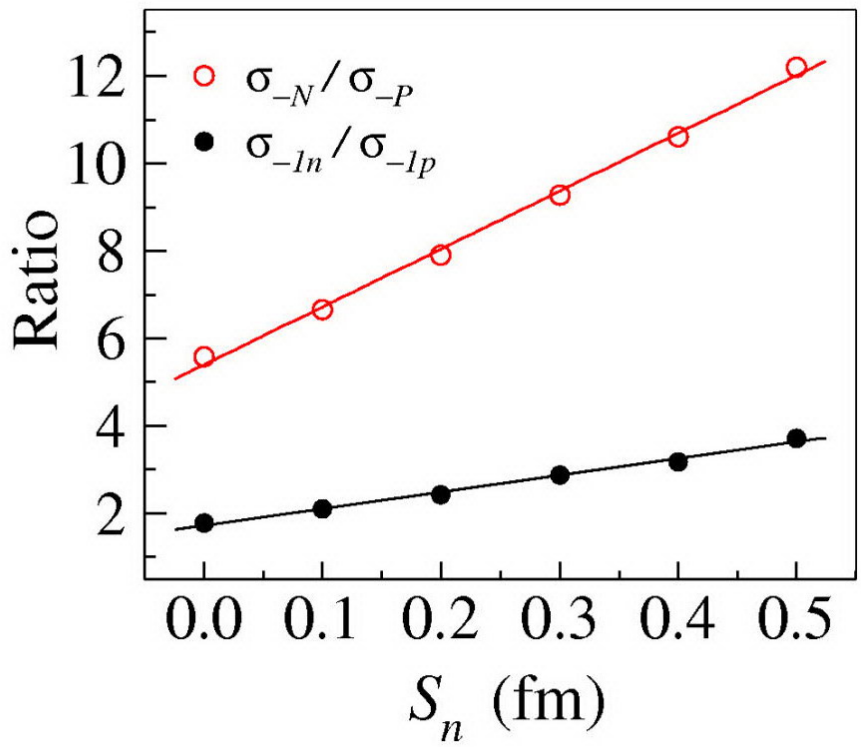

D. Q. Fang et al., Phys. Rev. C 81 (2010) 047603;
Chin. Phys. Lett 28 (2011) 102102.

中子皮与中子擦去截面

PRL 119, 262501 (2017) PHYSICAL REVIEW LETTERS week ending 29 DECEMBER 2017

Peeling Off Neutron Skins from Neutron-Rich Nuclei: Constraints on the Symmetry Energy from Neutron-Removal Cross Sections

T. Aumann,[1,2,*] C. A. Bertulani,[3,1] F. Schindler,[1] and S. Typel[1,2]
[1]*Institut für Kernphysik, Technische Universität Darmstadt, Schlossgartenstraße 9, D-64289 Darmstadt, Germany*
[2]*GSI Helmholtzzentrum für Schwerionenforschung, Planckstraße 1, D-64291 Darmstadt, Germany*
[3]*Department of Physics and Astronomy, Texas A&M University-Commerce, Commerce, Texas 75429-3011, USA*
(Received 30 September 2017; published 28 December 2017)

An experimentally constrained equation of state of neutron-rich matter is fundamental for the physics of nuclei and the astrophysics of neutron stars, mergers, core-collapse supernova explosions, and the synthesis of heavy elements. To this end, we investigate the potential of constraining the density dependence of the symmetry energy close to saturation density through measurements of neutron-removal cross sections in high-energy nuclear collisions of 0.4 to 1 GeV/nucleon. We show that the sensitivity of the total neutron-removal cross section is high enough so that the required accuracy can be reached experimentally with the recent developments of new detection techniques. We quantify two crucial points to minimize the model

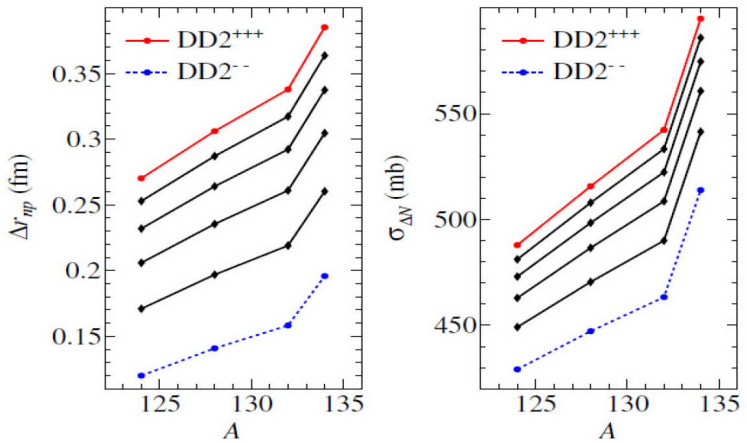

FIG. 2. Neutron-skin thickness Δr_{np} (left) and corresponding neutron-removal cross sections $\sigma_{\Delta N}$ (right) for Sn isotopes as

中子擦碎截面敏感于中子皮厚度的类似结论，并可用于约束对称能

中子皮与轻粒子产额比 (IQMD)

X. Y. Sun, D. Q. Fang, Y. G. Ma et al., PLB 682 (2010) 396.

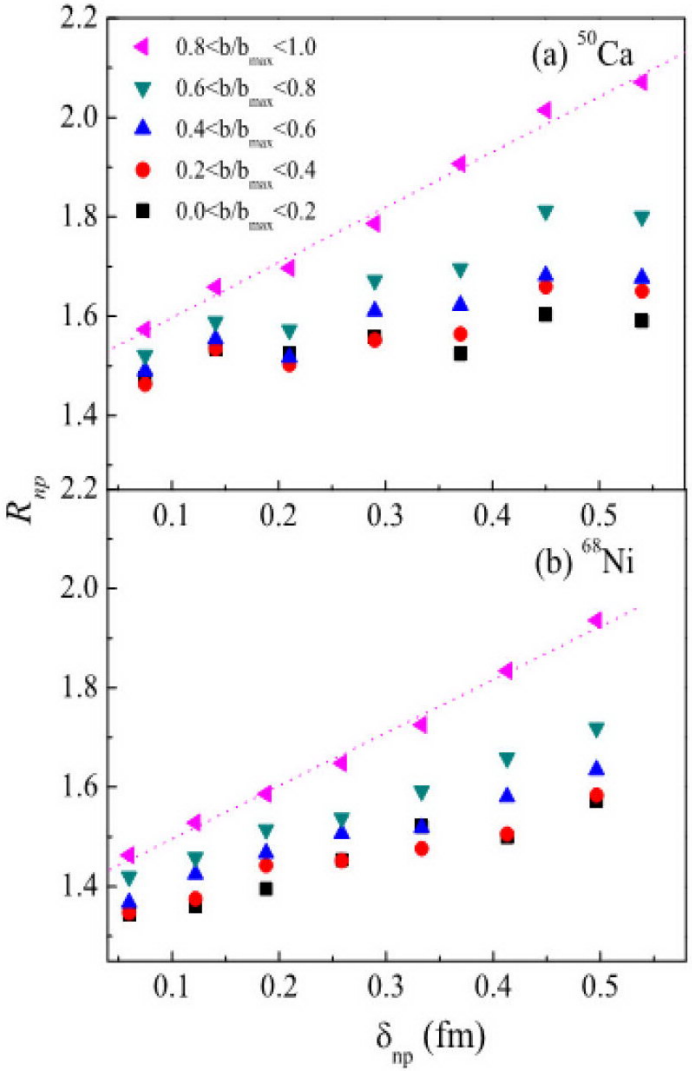

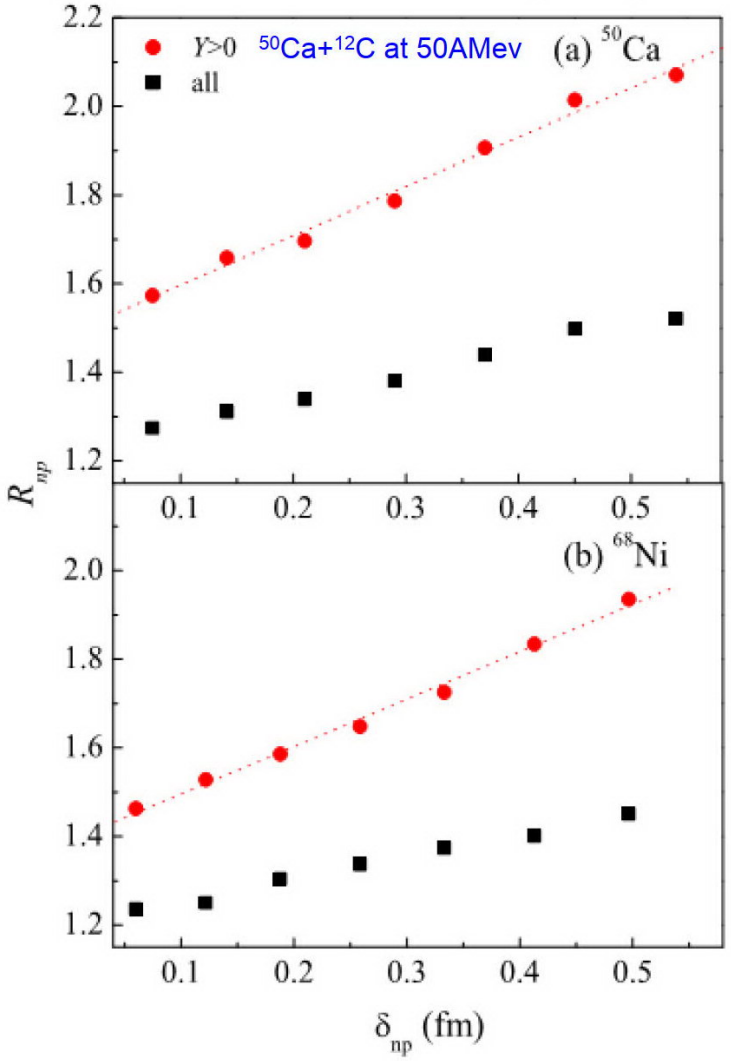

Strong correlation between R_{np} and neutron skin thickness

中子皮与轻粒子产额比 (IQMD)

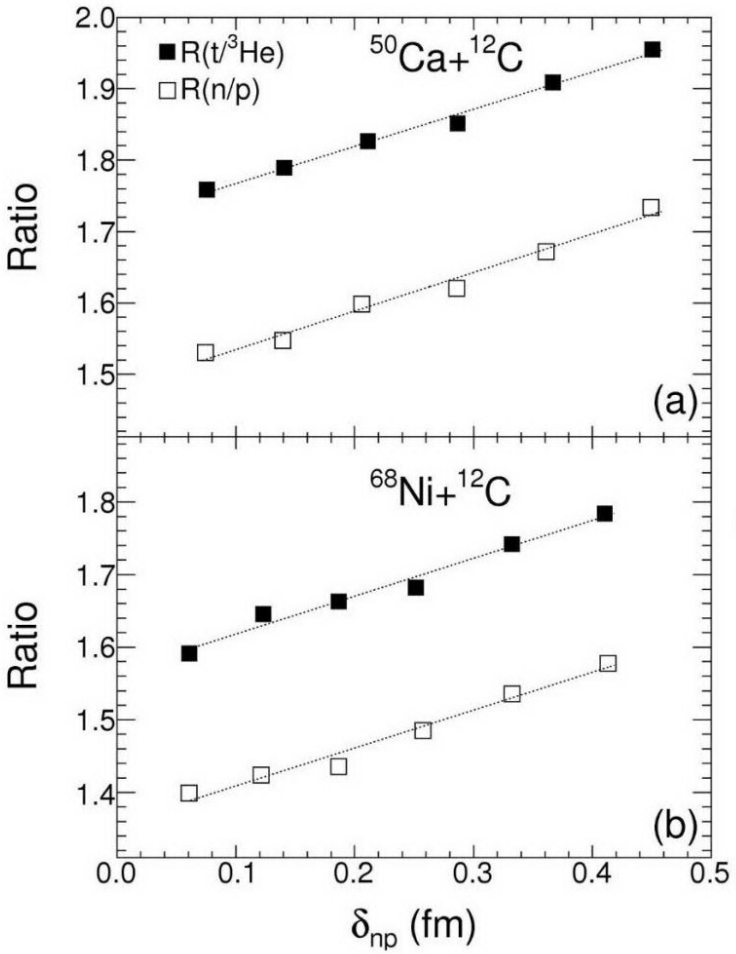

Z. T. Dai, D. Q. Fang et al., Phys. Rev. C 89 (2014) 014613

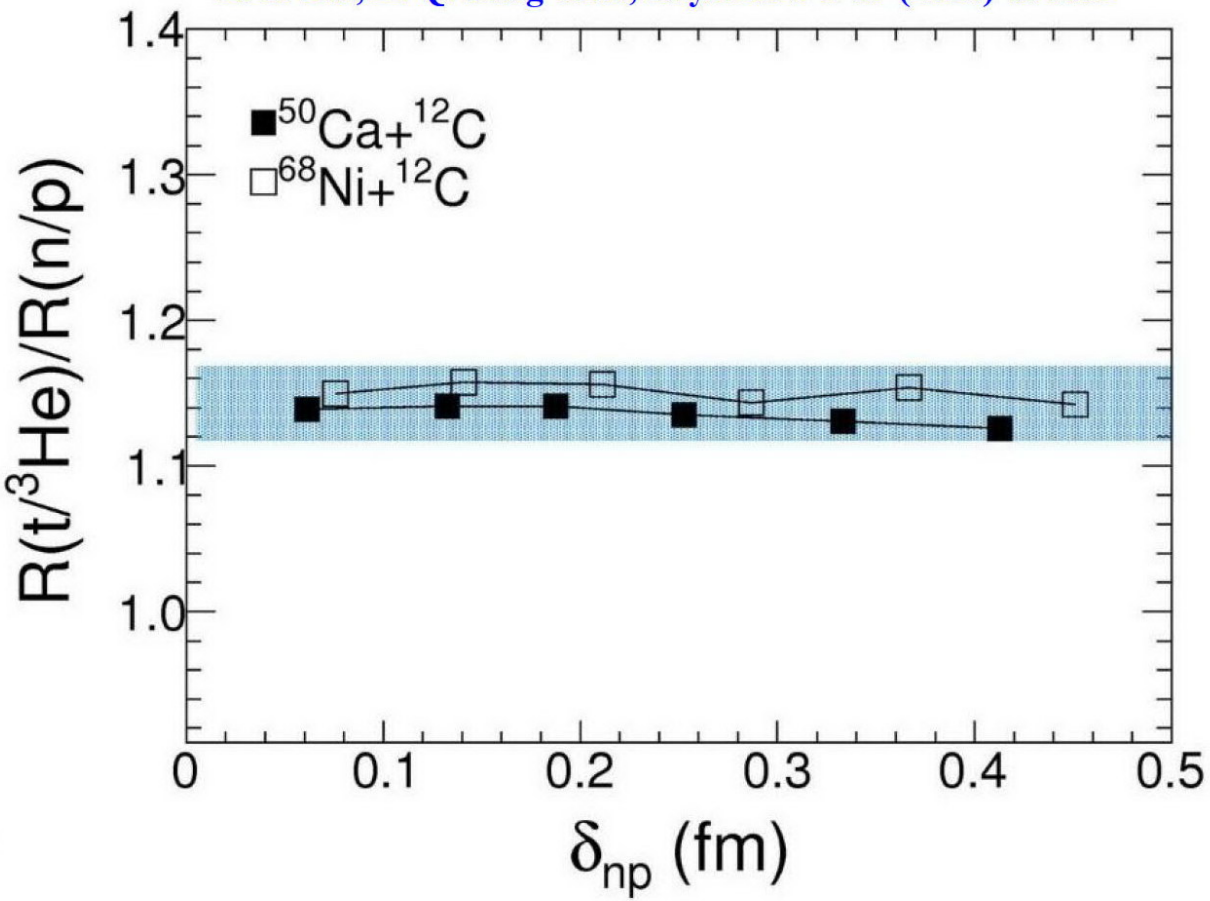

Correlation between t/³He and neutron skin thickness

中子皮与轻粒子产额比 (IQMD)

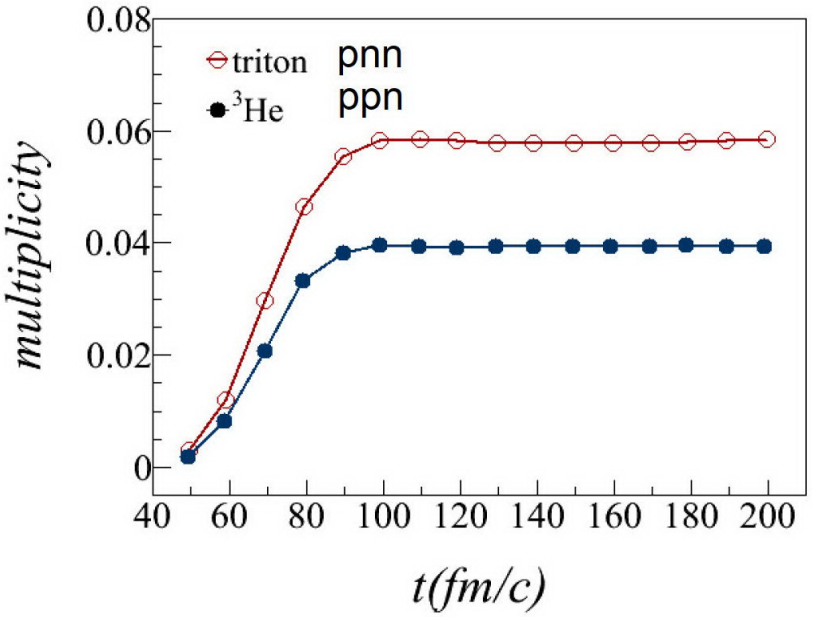

Time evolution of multiplicities for triton and ^{3}He under the condition of reduced impact parameter from 0.6 to 1.0 and Y>0 for ^{68}Ni+^{12}C at 50 A MeV

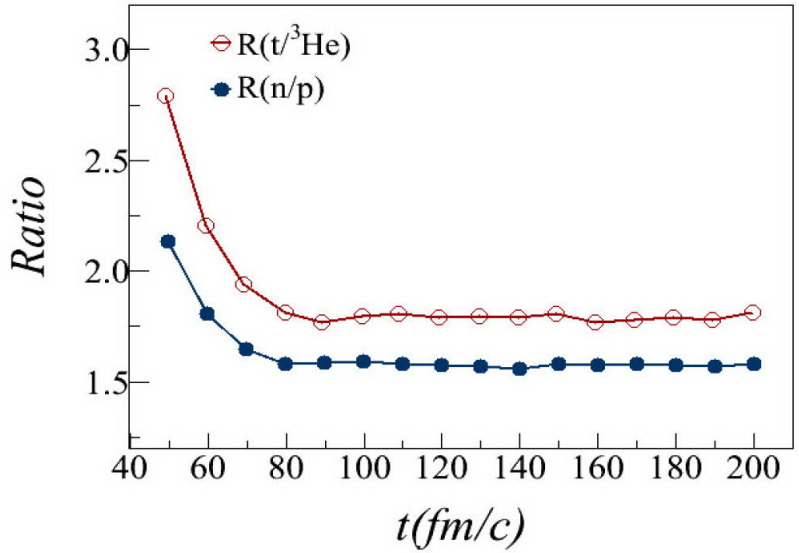

Time evolution of R(n/p) and R(t/^{3}He) under the condition of reduced impact parameter from 0.6 to 1.0 and Y>0 for ^{68}Ni+^{12}C at 50 A MeV.

中子皮与弹核碎裂反应

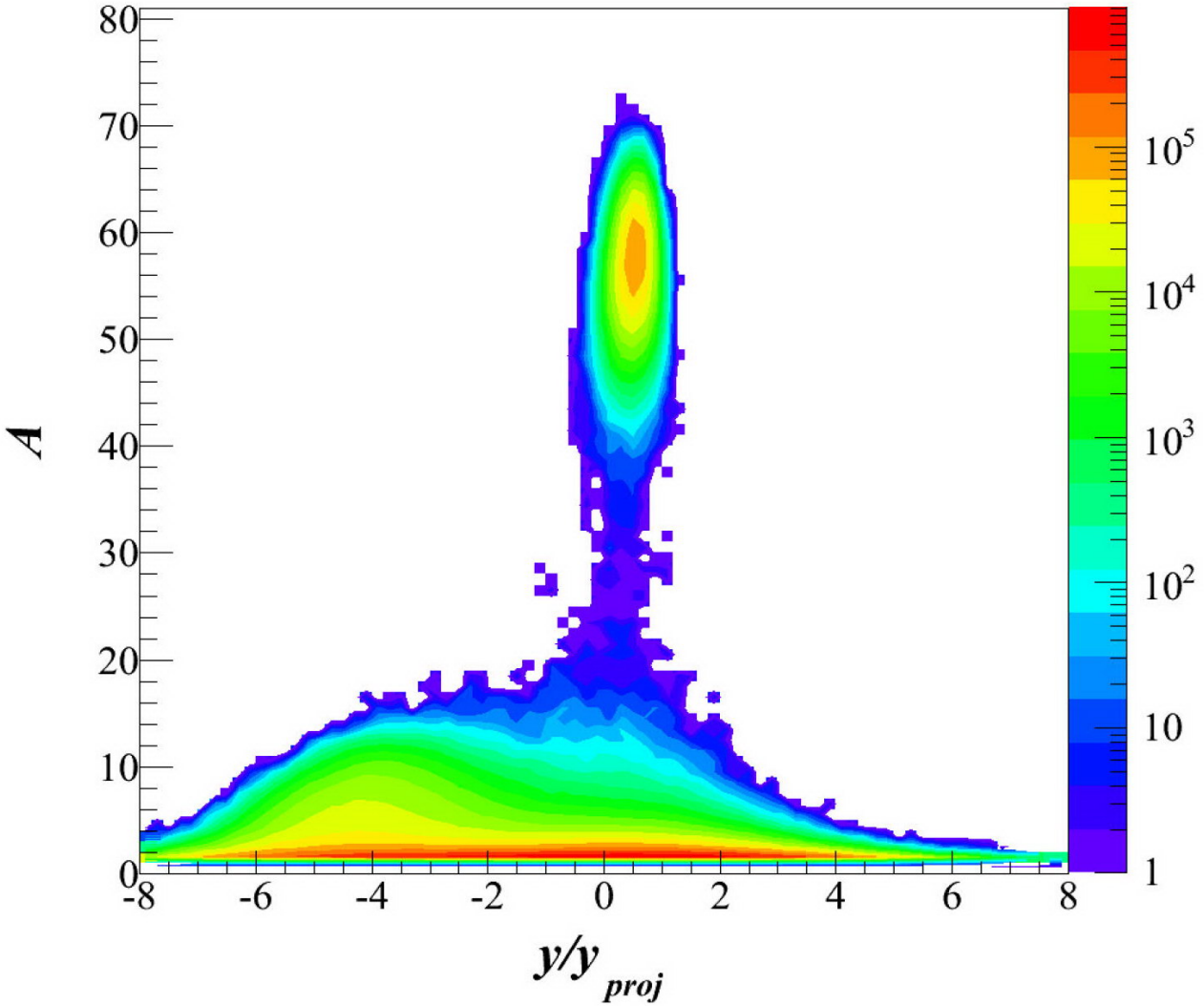

The multiplicities of fragment with different mass numbers under the condition of reduced impact parameter from 0.6 to 1.0 and Y>0 for $^{68}Ni+^{12}C$ at 50 A MeV.

同位旋标度现象

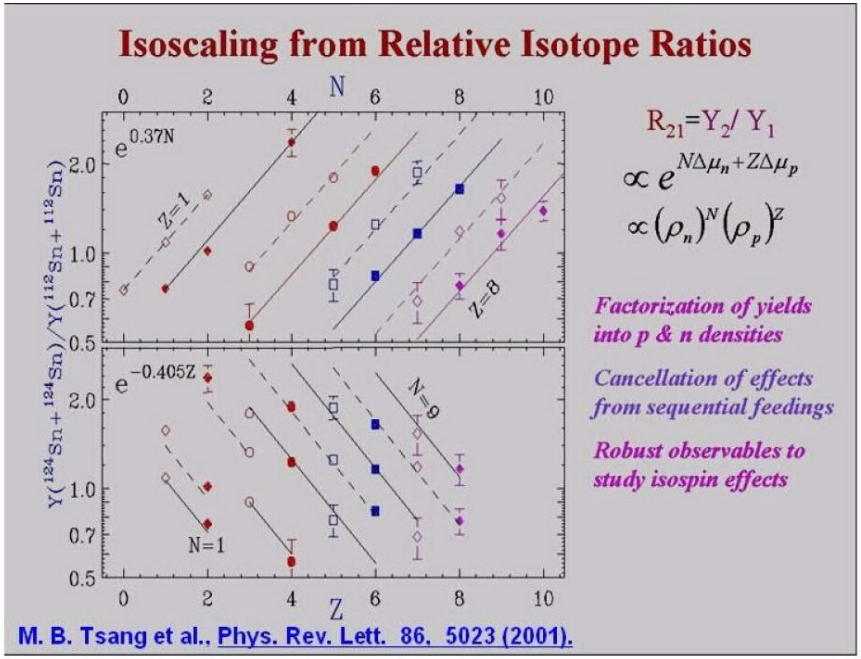

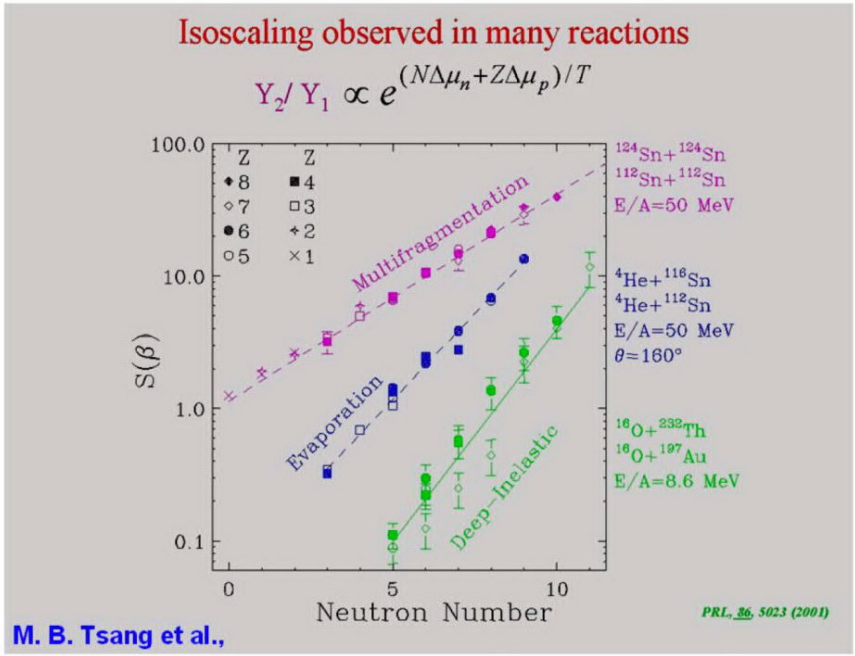

Isoscaling is the property that the ratio of fragment yields from similar but isotopically different reactions has a exponential dependence on N and Z:

$$R_{21}(N,Z)=\frac{Y_2(N,Z)}{Y_1(N,Z)}=C\exp(\alpha N+\beta Z),$$

$$\alpha=\frac{4C_{\rm sym}}{T}\Delta[(\frac{Z}{A})^2]=\frac{4C_{\rm sym}}{T}[(\frac{Z}{A})_1^2-(\frac{Z}{A})_2^2]$$

$$\beta=\frac{4C_{\rm sym}}{T}\Delta[(\frac{N}{A})^2]=\frac{4C_{\rm sym}}{T}[(\frac{N}{A})_1^2-(\frac{N}{A})_2^2]$$

同位旋标度现象

PRL 94, 162701 (2005) PHYSICAL REVIEW LETTERS week ending 29 APRIL 2005

Isotopic Scaling and the Symmetry Energy in Spectator Fragmentation

$$E_{\mathrm{sym}} = \tilde{\gamma}(A - 2Z)^2/A$$

$$\alpha T = \Delta\mu_n = \mu_{n,2} - \mu_{n,1} \approx 4\gamma\left(\frac{Z_1^2}{A_1^2} - \frac{Z_2^2}{A_2^2}\right)$$

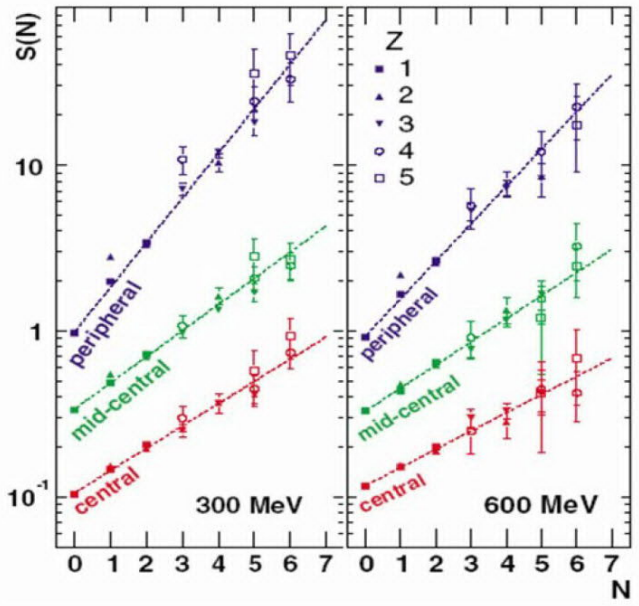

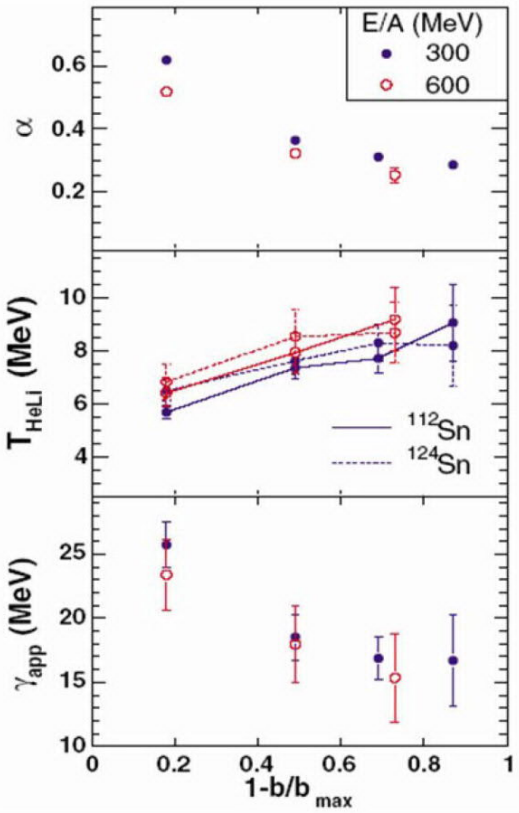

The isoscaling approach has become an important method in heavy ion collisions since it can isolate the nuclear symmetry energy in the fragment yields.

同位旋标度现象

SAA模型

^{36,40}Ar
^{40,48}Ca
^{58,60}Ni
^{78,86}Kr
^{112,124}Sn
^{129,136}Xe
$\Big\}$ + ^{112}Sn

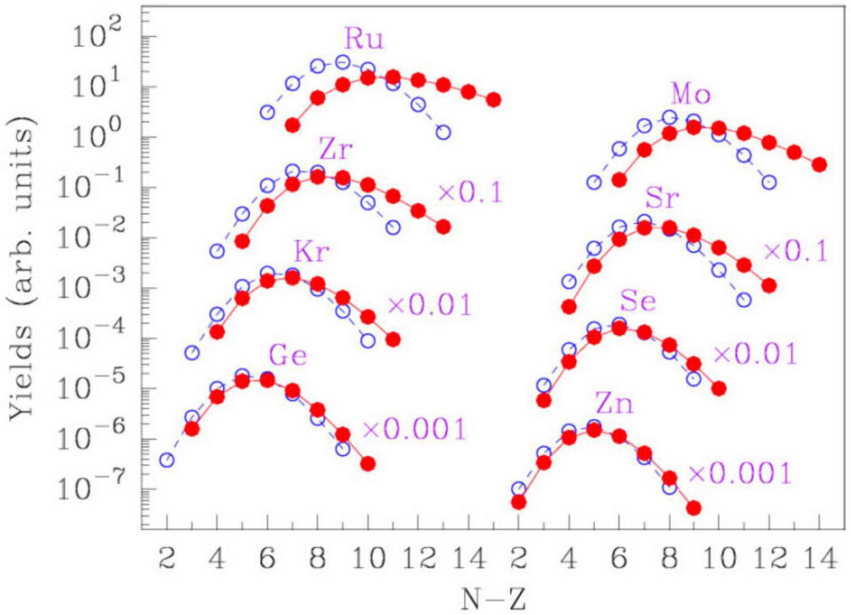

^{112,124}Sn+^{112}Sn at 60A MeV

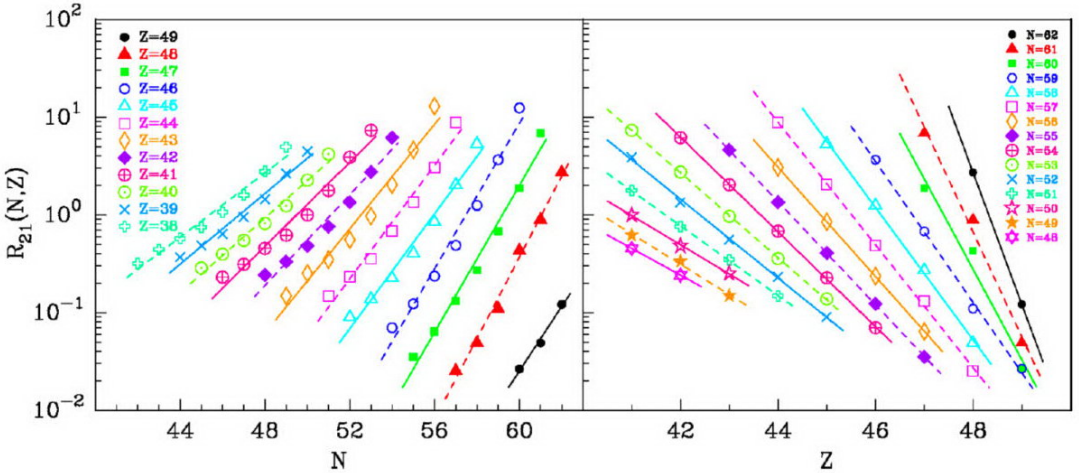

^{112,124}Sn+^{112}Sn

同位旋标度现象

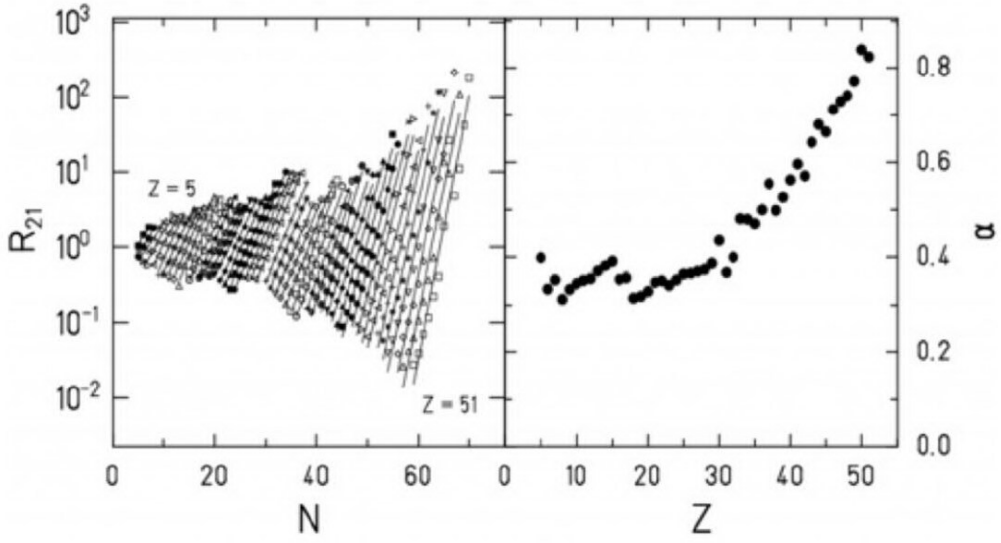

FRS data: ^{124,136}Xe+Pb at 1A GeV

D. Henzlova et al., arXiv:nucl-ex/0507003

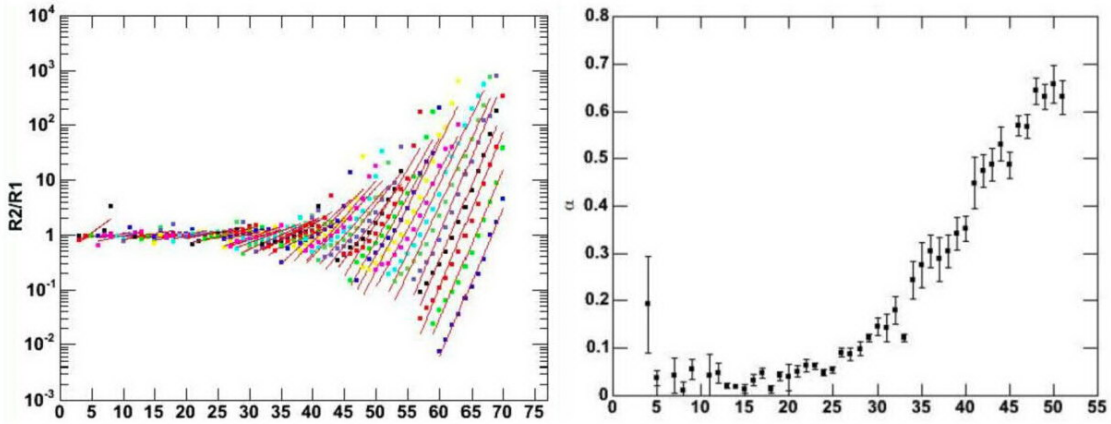

SAA calculation: ^{124,136}Xe+Pb at 1A GeV

同位旋标度现象

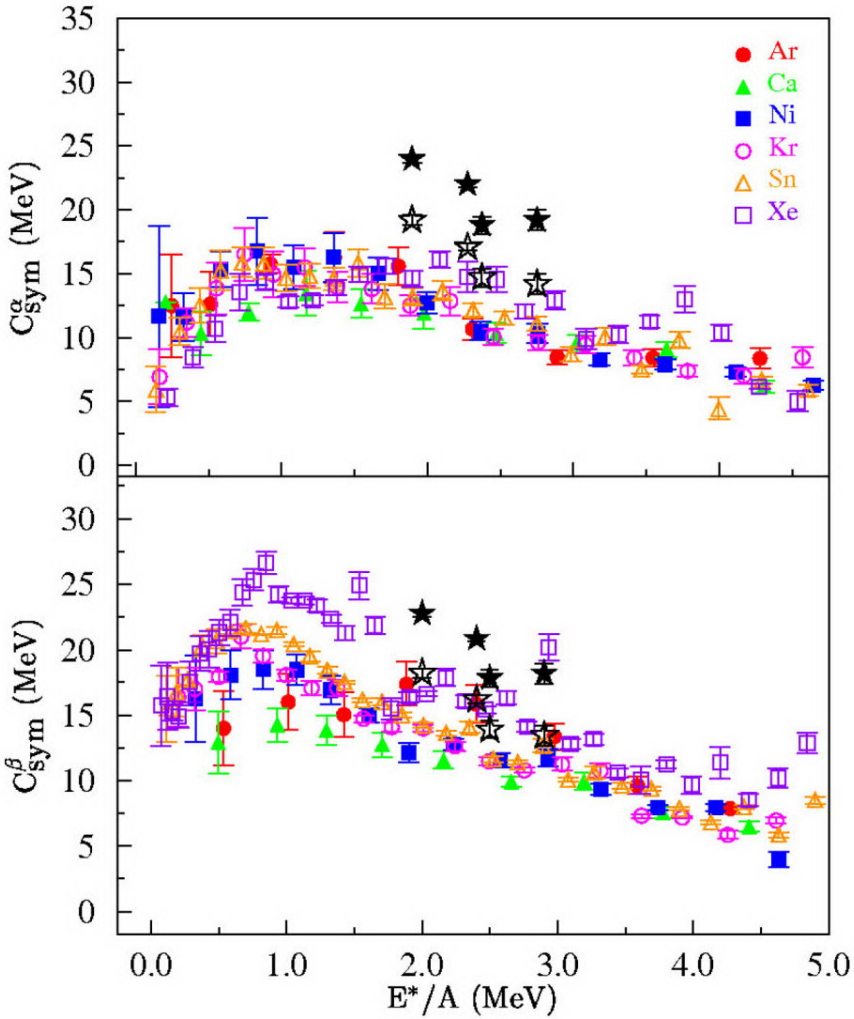

$$E^*/A = \frac{1}{a}T^2 \ (a \sim 10)$$

$$\begin{cases} \alpha = \frac{4C_{\rm sym}}{T}\left[\left(\frac{Z}{A}\right)_1^2 - \left(\frac{Z}{A}\right)_2^2\right] \\ \beta = \frac{4C_{\rm sym}}{T}\left[\left(\frac{N}{A}\right)_1^2 - \left(\frac{N}{A}\right)_2^2\right] \end{cases}$$

G. A. Souliotis *et al.*,
Phys. Rev. C **73**, 024606 (2006).

Q. M. Su, D. Q. Fang, Y. G. Ma *et al.*, Int. J. Mod. Phys. **15**, 1803 (2006).

D. Q. Fang, Y. G. Ma *et al.*, J. Phys. G **34**, 2173 (2007).

中子皮与同位旋标度现象 (IQMD)

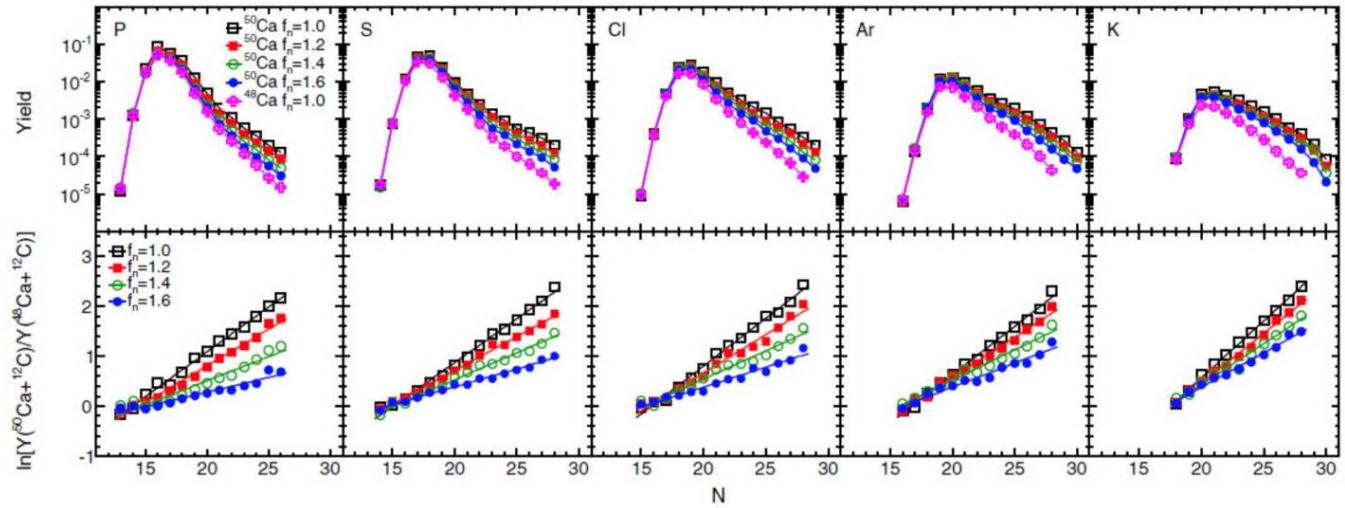

FIG. 4. (Color online) Isotopic yield per event as a function of the neutron number N with the charge number of fragment varying from 15 to 19 in ^{50}Ca+^{12}C and ^{48}Ca+^{12}C at 50 MeV/nucleon (upper row). The related isotopic yield ratios of the two reactions as functions of N are displayed in the lower row. In the calculations, f_n is varied from 1.0 to 1.6 for ^{50}Ca+^{12}C, while it is 1.0 for ^{48}Ca+^{12}C.

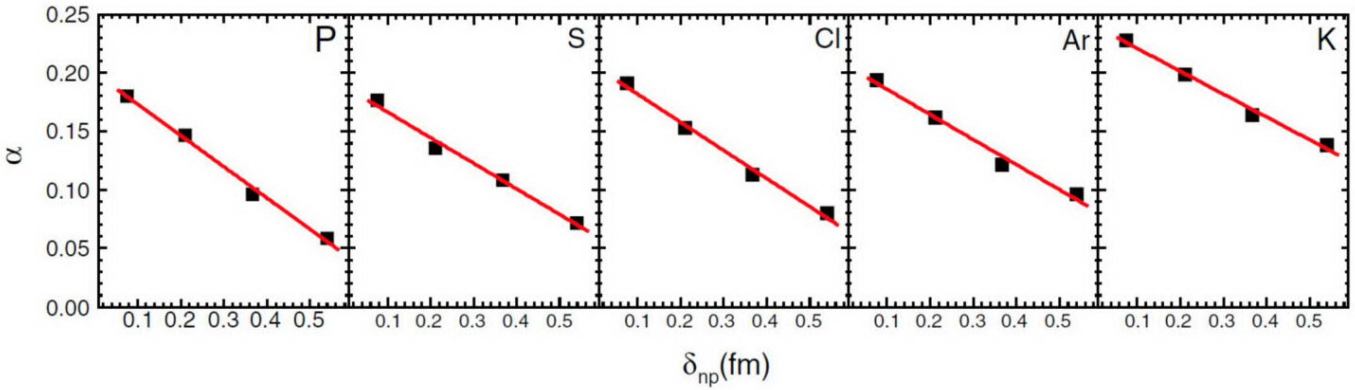

FIG. 5. (Color online) Isoscaling parameter α as a function of δ_{np} for fragments with the charge number varying from 15 to 19 in 50 MeV/nucleon ^{50}Ca+^{12}C.

Z. T. Dai, D. Q. Fang et al., Phys. Rev. C 91 (2015) 034618

中子皮与中子星、碎裂反应

PHYSICAL REVIEW C **100**, 015802 (2019)

Neutron skins as laboratory constraints on properties of neutron stars and on what we can learn from heavy ion fragmentation reactions

C. A. Bertulani[1,2] and J. Valencia[1]

[1]*Department of Physics and Astronomy, Texas A&M University-Commerce, Commerce, Texas 75429-3011, USA*

[2]*Institut für Kernphysik, Technische Universität Darmstadt, D-64289 Darmstadt, Germany*

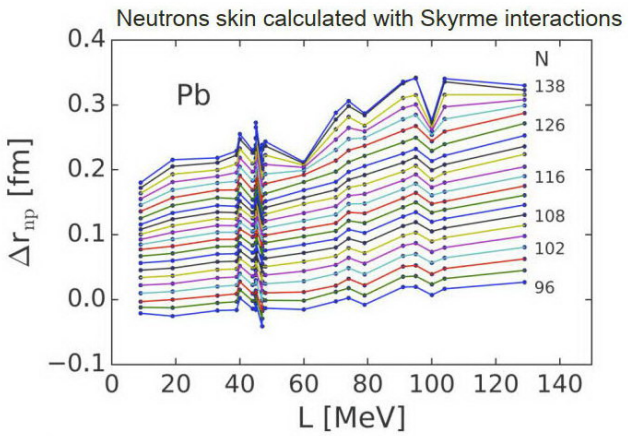

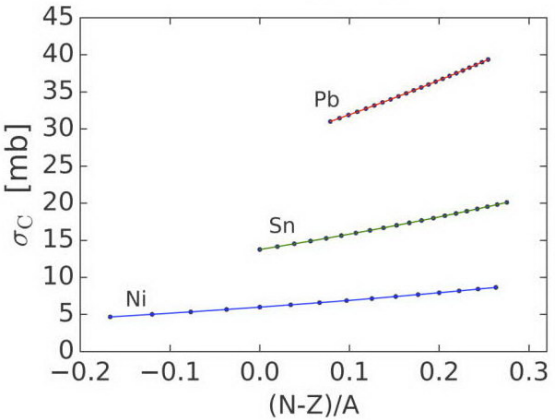

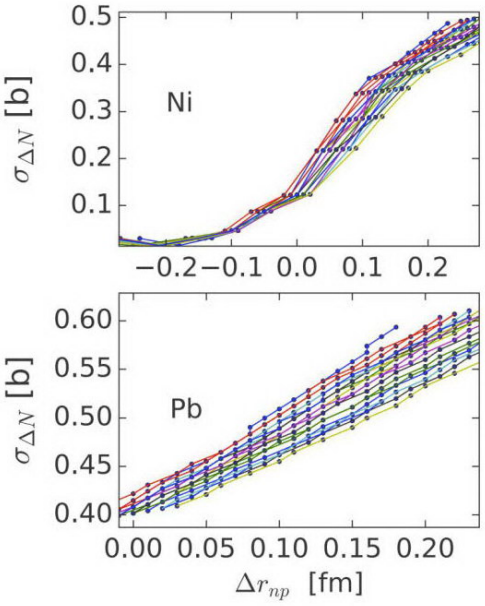

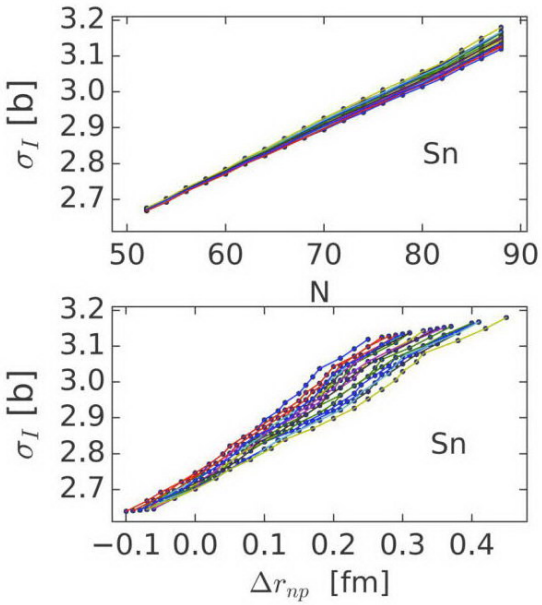

slope parameter of the symmetry energy. In this article, we explore a particular set of reactions using high-energy ($E_{\rm lab} \sim 1$ GeV/nucleon) neutron-rich projectiles. We explore measurements of all reaction fragments (a) in the same isotopic chain, i.e., only by removal of neutrons, (b) in all charge-changing channels, and (c) total interaction cross sections. Using Hartree-Fock-Bogoliubov (HBF) predictions for neutron and proton densities with Skyrme interactions, we explore the sensitivity of these cross sections with the neutron skin in nuclei.

中子皮与集团结构

Eur. Phys. J. A (2021) 57:157
https://doi.org/10.1140/epja/s10050-021-00465-0

THE EUROPEAN PHYSICAL JOURNAL A

α clustering and neutron-skin thickness of carbon isotopes

Q. Zhao[1], Y. Suzuki[2], J. He[2], B. Zhou[2,3], M. Kimura[1,2,4,a]

[1] Nuclear Reaction Data Centre (JCPRG), Hokkaido University, Sapporo 060-0810, Japan
[2] Department of Physics, Hokkaido University, Sapporo 060-0810, Japan
[3] Institute of Modern Physics, Fudan University, Shanghai 200433, China
[4] Research Center for Nuclear Physics (RCNP), Osaka University, Ibaraki 567-0047, Japan

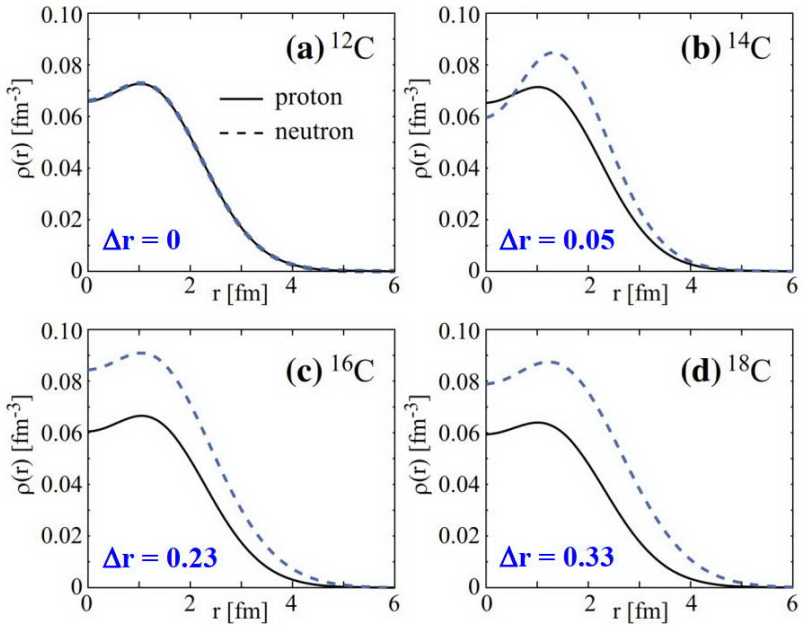

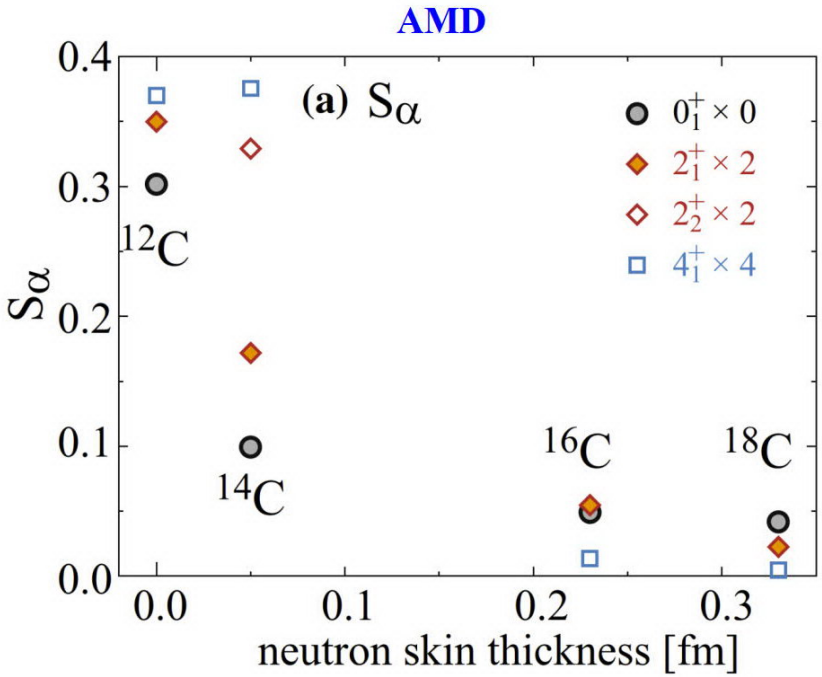

The growth of the neutron skin seems to suppress the α clustering of C isotopes similarly to those observed in Sn isotopes.

中子皮与集团结构

NUCL SCI TECH (2017) 28:22
DOI 10.1007/s41365-016-0174-7

Exploring the sensitivity of α-decay half-life to neutron skin thickness for nuclei around ^{208}Pb

Niu Wan[1] · Chang Xu[1] · Zhong-Zhou Ren[1,2]

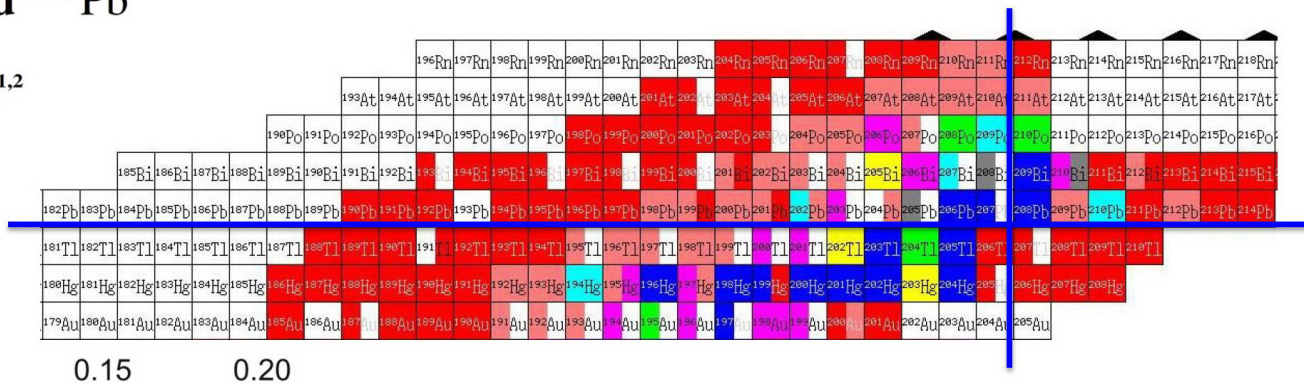

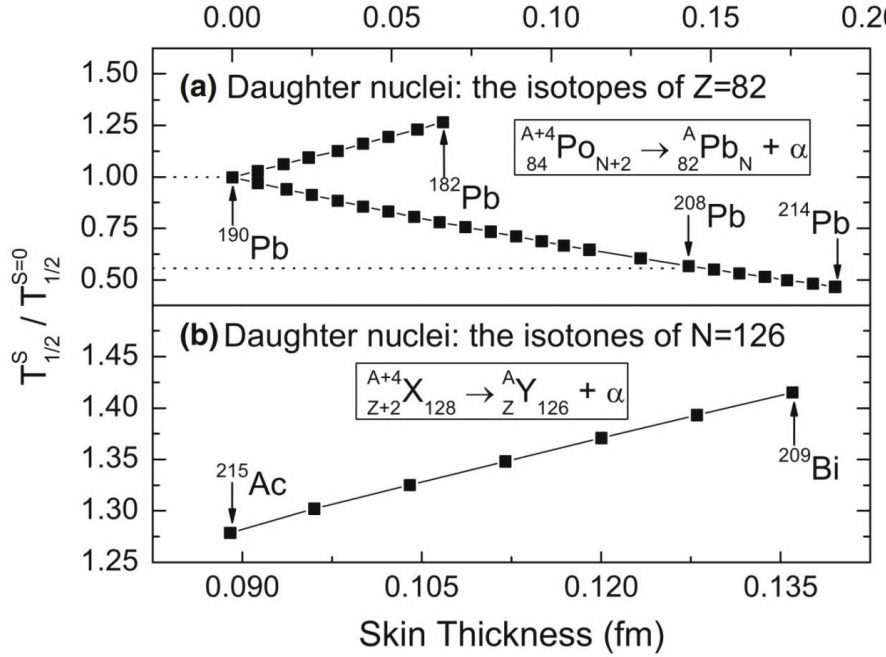

and isotones of $N_d = 126$. From the numerical results, we find there is a close correlation between α-decay half-life and nuclear skin thickness, and the former one can be changed by a factor from 0.466 to 1.415. So it is necessary to consider the skin thickness for investigations on α-decay half-lives, and it could be a possible way to extract nuclear skin thickness from measured α-decay half-lives.

中子皮与集团结构

PHYSICAL REVIEW C **96**, 054328 (2017)

Correlation between observed α decays and changes in neutron or proton skins from parent to daughter nuclei

W. M. Seif,[1,*] N. V. Antonenko,[2,3] G. G. Adamian,[2] and Hisham Anwer[1,4]
[1]*Cairo University, Faculty of Science, Department of Physics, 12613 Giza, Egypt*
[2]*Joint Institute for Nuclear Research, 141980 Dubna, Russia*
[3]*Mathematical Physics Department, Tomsk Polytechnic University, 634050 Tomsk, Russia*
[4]*Physics Department, Zewail City of Science and Technology, Egypt*
(Received 21 August 2017; published 29 November 2017)

The change of proton and neutron skin thicknesses is investigated in nuclei after α decay. The skin thicknesses are self-consistently calculated. The observed α decays lead to relatively large decrease of the proton skin in the daughter nuclei. A large increase of the neutron skin in the daughter nucleus reflects the hindered α decay. This hindrance is related to the decrease of both the Q_α value and the preformation probability in the parent nucleus. For each isotopic chain, the observed half-lives consistently correlate with the change of the proton (neutron) skin thickness, from parent to daughter nuclei.

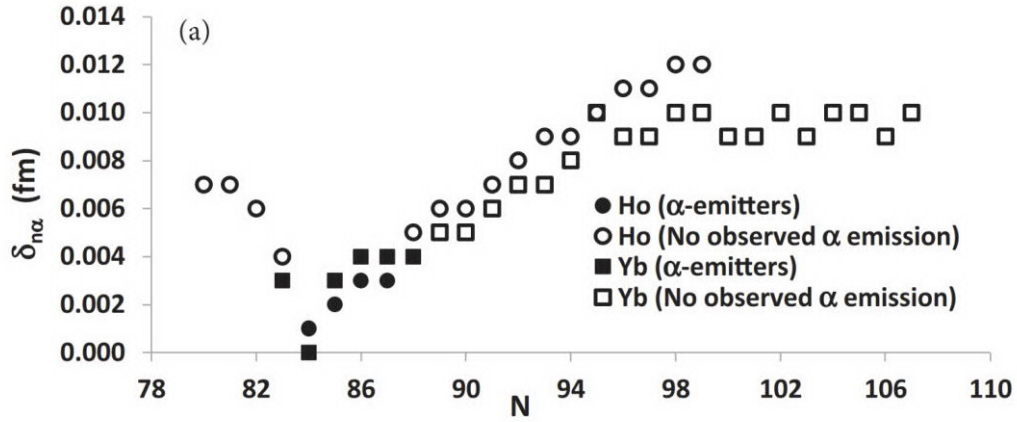

中子皮与核表面

PHYSICAL REVIEW C **96**, 035804 (2017)

Neutron-skin thickness determines the surface tension of a compressible nuclear droplet

W. Horiuchi,[1] S. Ebata,[2] and K. Iida[3]
[1]*Department of Physics, Hokkaido University, Sapporo 060-0810, Japan*
[2]*Nuclear Reaction Data Centre, Faculty of Science, Hokkaido University, Sapporo 060-0810, Japan*
[3]*Department of Mathematics and Physics, Kochi University, Kochi 780-8520, Japan*

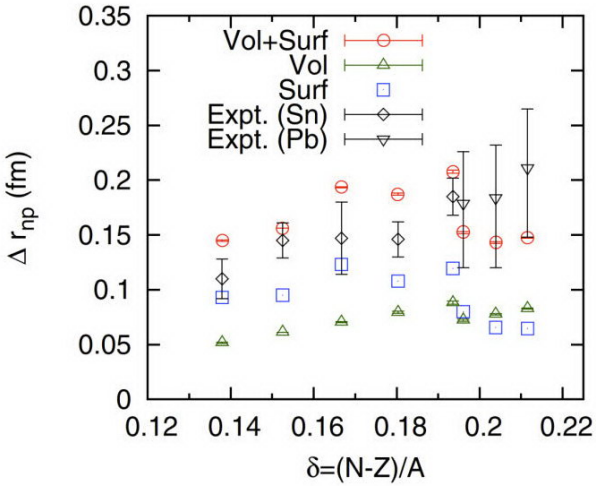

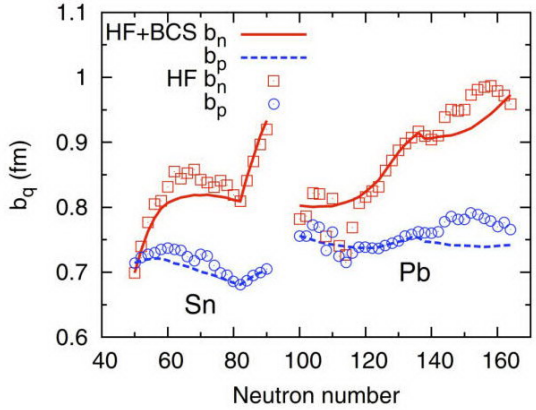

FIG. 6. Surface widths of Sn and Pb isotopes that are extracted from the neutron and proton density distributions calculated in the presence (HF+BCS) and absence (HF) of the pairing interaction. The SkM* interaction is employed for calculations of the density distributions.

Such a determination provides possible way of determining the density dependence of the surface tension, which is a key quantity to bridge a gap between microscopic and macroscopic nuclear models.

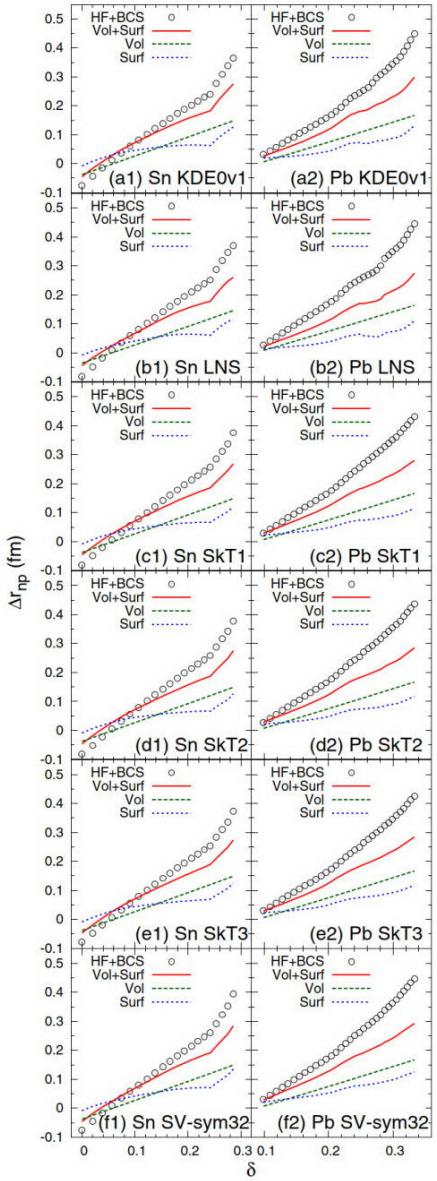

中子皮与核温度

PHYSICAL REVIEW LETTERS **125,** 222301 (2020)

Probing the Neutron Skin with Ultrarelativistic Isobaric Collisions

Hanlin Li,[1] Hao-jie Xu,[2,*] Ying Zhou,[3] Xiaobao Wang,[2] Jie Zhao,[4] Lie-Wen Chen,[3,†] and Fuqiang Wang[2,4,‡]
[1]*College of Science, Wuhan University of Science and Technology, Wuhan, Hubei 430065, China*
[2]*School of Science, Huzhou University, Huzhou, Zhejiang 313000, China*
[3]*School of Physics and Astronomy and Shanghai Key Laboratory for Particle Physics and Cosmology, Shanghai Jiao Tong University, Shanghai 200240, China*
[4]*Department of Physics and Astronomy, Purdue University, West Lafayette, Indiana 47907, USA*

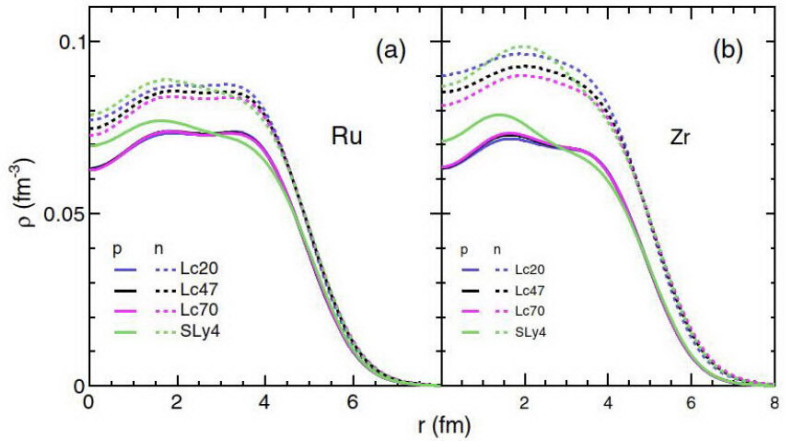

FIG. 1. Proton and neutron density distributions of (a) ^{96}Ru and (b) ^{96}Zr nuclei from eSHF (parameter sets Lc20, Lc47, Lc70) and SHF (SLy4).

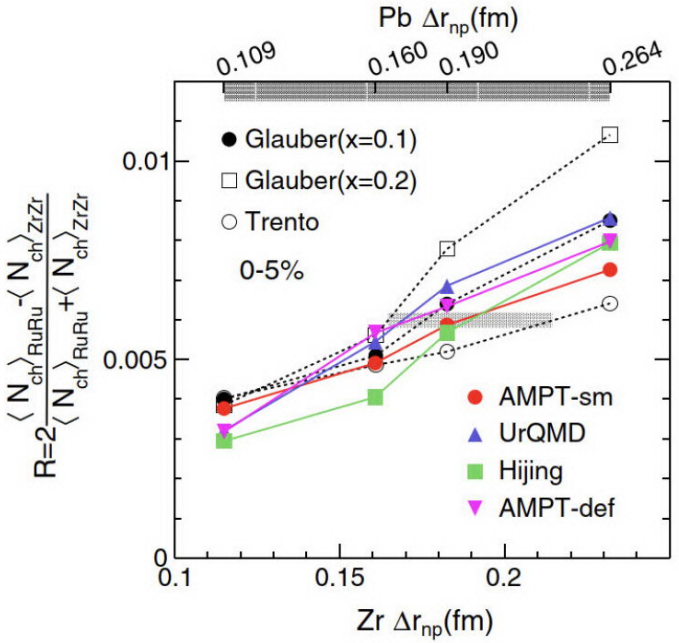

高能重离子碰撞中的中子皮效应

PHYSICAL REVIEW LETTERS **125,** 222301 (2020)

Probing the Neutron Skin with Ultrarelativistic Isobaric Collisions

Hanlin Li,[1] Hao-jie Xu,[2,*] Ying Zhou,[3] Xiaobao Wang,[2] Jie Zhao,[4] Lie-Wen Chen,[3,†] and Fuqiang Wang[2,4,‡]

[1]*College of Science, Wuhan University of Science and Technology, Wuhan, Hubei 430065, China*

[2]*School of Science, Huzhou University, Huzhou, Zhejiang 313000, China*

[3]*School of Physics and Astronomy and Shanghai Key Laboratory for Particle Physics and Cosmology, Shanghai Jiao Tong University, Shanghai 200240, China*

[4]*Department of Physics and Astronomy, Purdue University, West Lafayette, Indiana 47907, USA*

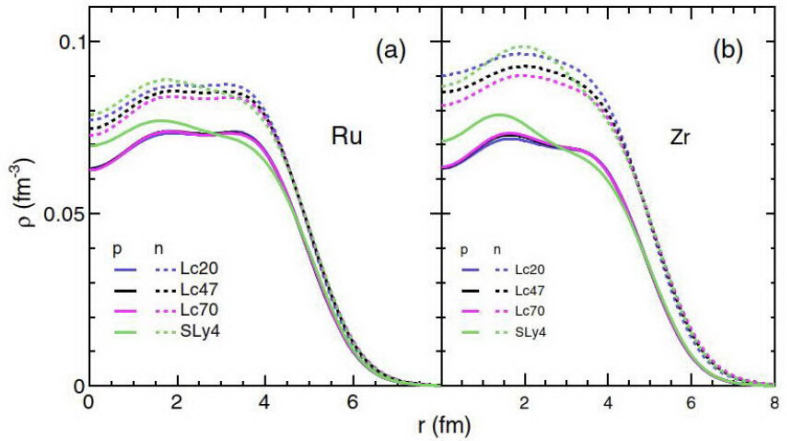

FIG. 1. Proton and neutron density distributions of (a) ^{96}Ru and (b) ^{96}Zr nuclei from eSHF (parameter sets Lc20, Lc47, Lc70) and SHF (SLy4).

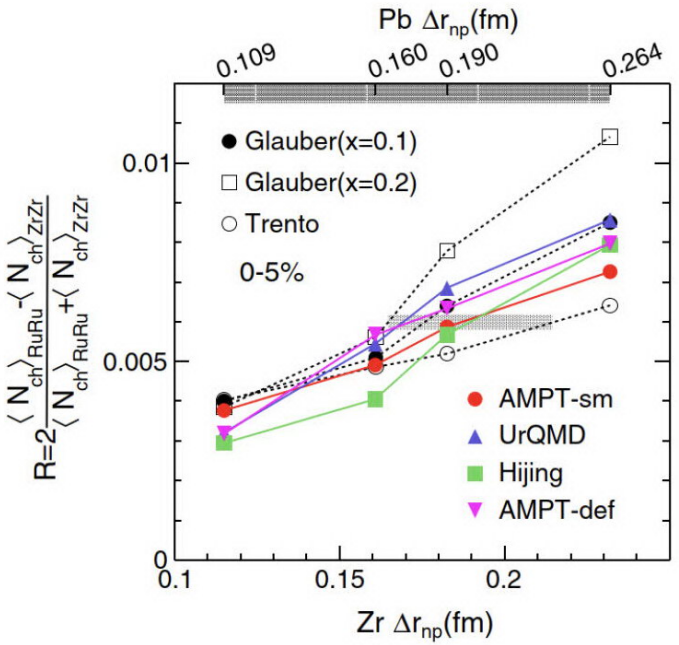

- ☆ 不稳定核的产生方法
- ☆ 晕结构的实验探测方法
- ☆ 中子皮的实验探测方法

兰州重离子加速器装置 (HIRFL-CSR)

SSC(K=450)
100 AMeV (H.I.), 110 MeV (p)

SFC (K=69)
10 AMeV (H.I.), 17~35 MeV (p)

CSRe

RIBLL1
RIBs at tens of AMeV

RIBLL2
RIBs at hundreds of AMeV

CSRm
1000 AMeV (H.I.), ≤ 2.8 GeV (p)

① Low energy site in general
② Atomic physics experimental site
③ Gas filled recoil separator
④ Heavy ion irradiation experimental site
⑤ RIBLL1 – 1st Radioactive Ion Beam Line in Lanzhou
⑥ CEE – CSR External target Experiment
⑦ CSRe – Experimental ring
⑧ PISA – Nuclear data measurements
⑨ Tumor therapy site

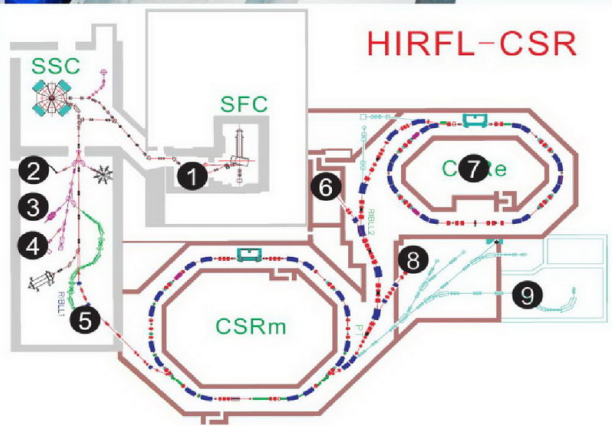

产生放射性核束的两种主要方法：PF、ISOL

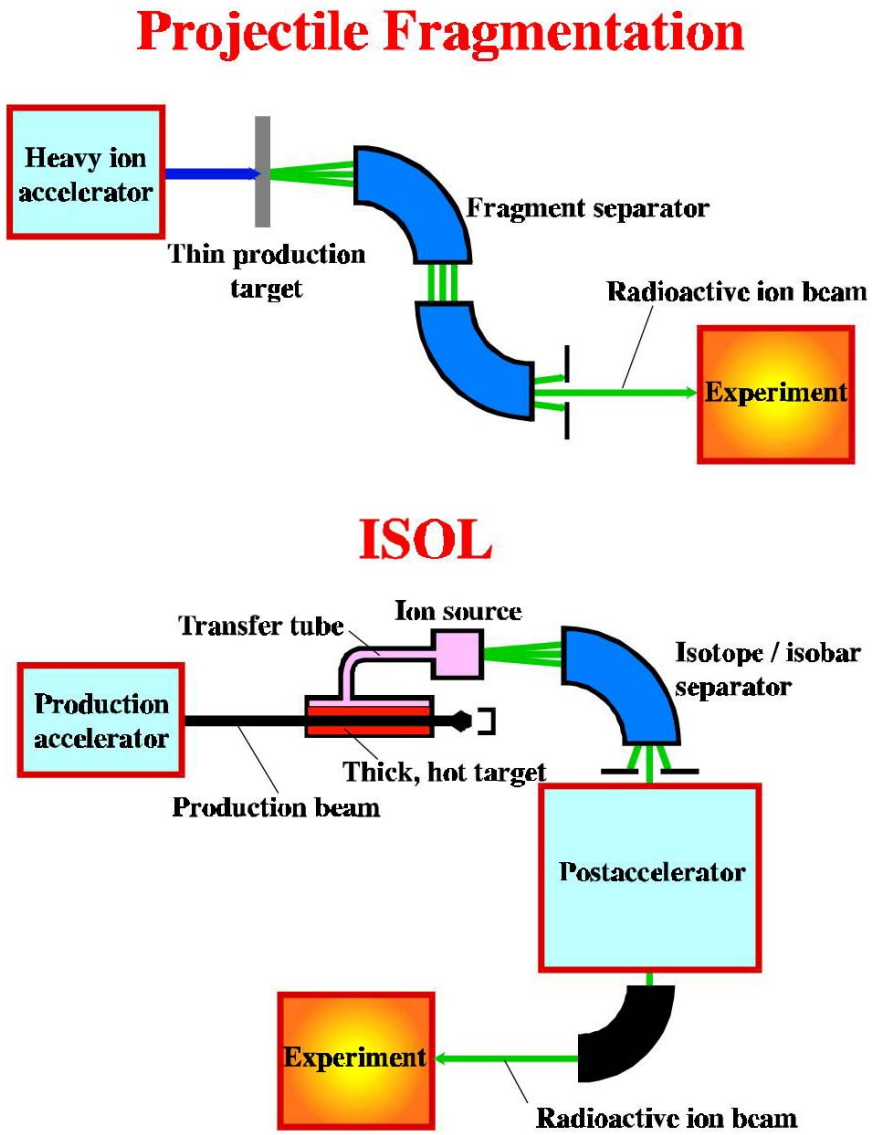

- **PF** 方法可产生寿命短至几百纳秒的不稳定核素，更加接近中子或质子滴线。束流能量与初级束流接近，较多研究需要降能，束流品质较差
- **ISOL(Isotope Separation On Line)** 方法局限于产生寿命较长的不稳定核素 (大于毫秒)，能量范围宽 (几十 **keV** 到 **100MeV/A**)，束流品质较好
- **PF** 与 **ISOL** 两种方法具有高度的互补性

兰州放射性束流线 (RIBLL)

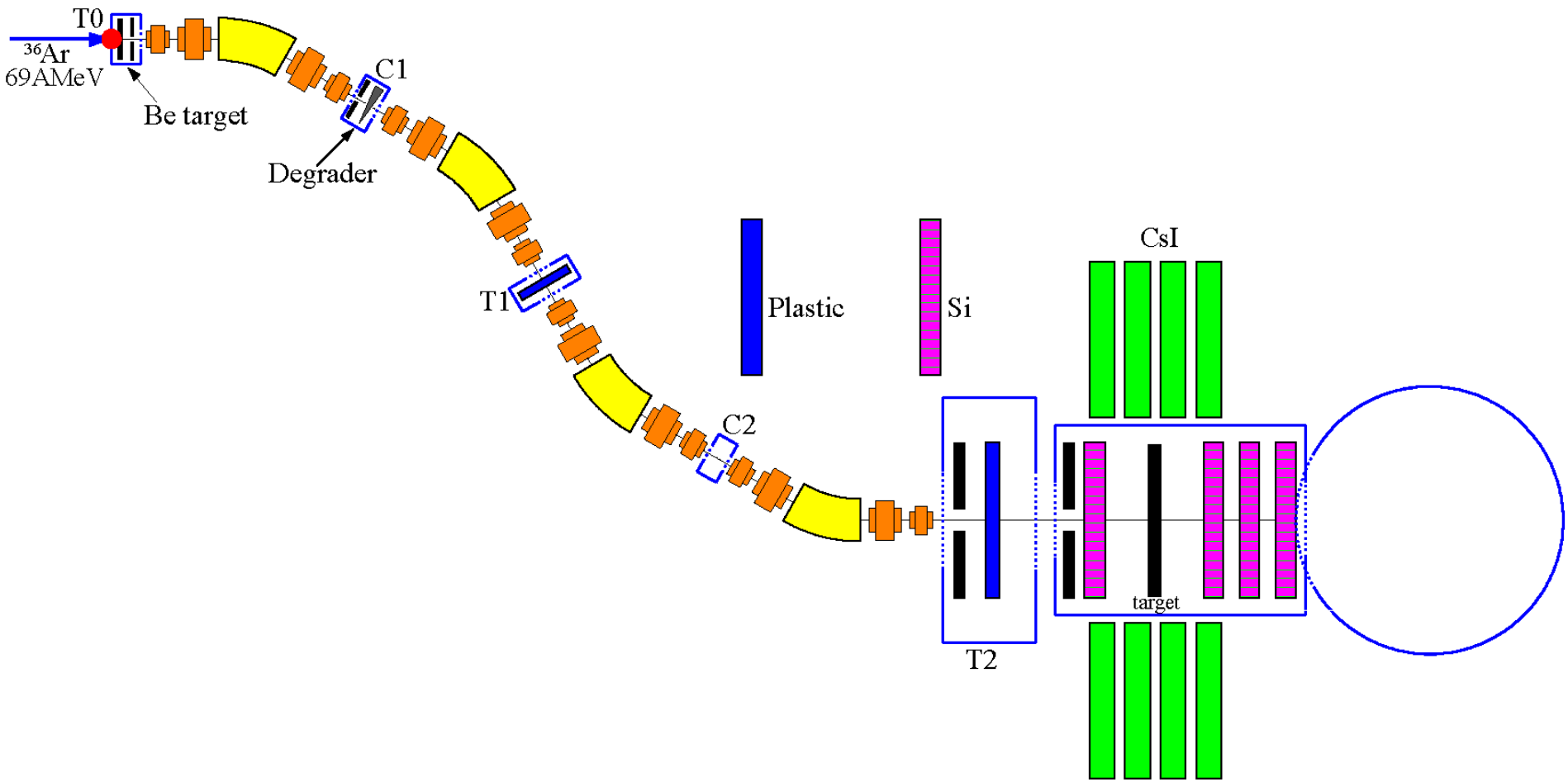

兰州放射性束流线 (RIBLL)

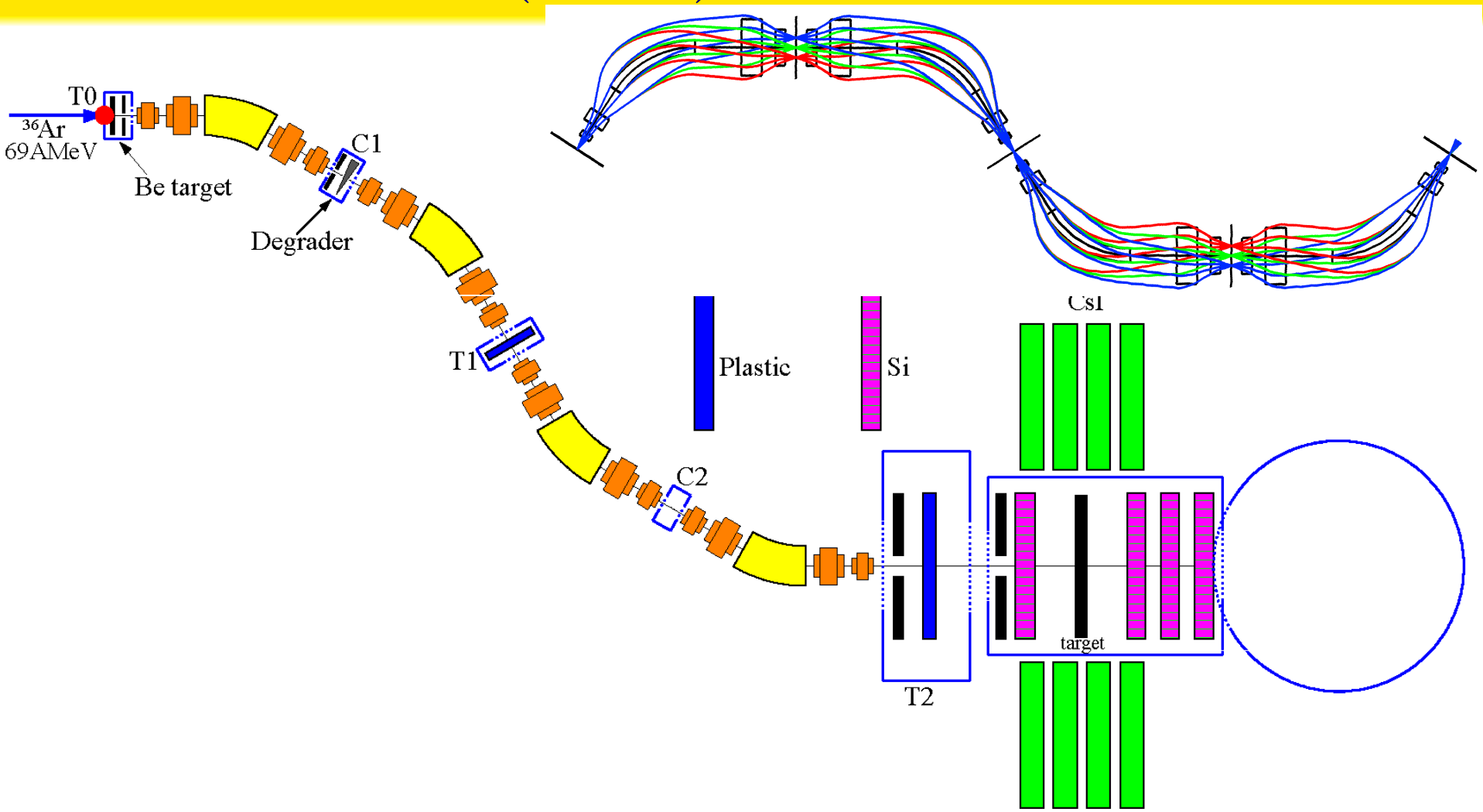

兰州放射性束流线 (RIBLL)

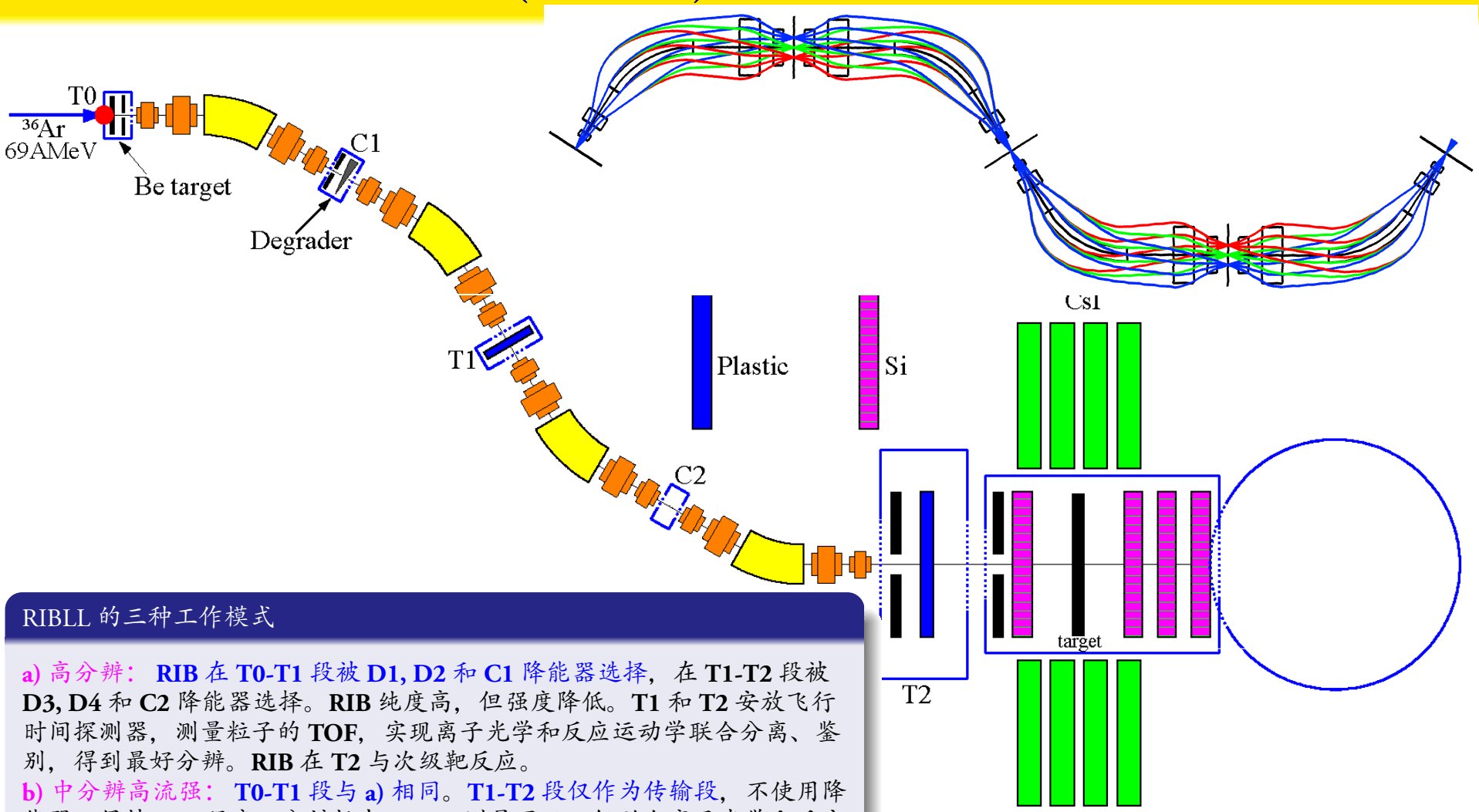

RIBLL 的三种工作模式

a) 高分辨：**RIB** 在 **T0-T1** 段被 **D1, D2** 和 **C1** 降能器选择，在 **T1-T2** 段被 **D3, D4** 和 **C2** 降能器选择。**RIB** 纯度高，但强度降低。**T1** 和 **T2** 安放飞行时间探测器，测量粒子的 **TOF**，实现离子光学和反应运动学联合分离、鉴别，得到最好分辨。**RIB** 在 **T2** 与次级靶反应。

b) 中分辨高流强：**T0-T1** 段与 **a)** 相同。**T1-T2** 段仅作为传输段，不使用降能器，保持 **RIB** 强度，分辨折中。**TOF** 测量同 **a)**，仍联合离子光学和反应运动学方法，改善分离质量。**RIB** 在 **T2** 与靶反应。

c) **RIB** + 磁谱仪：**T0-T1** 段同 **a)**。次级靶被放在 **T1**；**T1-T2** 段以磁谱仪方式工作，设置不同 **B**ρ，实现选择不同的次极反应产物。**TOF** 测量在 **T0** — **T1** 段完成。

兰州放射性束流线 (RIBLL)

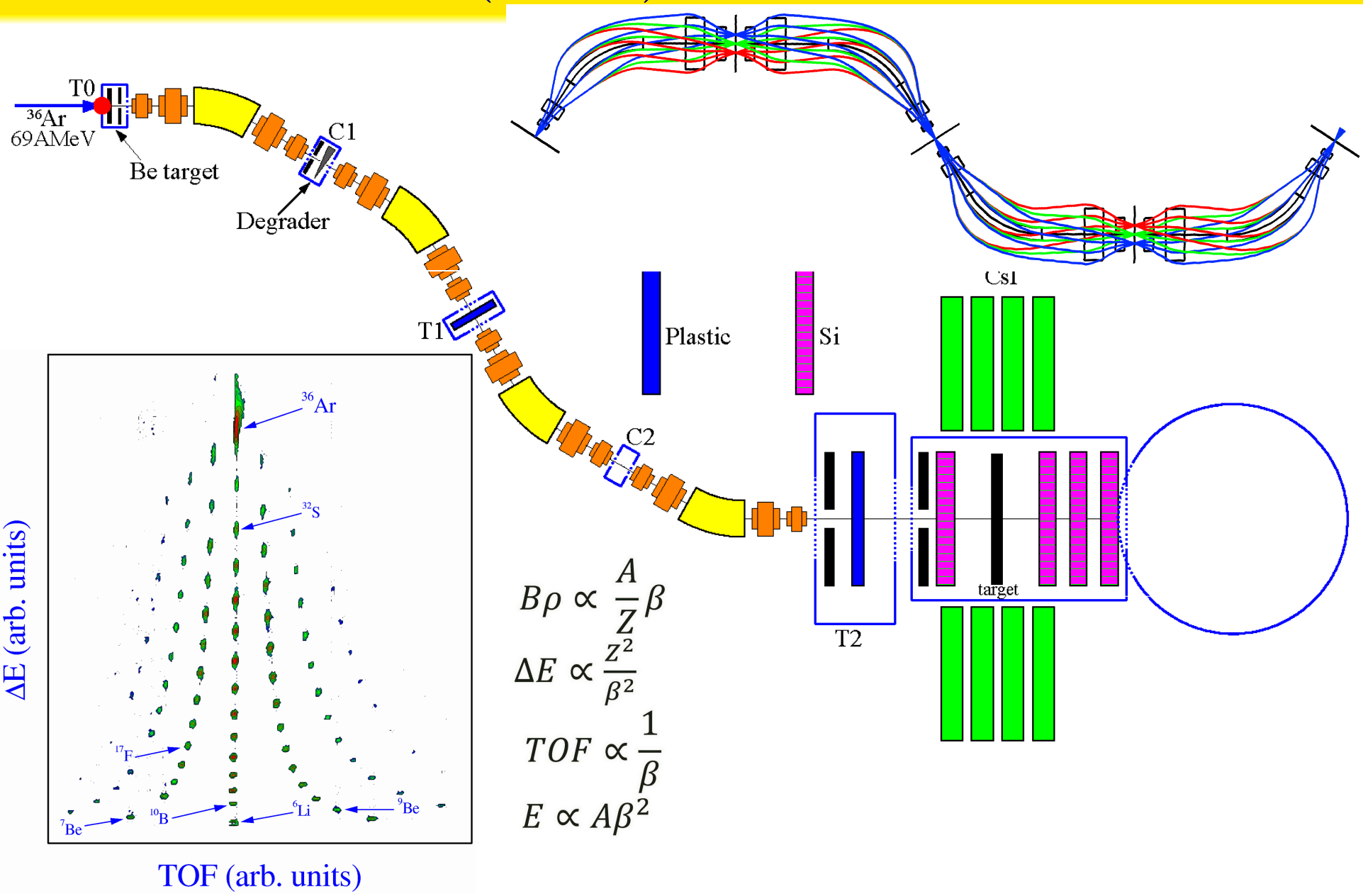

$$B\rho \propto \frac{A}{Z}\beta$$

$$\Delta E \propto \frac{Z^2}{\beta^2}$$

$$TOF \propto \frac{1}{\beta}$$

$$E \propto A\beta^2$$

兰州放射性束流线 (RIBLL)

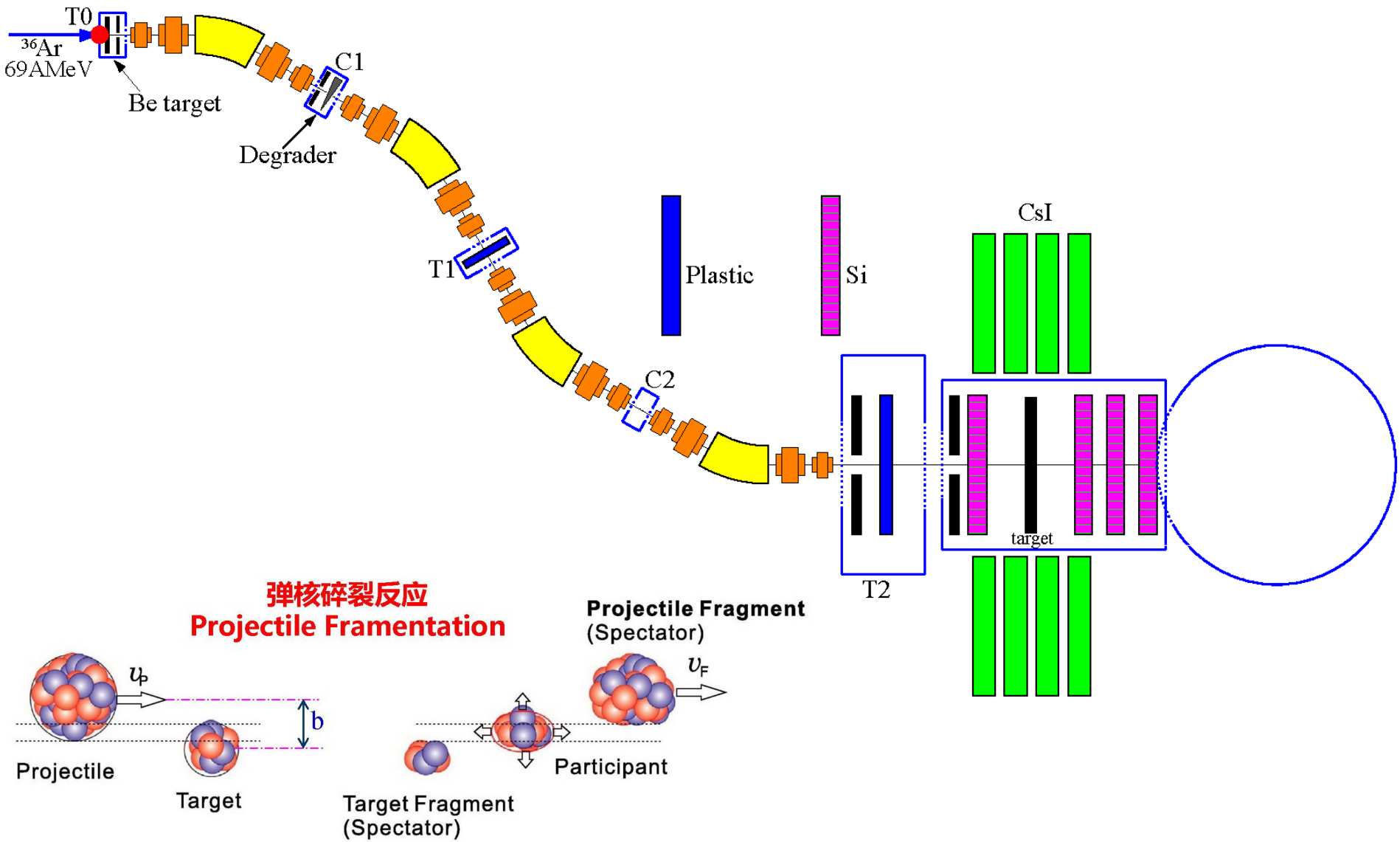

核反应总截面 (σ_R) 与核半径

核半径实验测量方法：

- Electron scattering $\Longleftrightarrow$ charge radii
- Isotope shift $\Longleftrightarrow$ charge radii
- Elastic scattering $\Longleftrightarrow$ matter radii
- Reaction cross section $\Longleftrightarrow$ matter radii

$$\sigma = \frac{n}{I \cdot Ns} \ [\text{mb}=10^{-27}\text{cm}^2]$$

(单位时间发生核反应的粒子数/单位时间入射粒子数/单位面积靶核数)

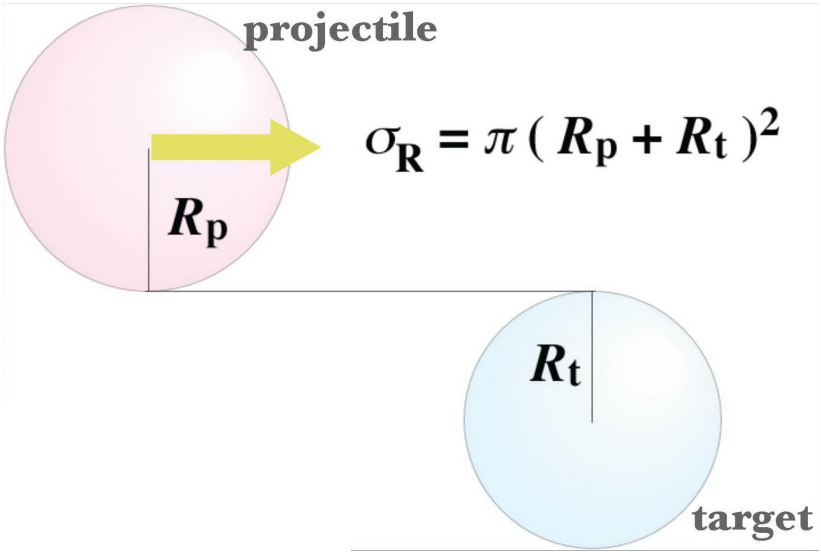

核反应总截面与核半径

Glauber Model:

$$\sigma_R = 2\pi \int [1 - T(b)] b \mathrm{d}b$$

$$T(b) = \exp\{-\sum_{ij} \int\int \sigma_{ij} \rho^z_{P_i}(s) \rho^z_{T_j}(b+s) \mathrm{d}s\}$$

$$\rho^z_{K_i}(s) = \int \rho_{K_i}(\sqrt{s^2 + z^2}) dz$$

$\sigma_R \longrightarrow$ Glauber model or other theory $\longrightarrow$ The matter density distribution

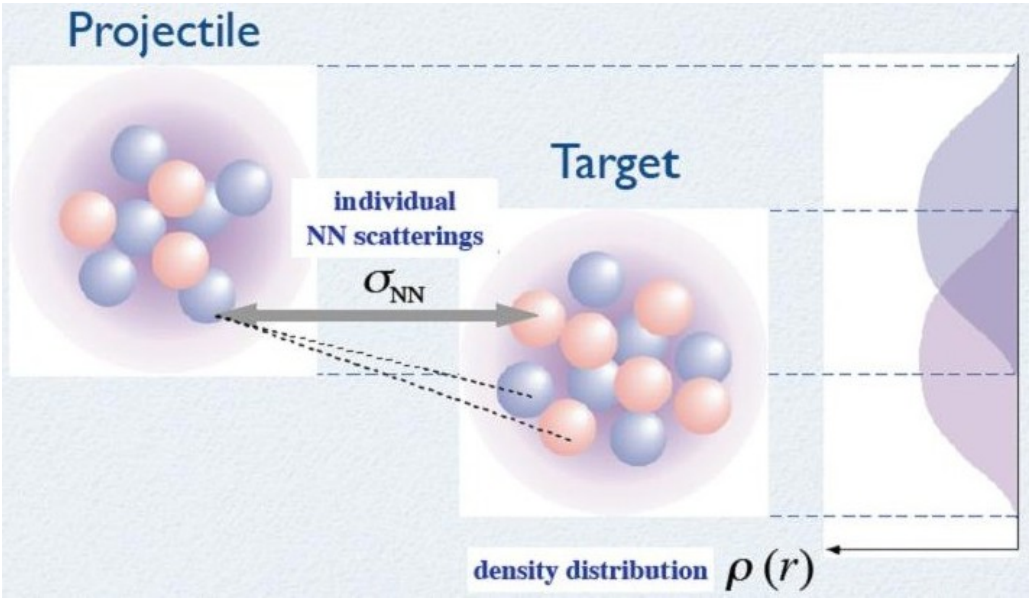

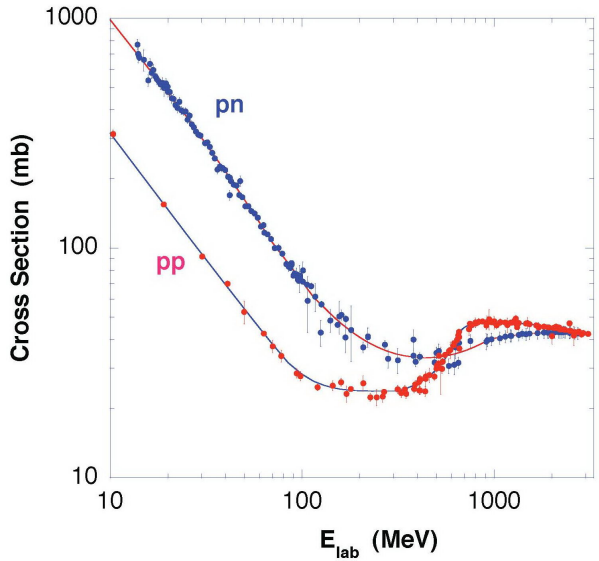

实验测量方法：透射法 (Transmission Method)

$$N_1 = N_0 \exp(-\sigma_R t)$$

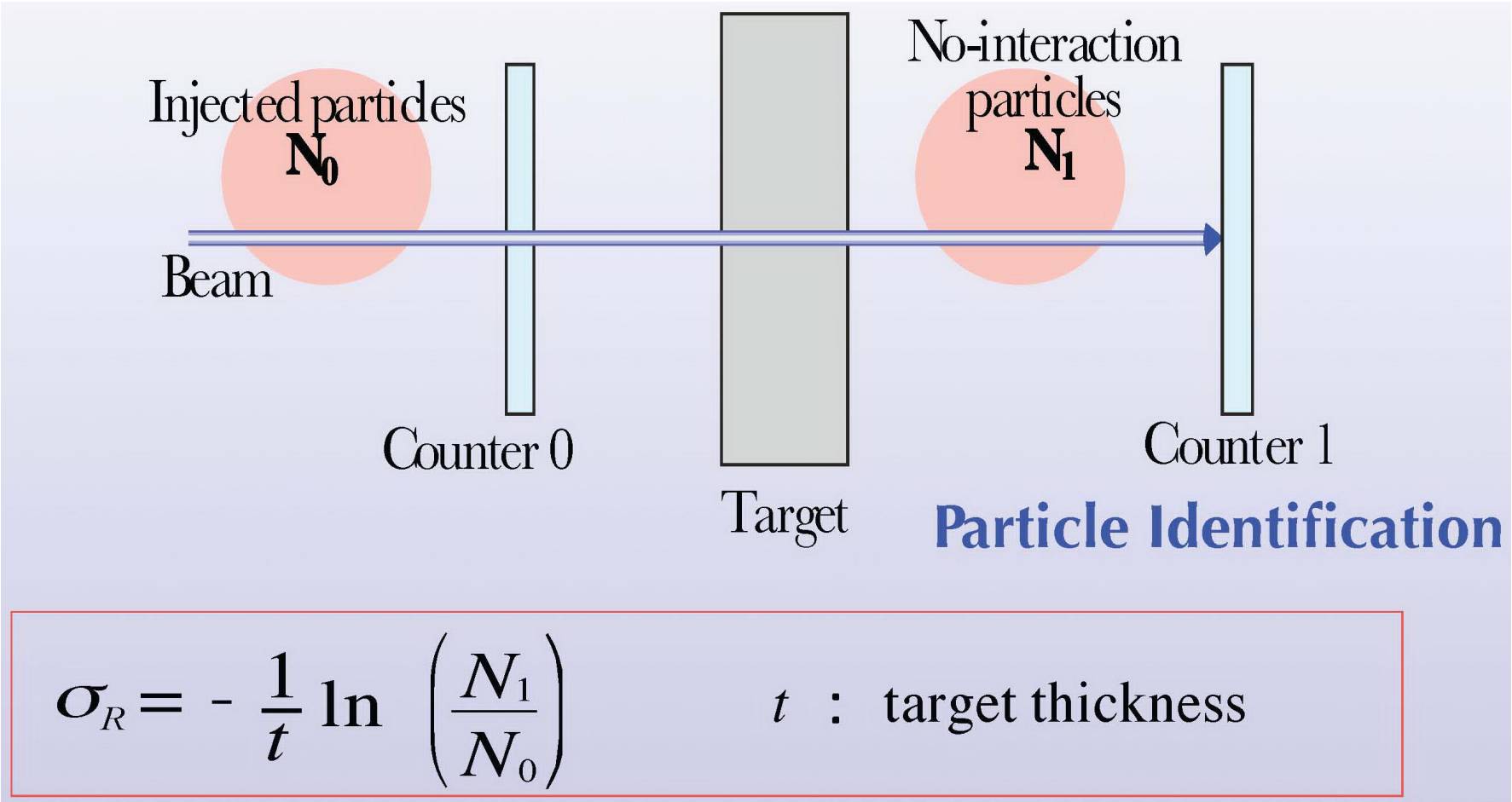

$$\sigma_R = -\frac{1}{t} \ln \left(\frac{N_1}{N_0} \right) \qquad t : \text{target thickness}$$

Target In/Out Measurements

Target-In :

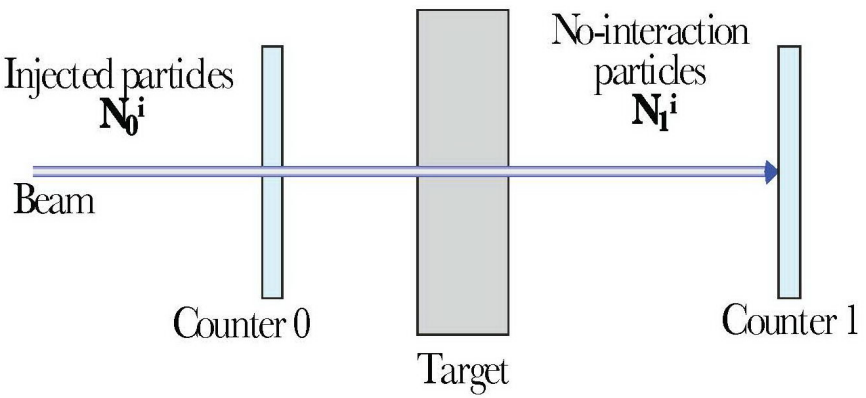

Target-Out :

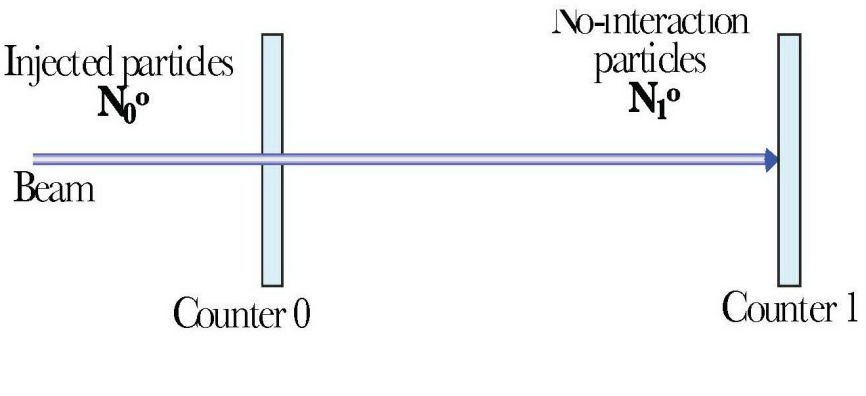

Correction for reactions in counters, etc. (other than target)

$$R_i = \frac{N_1^i}{N_0^i}, \quad R_o = \frac{N_1^o}{N_0^o}$$

$$\sigma_R = -\frac{1}{t}\ln\left(\frac{R_i}{R_o}\right)$$

价核子动量分布与密度分布的关系

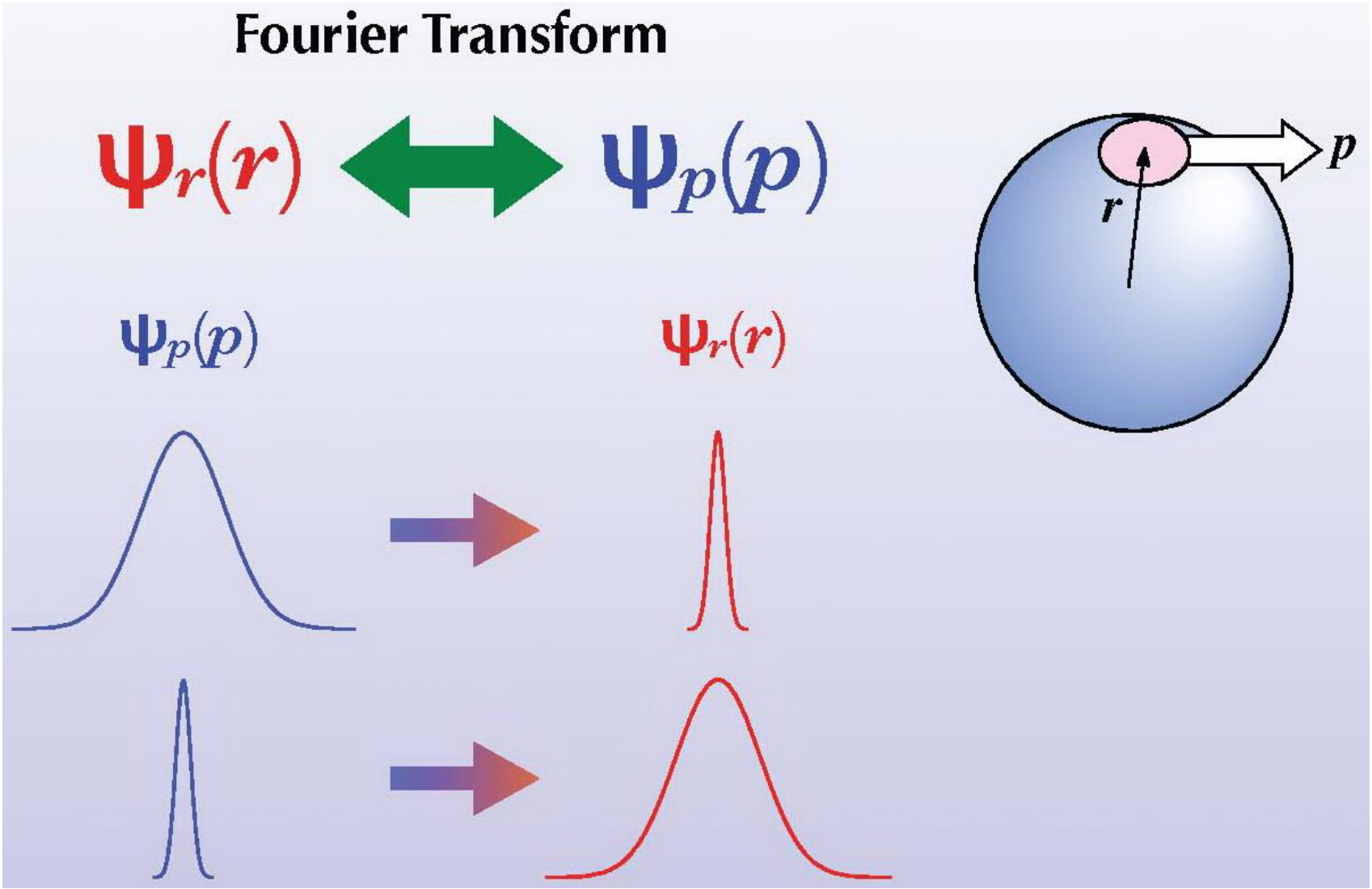

动量分布测量原理

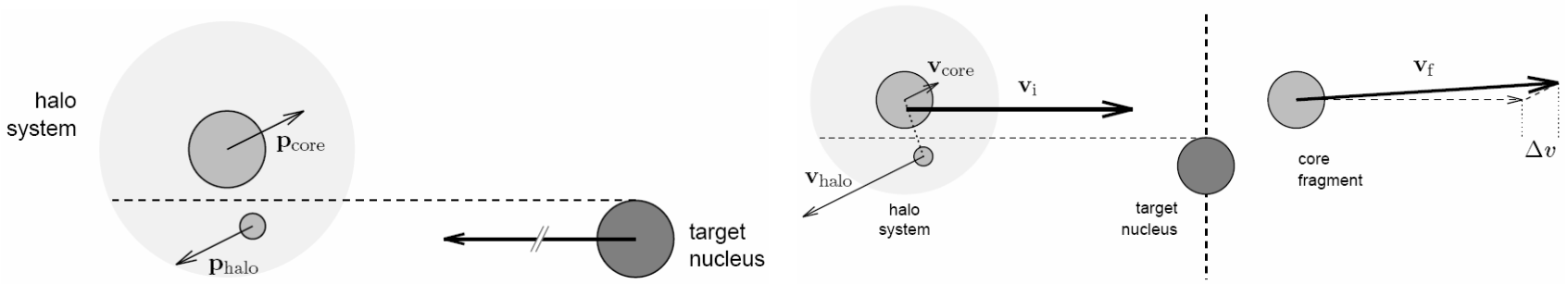

$$P_{\text{core}} = -P_{\text{halo}}$$

$P_{//}$ ⟶ Glauber model or other theory ⟶ The valence nucleon orbit

Fragment Momentum Distribution of Stable Nuclei

Goldhaber Model :

$$P(p) = A\exp\left[-\frac{(p-p_0)^2}{2\sigma^2}\right]$$

$$\sigma^2 = \sigma_0^2 \frac{A_F(A_P - A_F)}{A_P - 1},$$

$$\sigma_0 = 90\ \text{MeV/c}$$

(for stable nuclei)

σ_R 和 $P_{//}$ 实验测量 (^{15}C、^{23}Al)

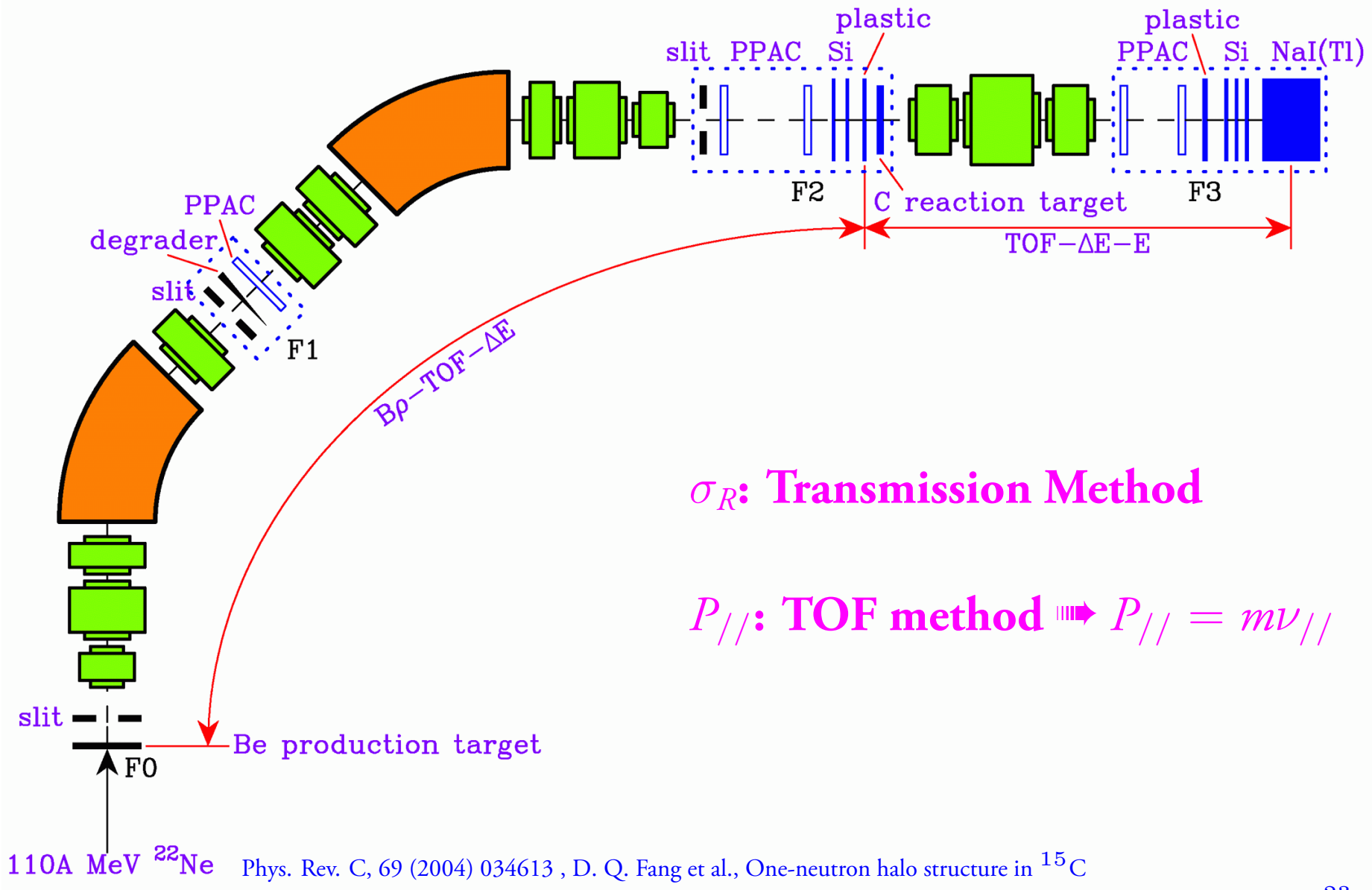

σ_R: **Transmission Method**

$P_{//}$: **TOF method** ➠ $P_{//} = m\nu_{//}$

Phys. Rev. C, 69 (2004) 034613 , D. Q. Fang et al., One-neutron halo structure in ^{15}C
Phys. Rev. C, 76 (2007) 031601(R), D. Q. Fang et al., Examining the exotic structure of the proton-rich nucleus ^{23}Al

靶前粒子鉴别

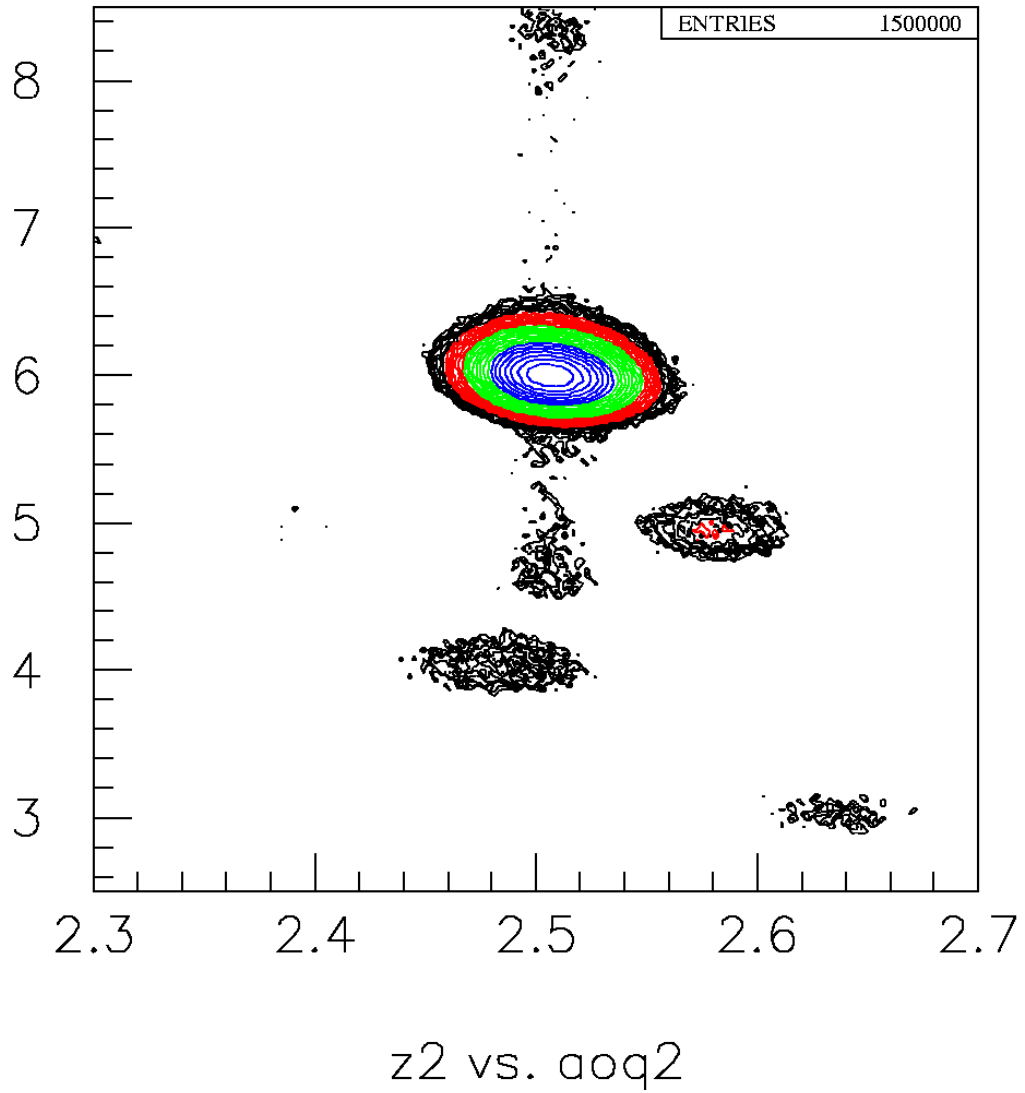

$$B\rho \propto \frac{A}{Z}\beta$$
$$TOF \propto \frac{1}{\beta}$$
$$\Delta E \propto \frac{Z^2}{\beta^2}$$

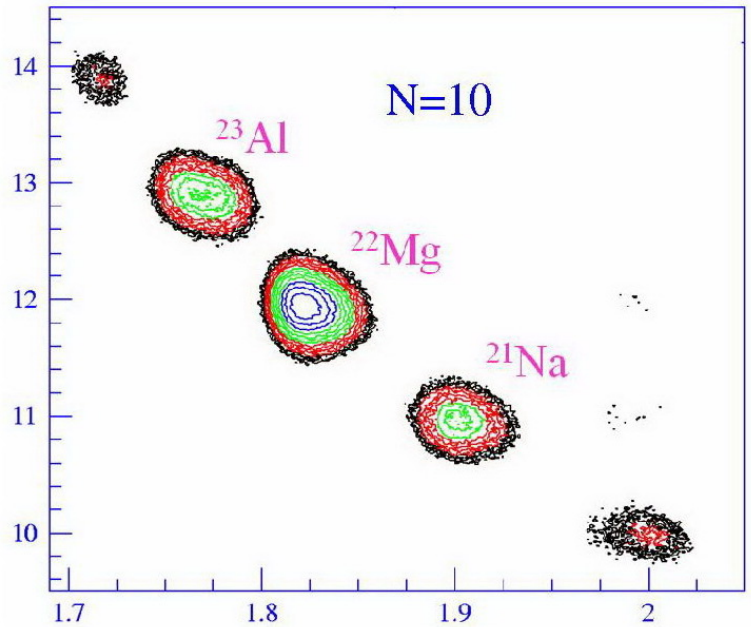

靶后粒子鉴别：电荷 (^{15}C)

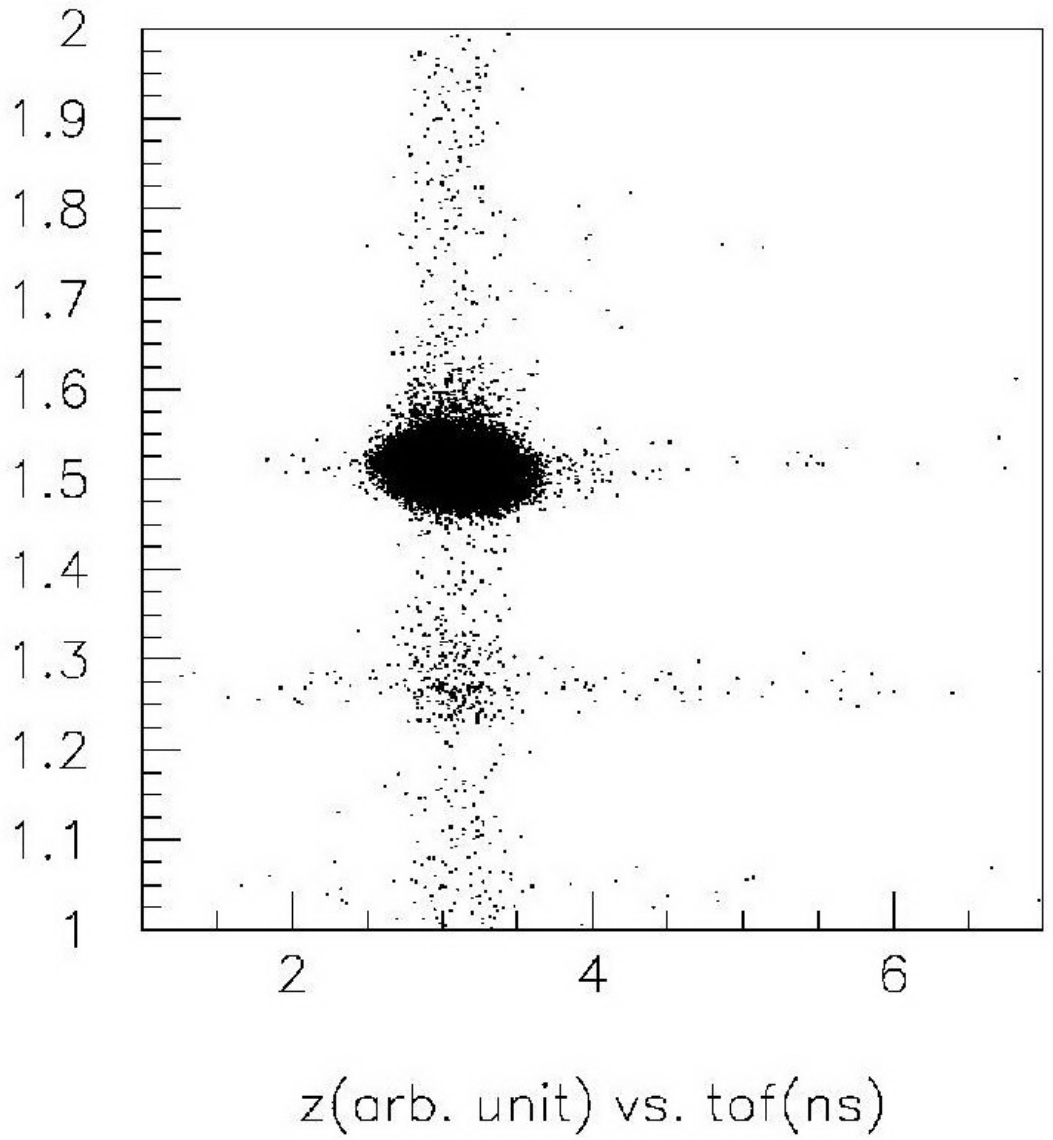

$$TOF \propto \frac{1}{\beta}$$
$$\Delta E \propto \frac{Z^2}{\beta^2}$$
$$E \propto A\beta^2$$

靶后粒子鉴别：质量 (^{15}C)

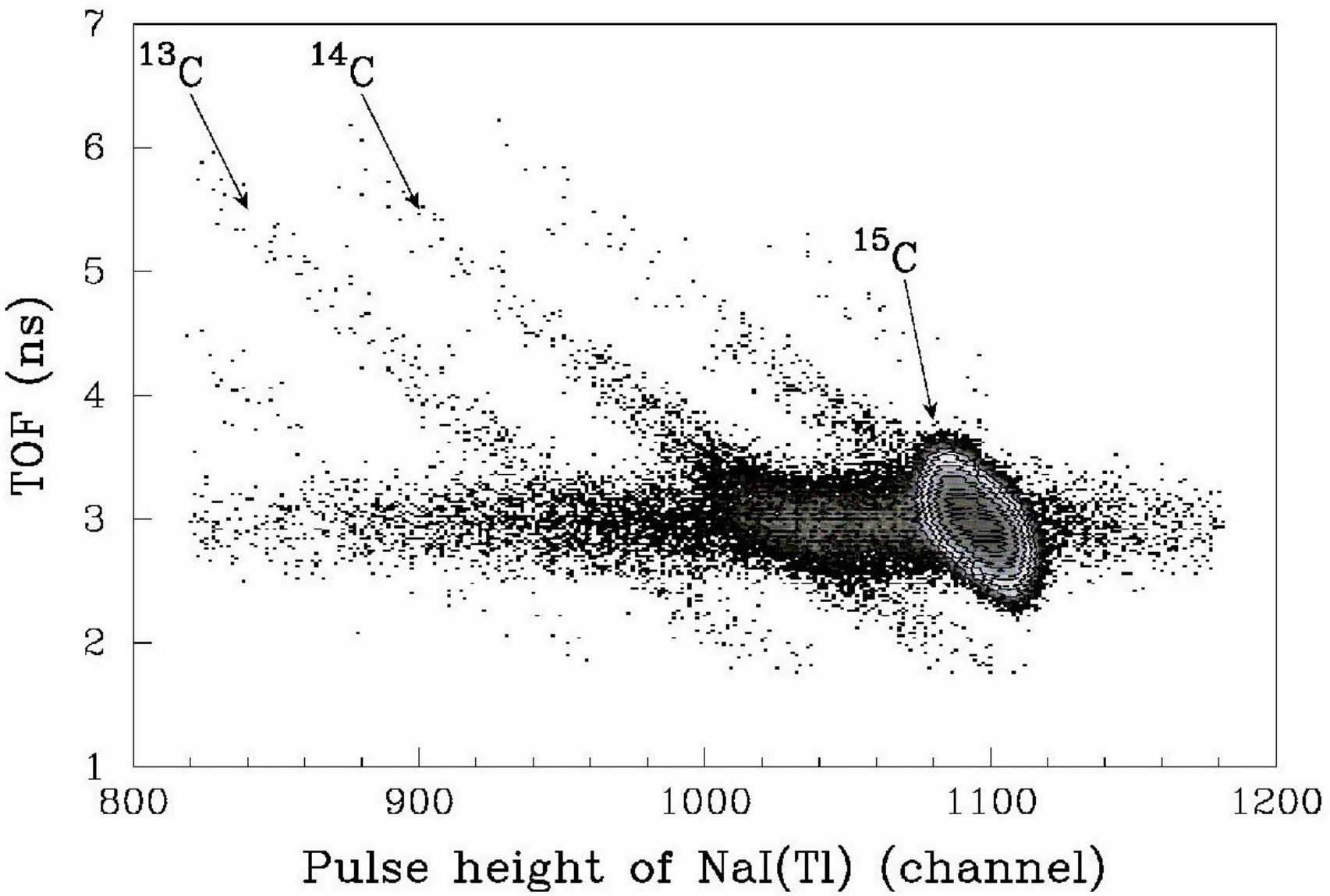

靶后粒子鉴别 (^{23}Al)

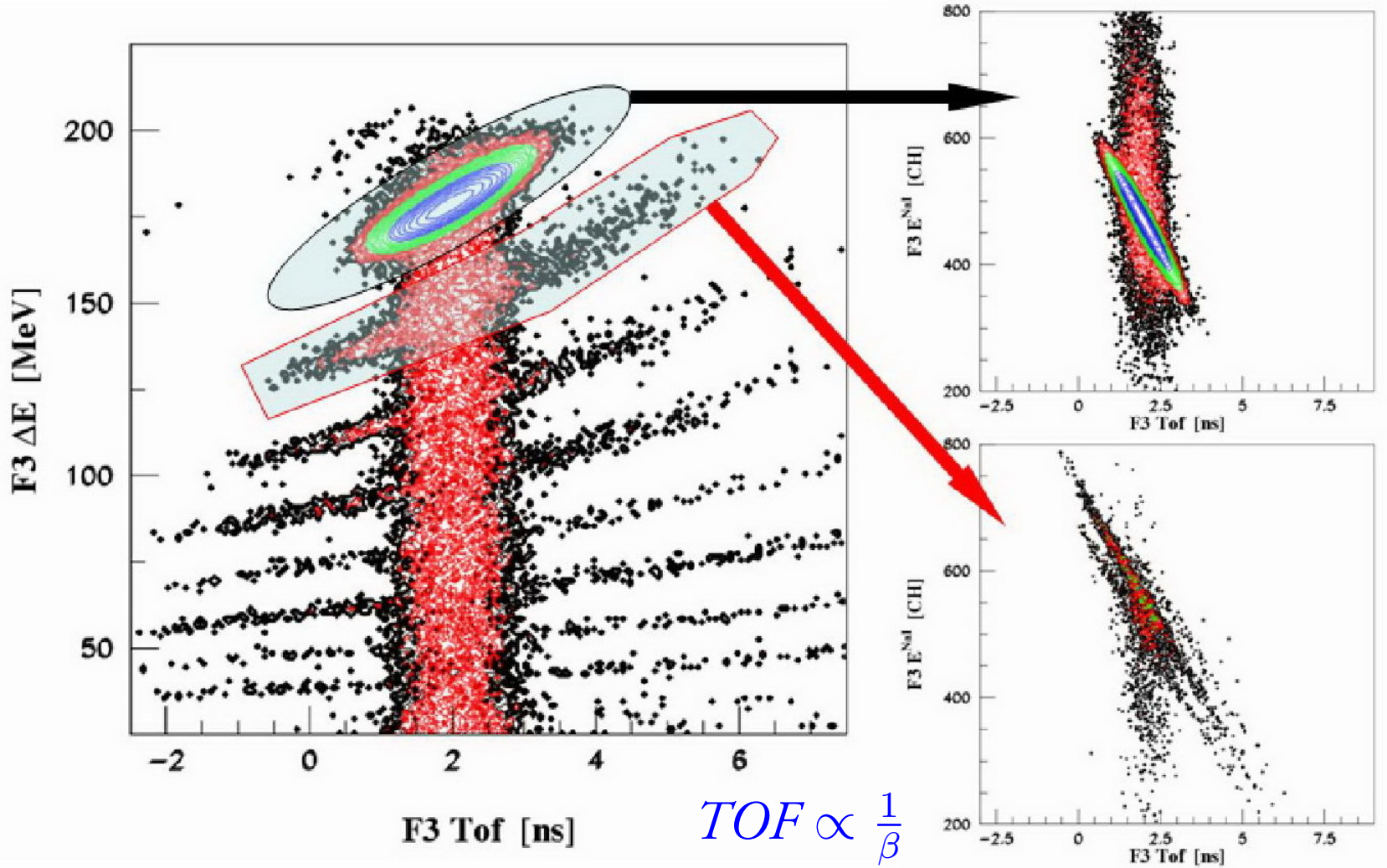

$$TOF \propto \frac{1}{\beta}$$

$$\Delta E \propto \frac{Z^2}{\beta^2}$$

$$E \propto A\beta^2$$

^{15}C 的动量分布结果

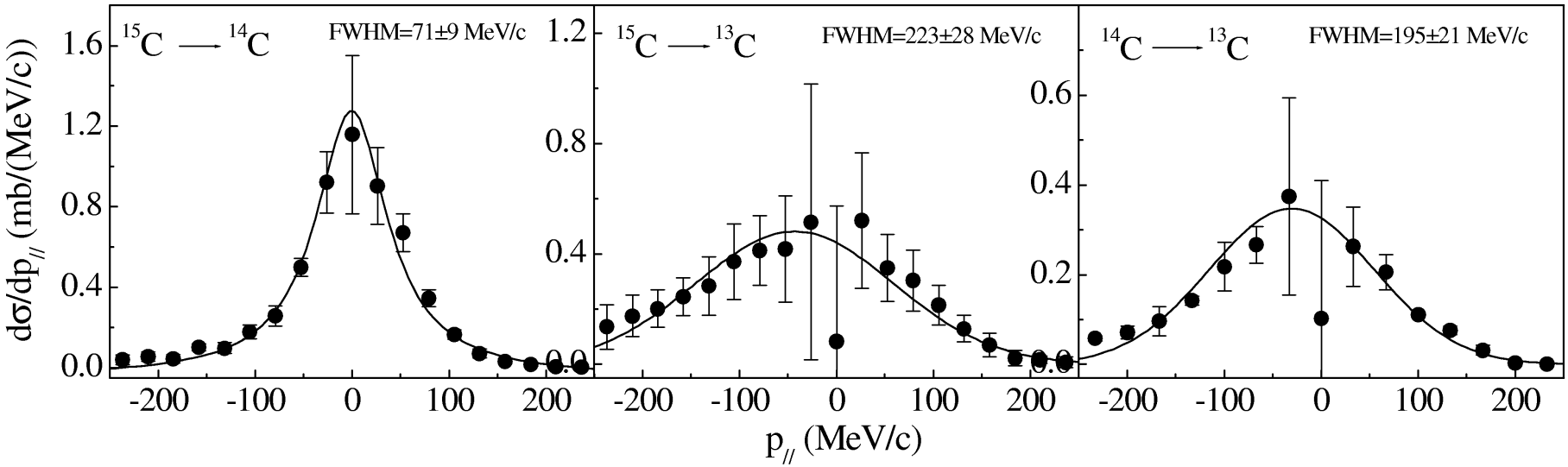
15C ⟶ 14C
FWHM=71±9 MeV/c
15C ⟶ 13C
FWHM=223±28 MeV/c
14C ⟶ 13C
FWHM=195±21 MeV/c
dσ/dp// (mb/(MeV/c))
p// (MeV/c)

与其他实验结果的比较

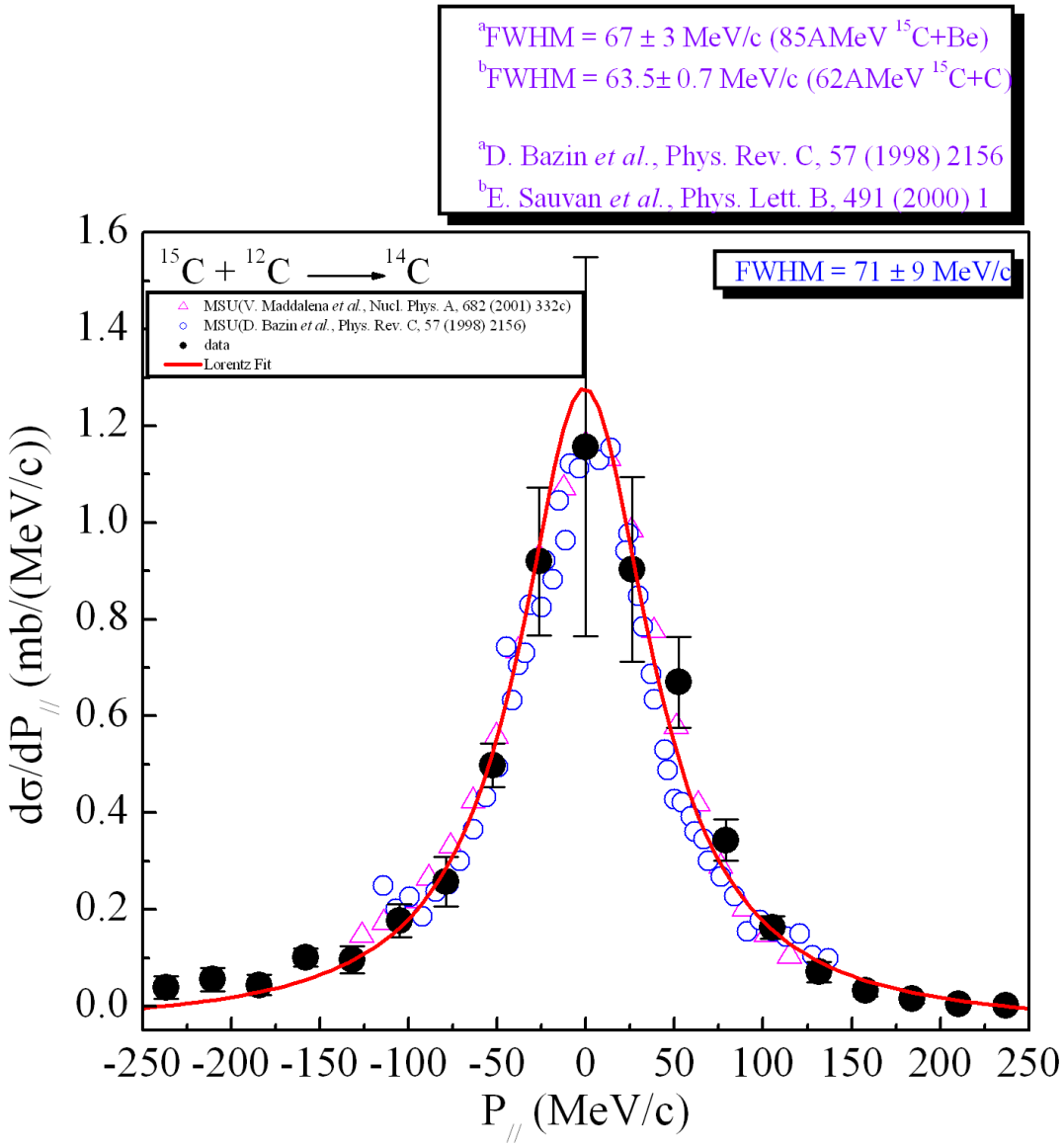
[a]FWHM = 67 ± 3 MeV/c (85AMeV 15C+Be)
[b]FWHM = 63.5± 0.7 MeV/c (62AMeV 15C+C)
[a]D. Bazin et al., Phys. Rev. C, 57 (1998) 2156
[b]E. Sauvan et al., Phys. Lett. B, 491 (2000) 1
15C + 12C → 14C
FWHM = 71 ± 9 MeV/c
MSU(V. Maddalena et al., Nucl. Phys. A, 682 (2001) 332c)
MSU(D. Bazin et al., Phys. Rev. C, 57 (1998) 2156)
data
Lorentz Fit
dσ/dP// (mb/(MeV/c))
P// (MeV/c)
1.6
1.4
1.2
1.0
0.8
0.6
0.4
0.2
0.0
-250 -200 -150 -100 -50 0 50 100 150 200 250

动量分布宽度

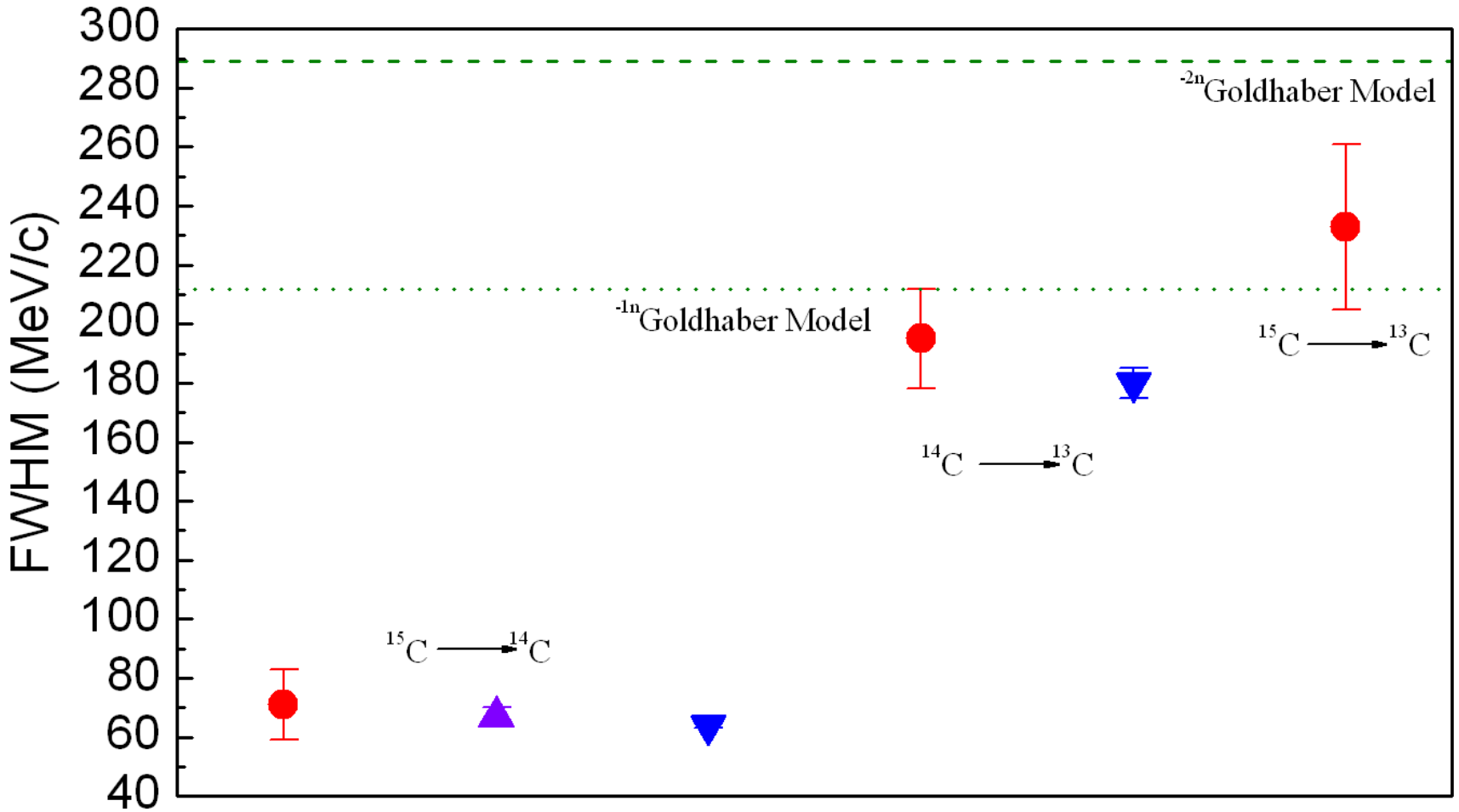
FWHM (MeV/c)
300
280
260
240
220
200
180
160
140
120
100
80
60
40
-2n Goldhaber Model
-1n Goldhaber Model
15C → 13C
14C → 13C
15C → 14C

Few-body Glauber 模型

Model description： Y. Ogawa *et al.*, Nucl. Phys. **A571**, 784 (1994).

Calculation method：

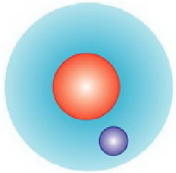

- core + valence nucleon
- the density distribution of the core is determined by reproducing the experimental σ_R data
- the wavefunction of the valence nucleon is calculated by resolving the Schrodinger equation

$$\frac{d^2R(r)}{dr^2}+\frac{2\mu}{\hbar^2}[E-U(r)-\frac{l(l+1)\hbar^2}{2\mu r^2}]R(r)=0$$

$$U(r)=-V_0f(r)+V_{ls}(\mathbf{l}\cdot\mathbf{s})r_0^2\frac{1}{r}\frac{d}{dr}f(r)+V_{\rm Coul}$$

where $f(r)=[1+\exp(\frac{r-R}{a})]^{-1}$, $R=r_0A_c^{1/3}$ ($V_{ls}=17$MeV). V_0 is the depth of the potential, $V_{\rm Coul}$ is the Coulomb potential. a=0.67 fm and r_0=1.27 fm.

价核子轨道分布

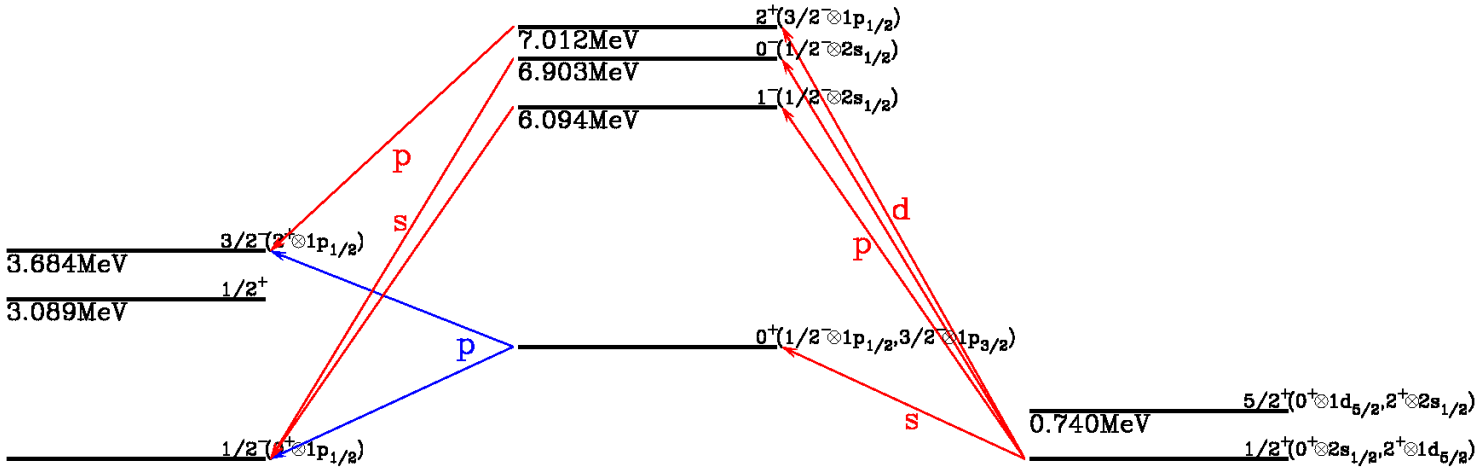
7.012MeV
6.903MeV
6.094MeV
3.684MeV
3.089MeV
0.740MeV
p
s
d
p
p
s

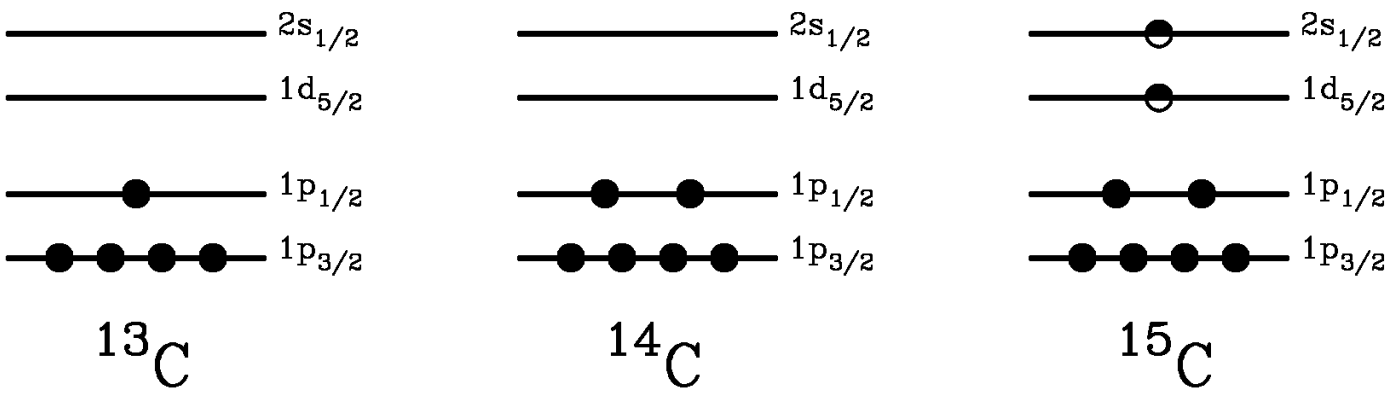
2s1/2
1d5/2
1p1/2
1p3/2
13C
14C
15C

价核子密度分布

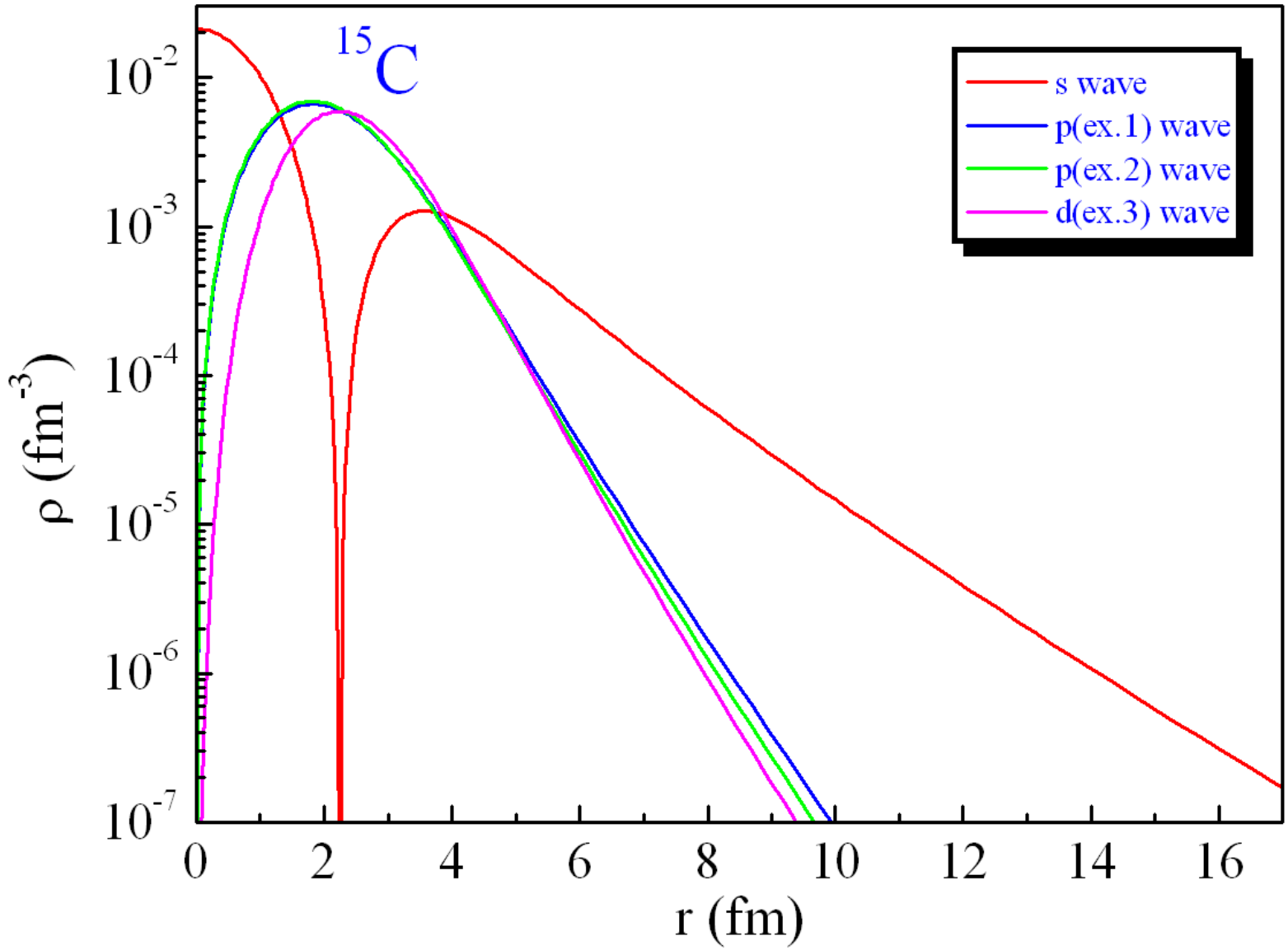
15C
s wave
p(ex.1) wave
p(ex.2) wave
d(ex.3) wave
ρ (fm-3)
r (fm)
10-2
10-3
10-4
10-5
10-6
10-7
0
2
4
6
8
10
12
14
16

计算与实验的比较

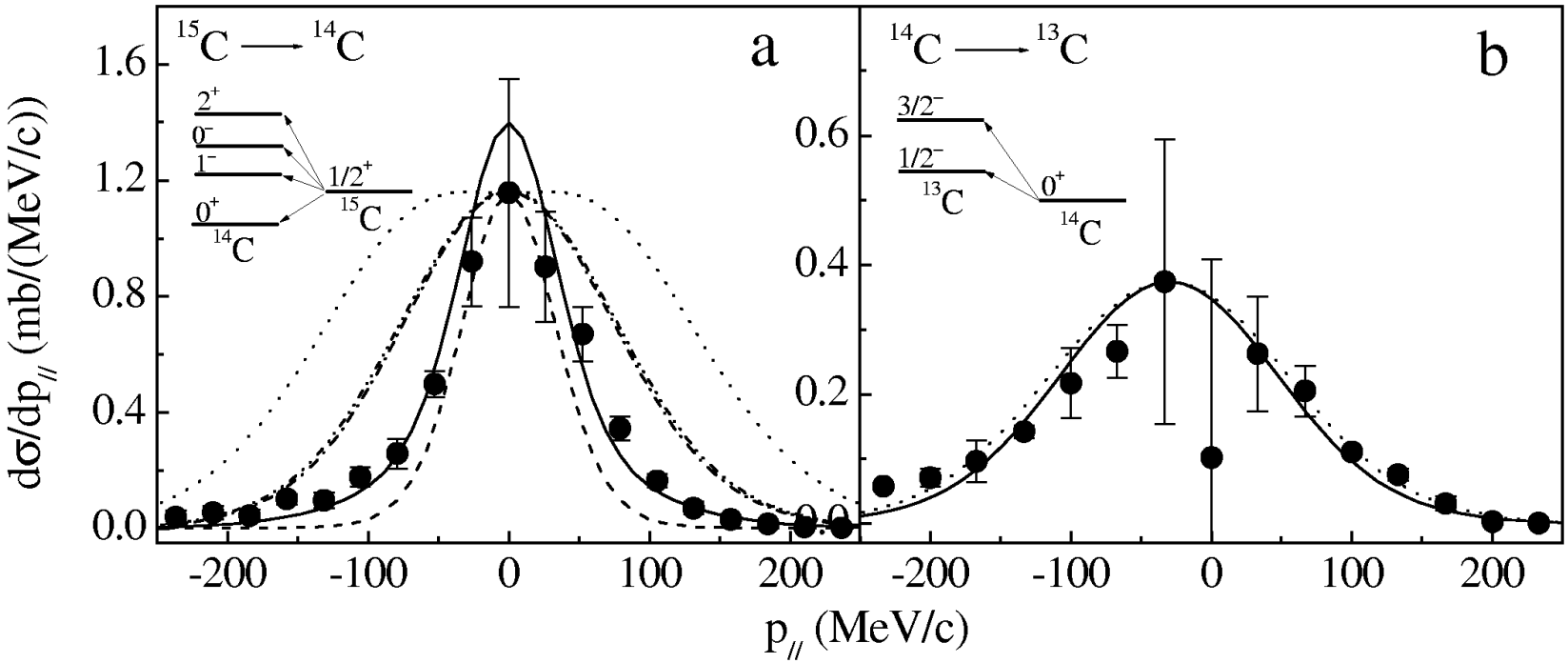
$^{15}C \longrightarrow {}^{14}C$
a
2^+
0^-
1^-
0^+
^{14}C
$1/2^+$
^{15}C
$^{14}C \longrightarrow {}^{13}C$
b
$3/2^-$
$1/2^-$
^{13}C
0^+
^{14}C
$d\sigma/dp_{//}$ (mb/(MeV/c))
$p_{//}$ (MeV/c)
1.6
1.2
0.8
0.4
0.0
0.6
0.4
0.2
0.0
-200
-100
0
100
200

价核子的组态混合

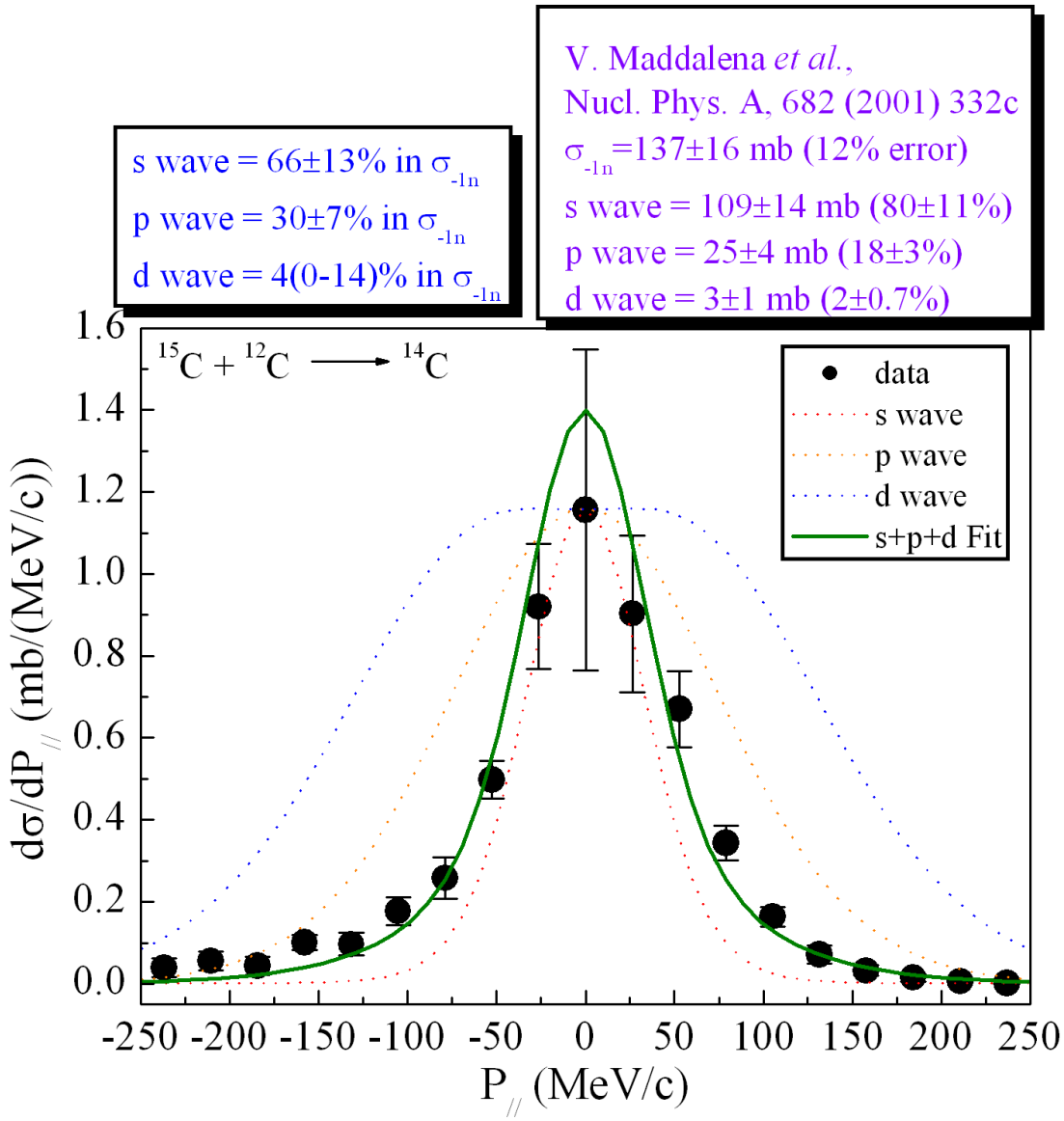
s wave = 66±13% in σ-1n
p wave = 30±7% in σ-1n
d wave = 4(0-14)% in σ-1n
V. Maddalena et al.,
Nucl. Phys. A, 682 (2001) 332c
σ-1n=137±16 mb (12% error)
s wave = 109±14 mb (80±11%)
p wave = 25±4 mb (18±3%)
d wave = 3±1 mb (2±0.7%)
15C + 12C → 14C
data
s wave
p wave
d wave
s+p+d Fit
dσ/dP// (mb/(MeV/c))
P// (MeV/c)
1.6
1.4
1.2
1.0
0.8
0.6
0.4
0.2
0.0
-250 -200 -150 -100 -50 0 50 100 150 200 250

^{15}C 的核反应总截面

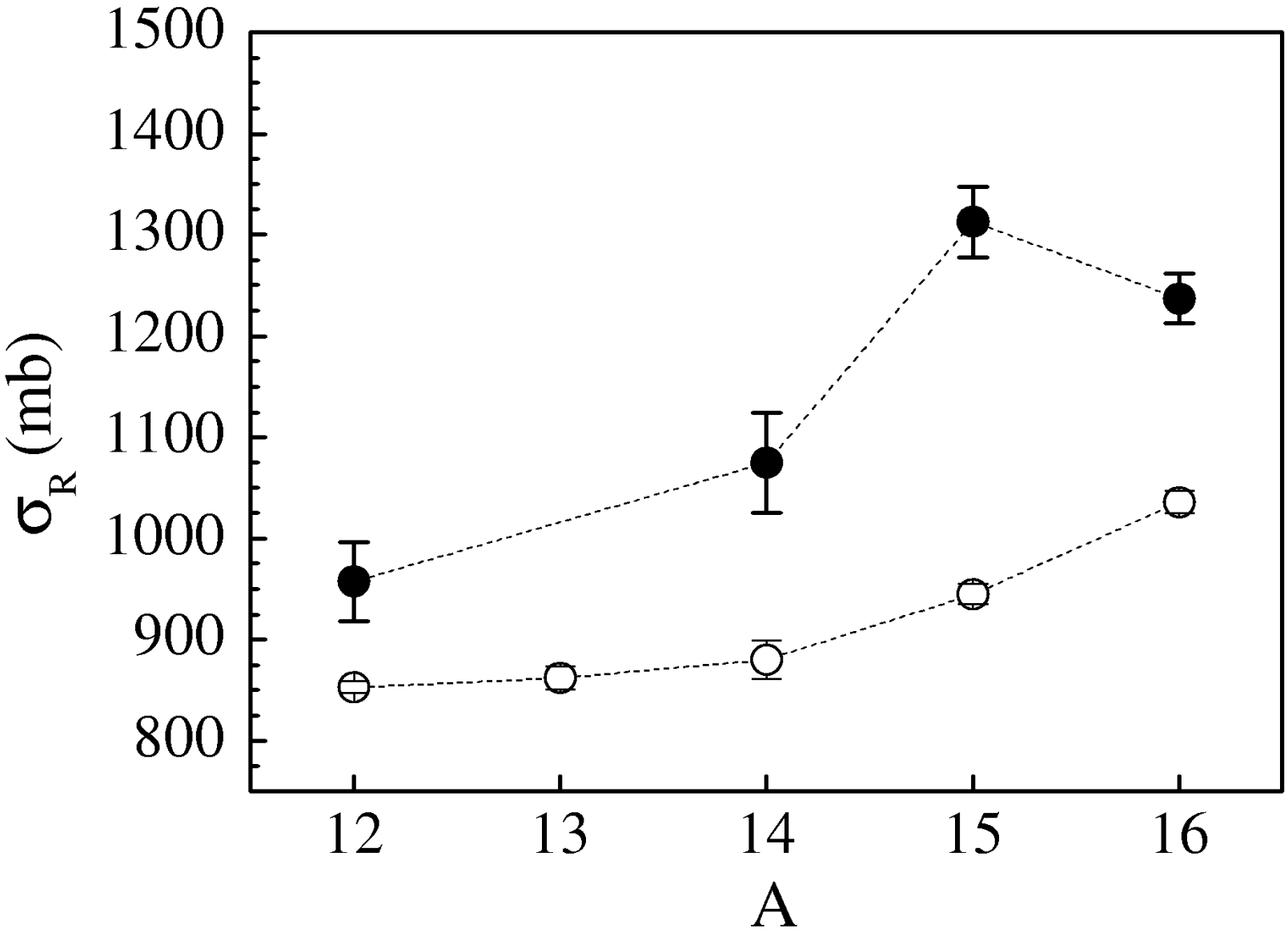

^{15}C 的半径参数

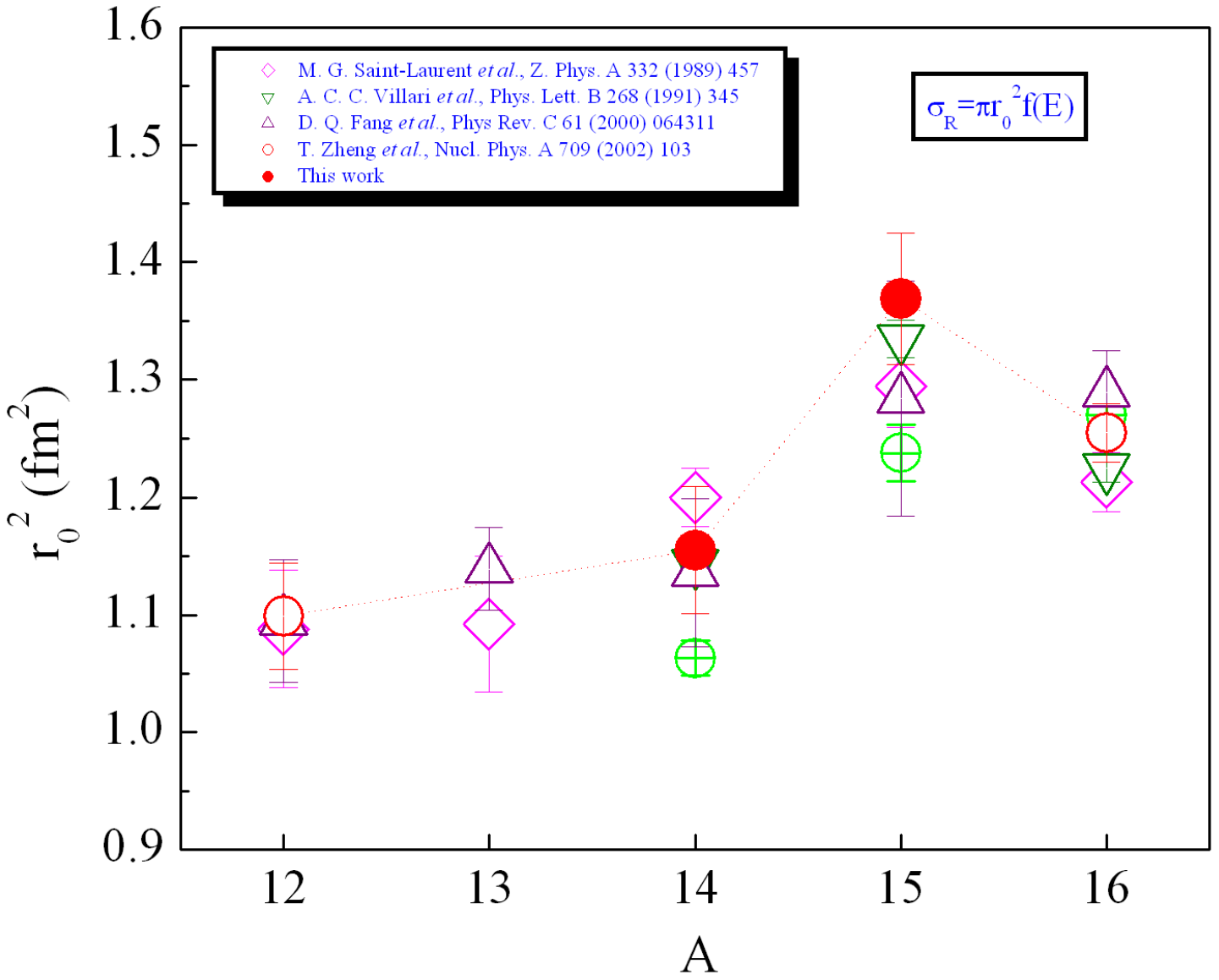
M. G. Saint-Laurent et al., Z. Phys. A 332 (1989) 457
A. C. C. Villari et al., Phys. Lett. B 268 (1991) 345
D. Q. Fang et al., Phys Rev. C 61 (2000) 064311
T. Zheng et al., Nucl. Phys. A 709 (2002) 103
This work
$\sigma_R=\pi r_0^2 f(E)$
r_0^2 (fm^2)
A
1.6
1.5
1.4
1.3
1.2
1.1
1.0
0.9
12
13
14
15
16

不同能量区的核反应总截面

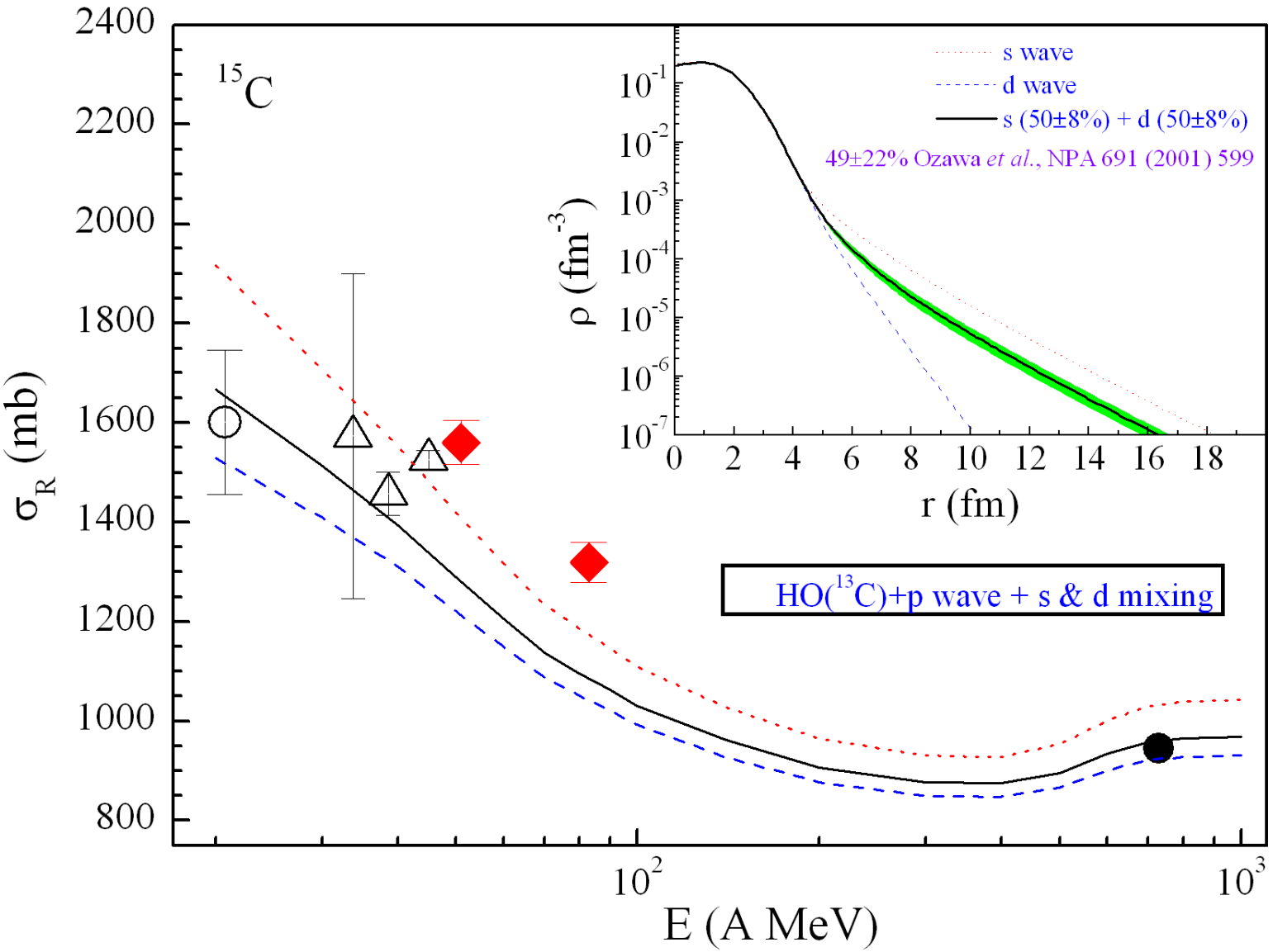

核反应总截面与中子皮探测

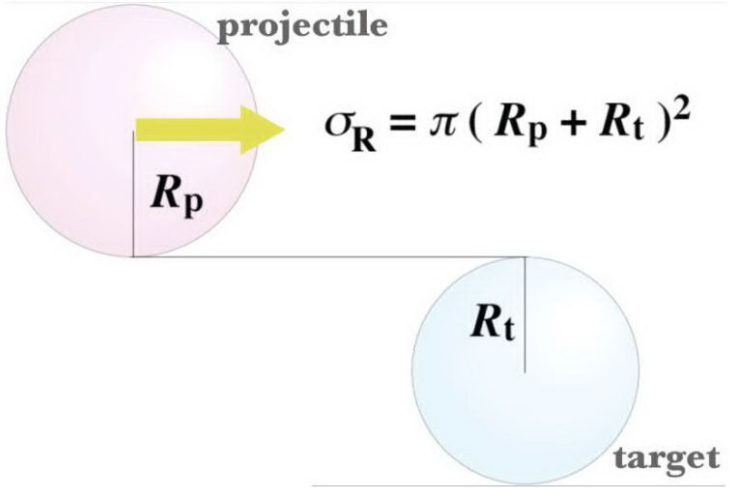

$R_p\ (r_p, r_n)$

核反应总截面： $\sigma_R = 2\pi \int_0^\infty [1 - T(b)] b db$

$$T(b) = \exp(-\int d^2 s \{\rho_n^P(s)\rho_n^T(s-b)\sigma_{nn} + \rho_p^P(s)\rho_p^T(s-b)\sigma_{pp} + \left[\rho_n^P(s)\rho_p^T(s-b) + \rho_p^P(s)\rho_n^T(s-b)\right]\sigma_{np}\})$$

核反应总截面、电荷改变截面与中子皮探测

$$T = T^p T^n$$

$$\begin{cases} T^p(b) = \exp[-(\sigma_{pp}\int \rho_p^{t\arg} \rho_p^{proj} + \sigma_{np}\int \rho_n^{t\arg} \rho_p^{proj}] \\ T^n(b) = \exp[-(\sigma_{pn}\int \rho_p^{t\arg} \rho_n^{proj} + \sigma_{nn}\int \rho_n^{t\arg} \rho_n^{proj}] \end{cases}$$

电荷改变截面： $\sigma_{cc} = 2\pi\int b[1 - T^p(b)]\varepsilon(E)db$

质子密度参数 → 质子密度分布ρ_p → 电荷改变截面 σ_{cc}

中子密度参数 → 中子密度分布ρ_n → 反应总截面

核反应总截面、电荷改变截面与中子皮探测

由于 $\sigma_{cc} = 2\pi \int b[1 - T^p(b)]\varepsilon(E)\,db$

令 $\tilde{\sigma}_{cc} = 2\pi \int b[1 - T^p(b)]\,db$

得 $\varepsilon(E) = \dfrac{\sigma_{cc}}{\tilde{\sigma}_{cc}}$

通过拟合实验数据得到 ε 函数

$$\varepsilon(E) = 1.107 + 0.01191 \times \exp(1.444 - 0.004623\,E)$$

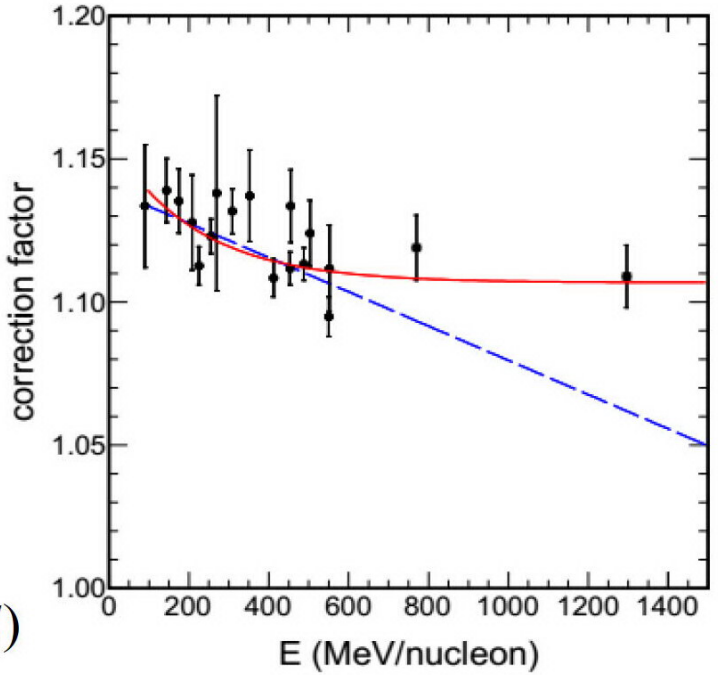

T. Yamaguchi et al., Energy-dependent charge-changing cross sections and proton distribution of ^{28}Si. Phys. Rev. C 82, 014609 (2010)

核反应总截面、电荷改变截面与中子皮探测

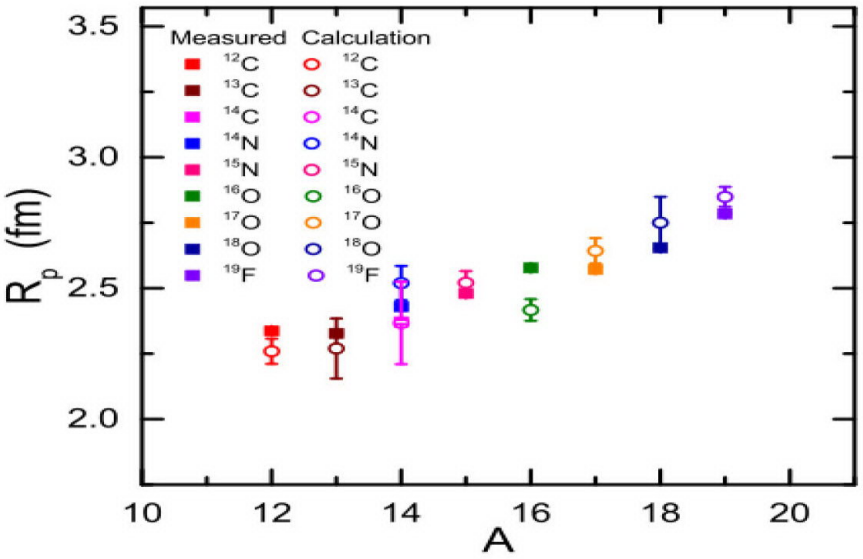

X. F. Li, D. Q. Fang, Y. G. Ma, Determination of the neutron skin thickness from interactioncross section and charge-changing cross section for B, C, N, O, F isotopes. Nucl Sci Tech 27 (2016) 71

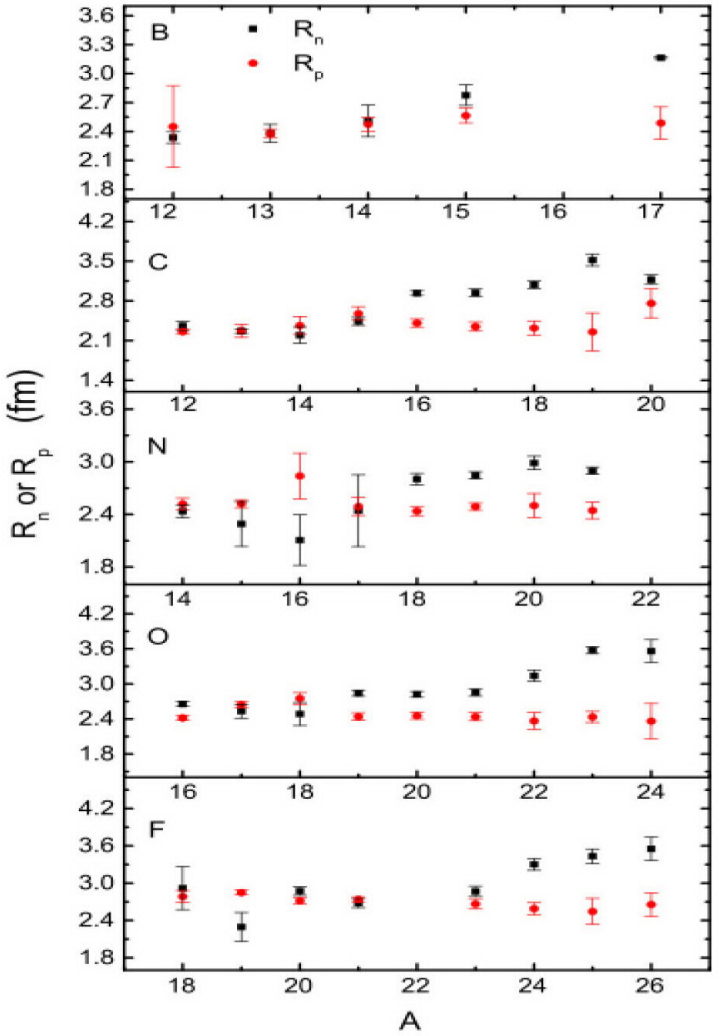

核反应总截面、电荷改变截面与中子皮探测

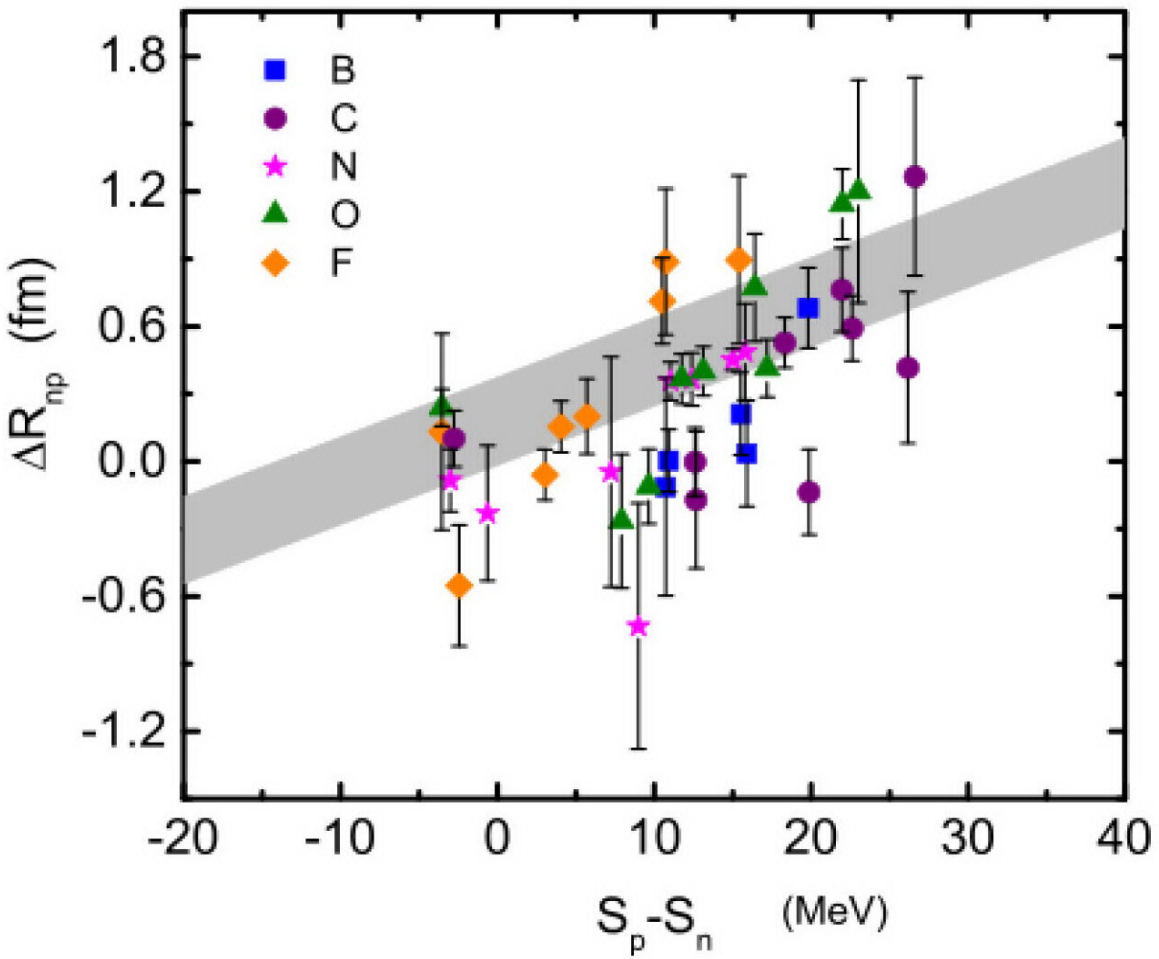

由公式$\Delta R_{np} = R_n - R_p$，得到B, C, N, O, F的中子皮厚度随单质子-中子分离能差的关系。阴影部分区域表示平均场理论计算预言的核的中子皮厚度的所在区域。

核反应总截面、电荷改变截面与中子皮探测

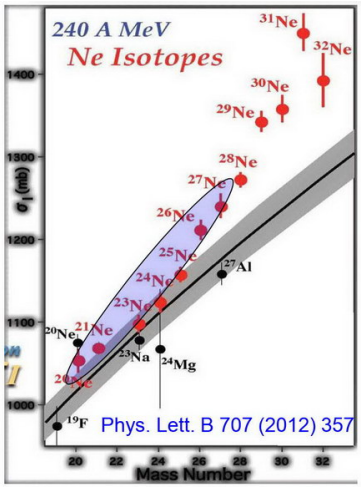

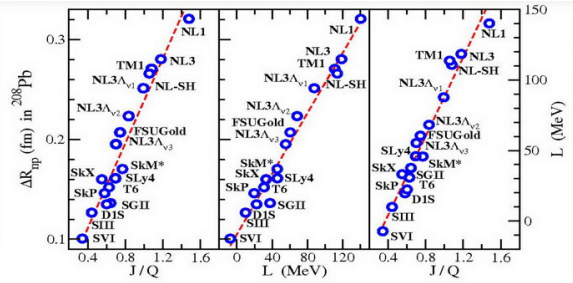

实验合作：近物所RIBLL束线组

实验目标：
测量$^{21-27}$Ne的电荷改变截面，提取Ne同位素的质子半径并得到中子皮厚度，结合理论计算提取对称能。

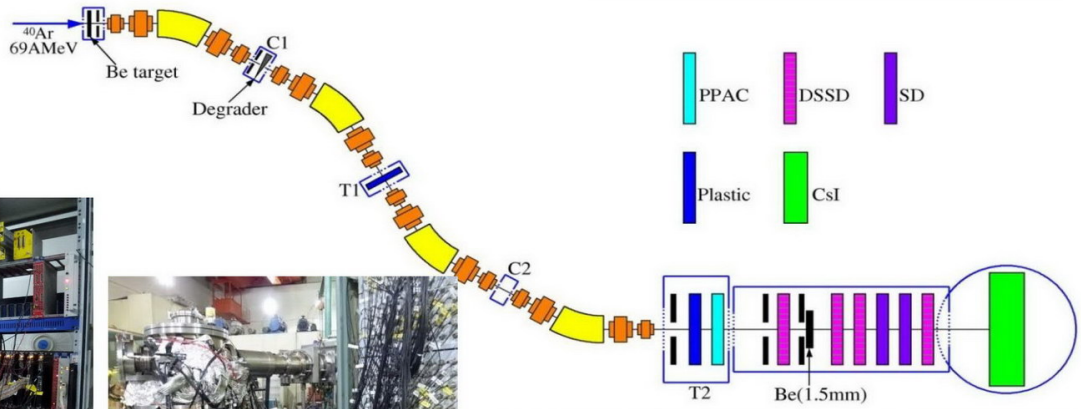

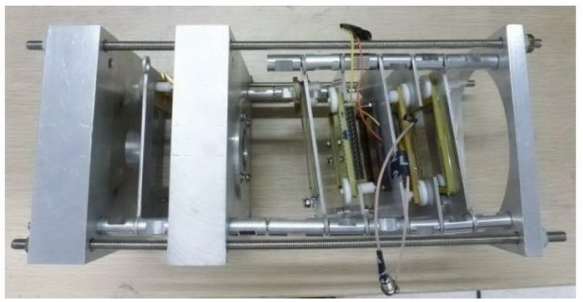

电荷改变截面与质子半径

$$\sigma_{cc} = \int [1 - T_c(b)] d\mathbf{b}$$

$$T_c(\mathbf{b}) = \exp[-\sigma_{pp} \int \rho_{Pp}(\mathbf{r}-\mathbf{b}) \cdot \rho_{Tp}(\mathbf{r}) d\mathbf{r} - \sigma_{pn} \int \rho_{Pp}(\mathbf{r}-\mathbf{b}) \cdot \rho_{Tn}(\mathbf{r}) d\mathbf{r}]$$

中子皮的可能实验观测量

中子皮厚度可能的实验观测量：

中子擦去截面：需鉴别炮弹及炮弹的同位素

轻粒子产额比：需测量中子、质子及轻带电粒子

重碎片产额比：需鉴别、测量重碎片

range of our calculation. We estimate the uncertainty of δ_{np} for $0.6 < b/b_{\max} < 1.0$ to be around 0.1 fm when the uncertainty of R_{np} is 5%. To achieve high resolution, well defined experimental

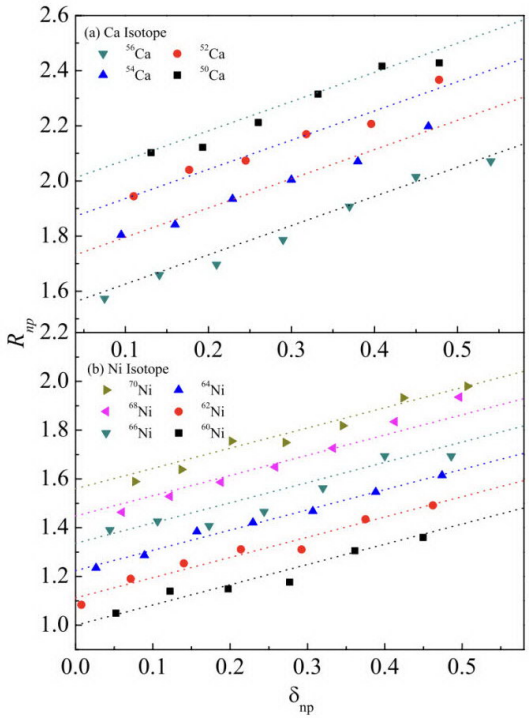

相对论重离子碰撞中的探针： 稳定核

PREX-II 实验

Jefferson Lab
Thomas Jefferson National Accelerator Facility

PRL 108, 112502 (2012) PHYSICAL REVIEW LETTERS week ending 16 MARCH 2012

Measurement of the Neutron Radius of ^{208}Pb through Parity Violation in Electron Scattering

S. Abrahamyan,[38] Z. Ahmed,[29] H. Albataineh,[17] K. Aniol,[2] D. S. Armstrong,[5] W. Armstrong,[31] T. Averett,[5] B. Babineau,[19] A. Barbieri,[36] V. Bellini,[11] R. Beminiwattha,[23] J. Benesch,[32] F. Benmokhtar,[6] T. Bielarski,[34] W. Boeglin,[7] A. Camsonne,[32] M. Canan,[24] P. Carter,[6] G. D. Cates,[36] C. Chen,[8] J.-P. Chen,[32] O. Hen,[30] F. Cusanno,[13,†] M. M. Dalton,[36] R. De Leo,[10] K. de Jager,[32,36] W. Deconinck,[21,5] P. Decowski,[28] X. Deng,[36] A. Deur,[32] D. Dutta,[22] A. Etile,[17] D. Flay,[31] G. B. Franklin,[3] M. Friend,[3] S. Frullani,[13] E. Fuchey,[4,31] F. Garibaldi,[13] E. Gasser,[17] R. Gilman,[26] A. Giusa,[11] A. Glamazdin,[16] J. Gomez,[32] J. Grames,[32] C. Gu,[36] O. Hansen,[32] J. Hansknecht,[32] D. W. Higinbotham,[32] R. S. Holmes,[29] T. Holmstrom,[19] C. J. Horowitz,[14] J. Hoskins,[5] J. Huang,[21] C. E. Hyde,[24,4] F. Itard,[17] C.-M. Jen,[29] E. Jensen,[5] G. Jin,[36] S. Johnston,[33]

PREX-I Result

PRL 108 (2012) 112502
PRC 85 (2012) 03250(R)

$$A = 0.656\ ppm \pm 0.060(stat) \pm 0.014(syst)$$

Neutron Skin = R_N - R_P = 0.33 + 0.16 - 0.18 fm

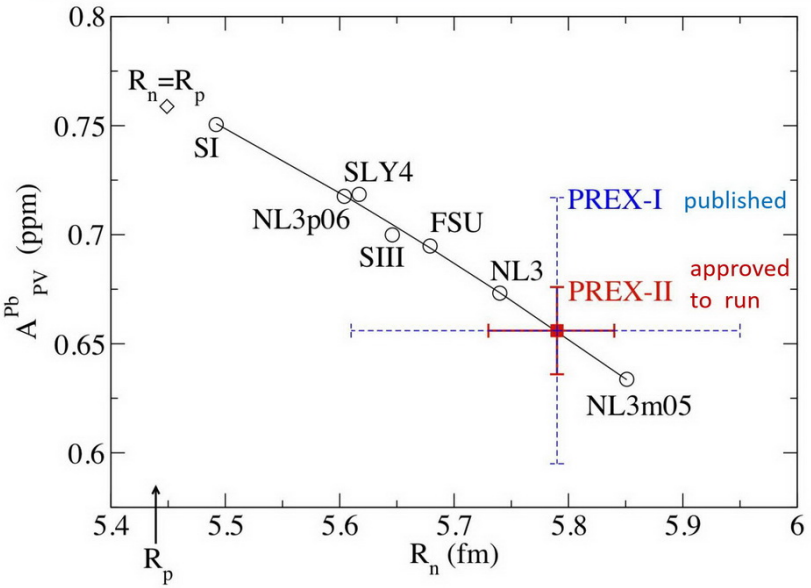

Parity Radius Experiment

- Parity violation probes neutrons because weak charge of a n ≫ p.
- Elastic scattering of 850 MeV e from ^{208}Pb at 6°.

$$A = \frac{\frac{d\sigma}{d\Omega}_+ - \frac{d\sigma}{d\Omega}_-}{\frac{d\sigma}{d\Omega}_+ + \frac{d\sigma}{d\Omega}_-}$$

- Measure A ≈ 0.6 ppm to 3%. This gives neutron radius to 1% (± 0.05 fm).
- Purely electroweak reaction is model independent

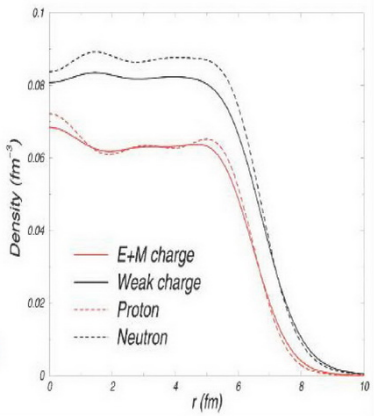

C-REX Proposal

(conditionally approved)

$$\frac{dR_N}{R_N} = 0.9\%$$

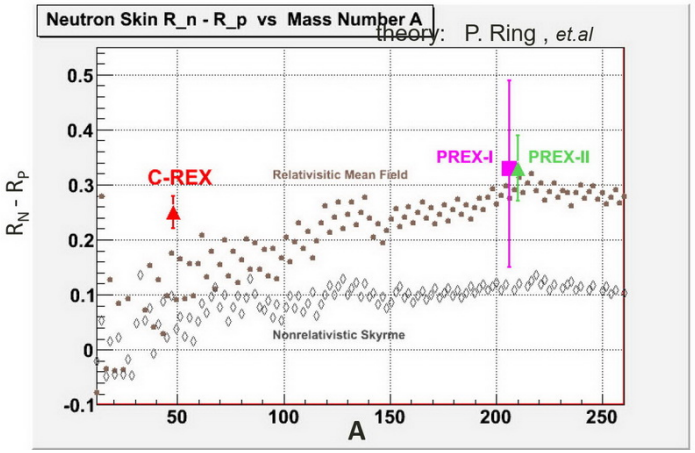

PREX-II 实验

PHYSICAL REVIEW LETTERS **126,** 172502 (2021)

Editors' Suggestion Featured in Physics

Accurate Determination of the Neutron Skin Thickness of ^{208}Pb through Parity-Violation in Electron Scattering

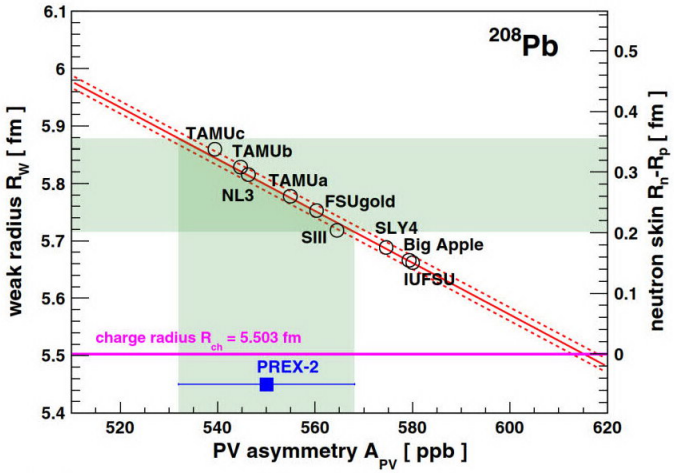

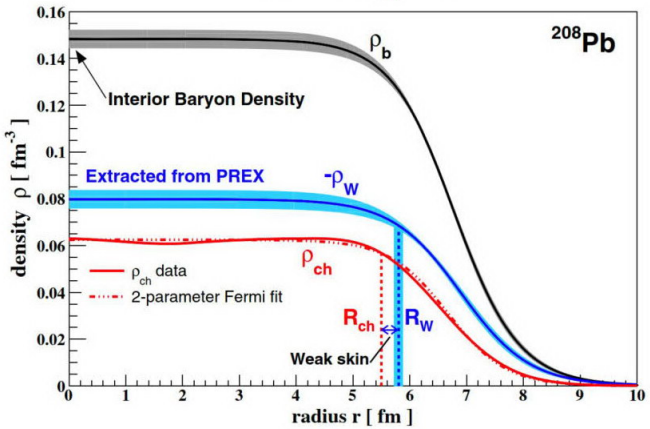

$R_N - R_P = 0.283 \pm 0.071$ fm

PHYSICAL REVIEW LETTERS **126,** 172503 (2021)

Editors' Suggestion

Implications of PREX-2 on the Equation of State of Neutron-Rich Matter

Brendan T. Reed,[1,2,*] F. J. Fattoyev,[3,†] C. J. Horowitz,[2,‡] and J. Piekarewicz[4,§]
[1]*Department of Astronomy, Indiana University, Bloomington, Indiana 47405, USA*
[2]*Center for Exploration of Energy and Matter and Department of Physics, Indiana University, Bloomington, Indiana 47405, USA*
[3]*Department of Physics, Manhattan College, Riverdale, New York 10471, USA*
[4]*Department of Physics, Florida State University, Tallahassee, Florida 32306, USA*

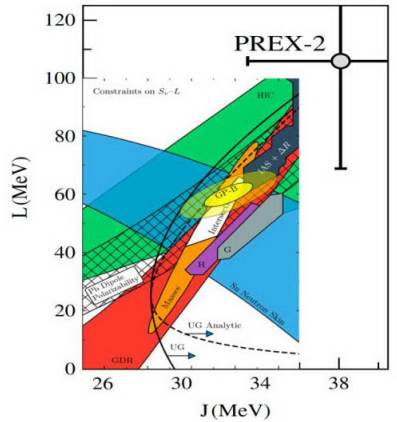

$J = (38.1 \pm 4.7)$ MeV,

$L = (106 \pm 37)$ MeV,

$\tilde{L} = (71.5 \pm 22.6)$ MeV.

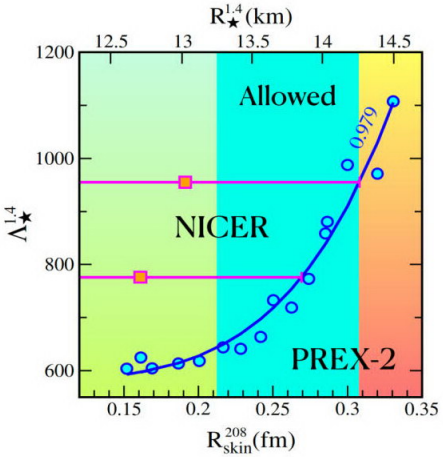

$0.21 \lesssim R_{\rm skin}({\rm fm}) \lesssim 0.31,$

$13.25 \lesssim R_\star^{1.4}({\rm km}) \lesssim 14.26,$

$642 \lesssim \Lambda_\star^{1.4} \lesssim 955.$

中子皮：原子核物理研究热点之一

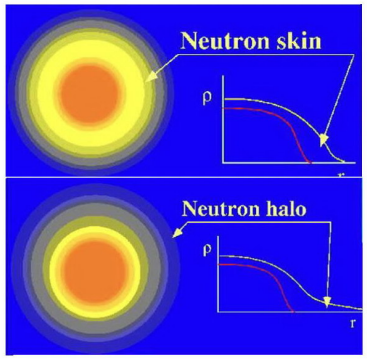

不稳定核结构

稳定核：～300；理论预言：～8000；已发现：～3000

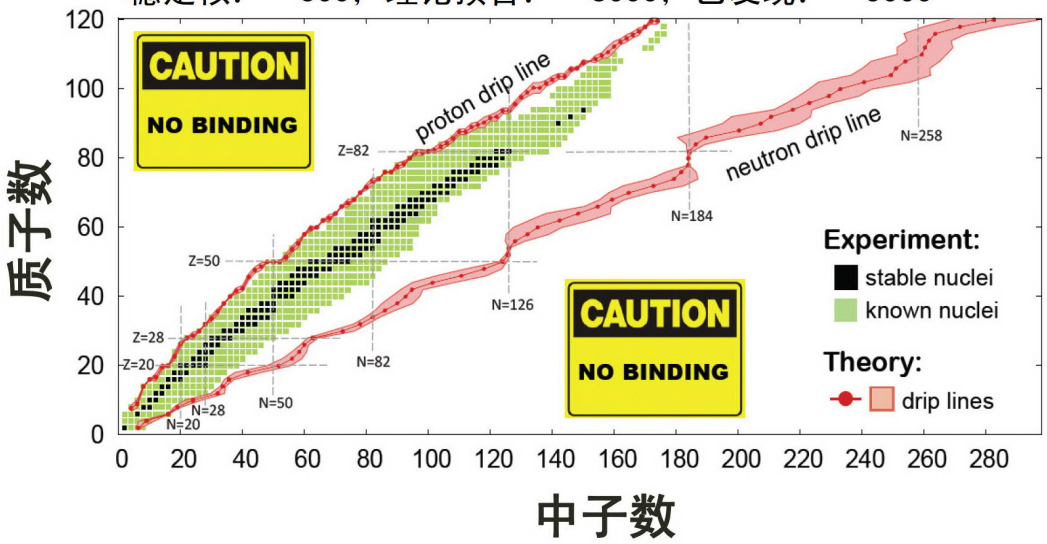

中子皮 ⟺ **核物质状态方程** ⟺ **核天体性质**

中子皮与核态方程参数的依赖

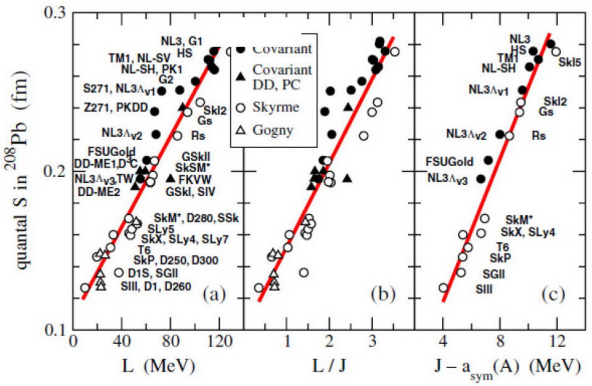

核态方程不确定

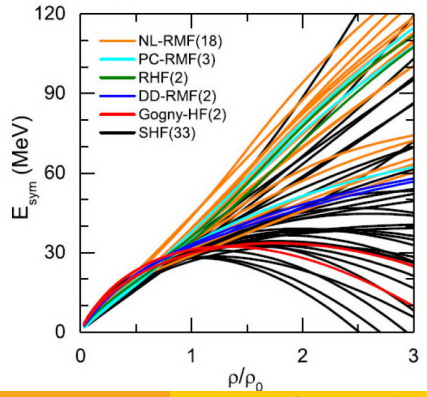

中子星的质量-半径关系